2019

Drp1 inhibition is protective against mitochondrial and autophagic impairment induced by alpha-synuclein

Fan, Zhangqiuzi

UNIVERSITY OF PLYMOUTH

Drp1 inhibition is protective against mitochondrial and autophagic impairment induced by alpha-synuclein.

by

Rebecca Zhangqiuzi Fan

A thesis submitted to the University of Plymouth
in partial fulfilment for the degree of

DOCTOR OF PHILOSOPHY

Peninsula Schools of Medicine and Dentistry

November 2019

Copyright Statement

Acknowledgements

The journey to a PhD has never been easy, and I cannot be more thankful for the support and help I have received all the way. It almost feels impossible to convey all my gratitude in a short acknowledgement; nevertheless, I will give it my best effort.

I would like to begin by acknowledging my primary supervisor, Dr Kim Tieu. It was a bold decision to change my study area to a more neuroscience-based field with little background; Dr Tieu gave me the chance to make it happen, to which I'm dearly grateful. Not only has Dr Tieu been a great mentor for me, he has also taken the time and effort to work closely with me and train me with techniques. Nor should I fail to thank other people who have been part of the Tieu lab: Dr Wai Ling Kok, who taught me about molecular biology; and all the fellow students I had the pleasure to work with - Monica Bussaca, Claire Moss, Carolina Sportelli and the list goes on. Also, thanks goes to my other supervisors, Dr Iain Robinson and Dr Camille Carroll, for their constructive comments and expertise shared with me in all my supervisory meetings. I have had the pleasure to collaborate with Dr Shouqing Luo, whose expertise and generosity in providing us the essential tools in assessing autophagy have greatly helped the development of this study and future ones to come. Thanks also to Dr Paul Waines from main campus Plymouth University, who trained me and helped me with FACS sorting for a better cell line to work with, and at a later stage kindly provided lab workspace as well as a high-speed centrifuge that made synaptosome isolation study possible. On the same note, I would also like to address Dr Martin Helley, who undertook all the animal injections and worked with me on the isolations, and Mrs Andrea Heath from reception who arranged all the transportation that enabled me to carry out the experiment between campuses. I also would like to

acknowledge the PSMD research administrator, Ms Francesca Niedzielski. Although we've never met in person, Francesca has always 'come to the rescue' when a paperwork problem emerges along the way since the lab relocation to Miami, which has been a great help for me to focusing on my study.

For a PhD student from a foreign country, life in Plymouth was a bit unsettling at the start. Thanks to my wonderful peers from PSMD, I was very lucky to have you as my friends to be alongside with me through the journey. Ms Jemma Walker, my first friend who also turns out to be best, my sister from another mister. None of the many memorable events would have happened if it has not for her, who drags me out of my shell and encourages me to grow. Not to mention all the unbearable moments of me she has to put up with. Another very special person is Mrs Tracey Evans (hopefully Dr Evans by now), who has always been there for me to help me get through the most difficult times in every stage of my PhD life, whether it's academia or personal obstacles. Friendship is not enough to summarise the incredible support and care Tracey has offered me, and all the laughter and tears we have shared together, she is my second family. Also, cheers to Dr Dan Felmlee, and my peer who has successfully upgraded to the next level, Dr Robert Button, for some quality company that acted as great anti-dote to the pressure. The witty duo enjoy cracking silly jokes for a good laugh yet are serious scientists at heart. Nor should I forget to mention my yoga pals, Dr Karolina Jaworek and Dr Mona Nasser, two busy ladies who like to live life to the fullest.

Outside academia, it is an understatement to say that I owe a great deal to my family. My parents who have been supporting every decision I have ever made even in my career throughout the entire journey, even when they don't understand it. I wouldn't have gone this far without your unconditional support. And I would like to

delicate this work to my grandmother, who was hospitalised upon diagnosis of Parkinson's with Dementia over a year ago. It almost seems ironic at times, that I haven't been able to visit her, being busy doing research related to finding effective therapeutics for the disease that strangles her in hospital bed. However, in the difficult time when I think about giving up and seek a more comfortable way of living, deep down I know there's always a reason to carry on. And, if this study could, in any way, serve any use to the development of potential therapies that would relieve the pain of patients and their loved ones, the effort would not be in vain.

Last, but not least, I would like to give special thanks to my examiners, Prof. David Parkinson and Dr Claudia Barros, for patiently sitting through the process for the second time. I hope you can get some useful information from reading this work, I am very grateful and wish you every success in your career.

Author's Declaration

At no time during the registration for the degree of *Doctor of Philosophy* has the author been registered for any other University award without prior agreement of the Graduate Sub-Committee.

Work submitted for this research degree at the Plymouth University has not formed part of any other degree either at Plymouth University or at another establishment.

This study was financed with the aid of a studentship from Plymouth University and carried out with a partial stipend support from Florida International University.

Relevant scientific seminars and conferences were attended at which work was presented; some of these results have either been published or prepared for publication submission.

Publications (or presentation of other forms of creative and performing work):

1) ***Rebecca Z Fan****, Min Guo, Shouqing Luo, Mei Cui, Tieu Kim Exosome release and neuropathology induced by α-synuclein: new insights into protective mechanisms of Drp1 inhibition.* (*Acta Neuropathologica Communications,* in press)
   DOI: https://doi.org//10.1186/s40478-019-0821-4
2) Bido S, Soria FN, **Fan RZ**, Bezard E, and Tieu K. Mitochondrial division inhibitor-1 is neuroprotective in the A53T-α-synuclein rat model of Parkinson's disease. *Scientific Reports* (2017), 7(1):7495.
   DOI: https://doi.org//10.1038/s41598-017-07181-0
3) Phillip Rappold, Mei Cui, Jonathan Grima, **Rebecca Fan,** Karen Bentley, Linan Chen, Xiaoxi Zhuang, William Bowers and Kim Tieu. Drp1 inhibition attenuates neurotoxicity and dopamine release deficits in vivo, *Nature Communications (2014),* 5:5244
   DOI: https://doi.org//10.1038/ncomms6244

Presentations at conferences:

1. Poster presentation (with travel grant awarded):

XXI World Congress on Parkinson's disease and Related Disorders, Milan Italy. 2015

Abstract published:

'Blocking mitochondrial fission is protective in dopaminergic neuronal cells with inducible α-synuclein expression'

Parkinsonism & Related Disorders 22(2):e191 DOI10.1016/j.parkreldis.2015.10.492

2. Poster presentation

5th World Parkinson Congress (WPC), Kyoto, Japan. 2019-

"Protein aggregation and exosomal release induced by α-synuclein: New Insights into protective mechanisms of Drp1 inhibition."

Word count of main body of thesis: 28502

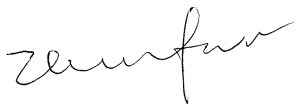

Signed…….

Date……03/09/2019…….

List of Contents

Rebecca Zhangqiuzi Fan

‘ Blocking mitochondrial fission protects against toxicity induced by α-synuclein overexpression’

Abstract

Parkinson’s disease (PD) is the second most common neurodegenerative disorder with currently no effective neuroprotective or neurorestorative treatments available. Alpha-synuclein (α-syn) pathology is one of the key proteins involved in PD pathology, it has been found to induce mitochondrial dysfunction, yet the mechanism is not entirely understood. This thesis project tests the hypothesis that α-syn induces mitochondrial dysfunction through disruption of fission/fusion pathway. Using an inducible cell line, I successfully demonstrated that in a time-dependent manner α-syn overexpression induces mitochondrial fragmentation through disruption of fission/fusion dynamics, collapse of mitochondrial membrane potential, increased oxidative stress and impaired mitochondrial respiratory capacity. In addition, accumulation of protein aggregation was also observed due to impaired autophagy flux. More importantly, blocking the fission protein Dynamin Related protein 1 (Drp1) either genetically or pharmacologically confers protection against these abnormalities. Although further investigation is needed to better understand this protective mechanism, these results are consistent with our previous published data and those from other laboratories that Drp1 inhibition is a promising therapeutic target for PD.

List of Figures

Chapter 4

Chapter 5

List of tables

List of Abbreviations

Abbreviation	Unabbreviated form
AD	Alzheimer's Disease
DHE	Dihydroethidium
DMSO	Dimethyl Sulfoxide
Drp1	Dynamic-related protein 1
EM	Electron Microscopy
ER	Endoplasmic Reticulum
FBS	Foetal Bovine Serum
FCCP	Carbonyl cyanide 4-(trifluoromethoxy)phenylhydrazone
GFP	Green Fluorescent Protein
ICC	Immunocytochemistry
LC 3	microtubule-associated protein 1A/1B Light Chain 3B
Mdivi-1	Mitochondrial division inhibitor-1
Mfn2	Mitofusin-2
MPTP	1-methyl-4-phenyl-1,2,3,6-tetrahydropyridine
mTOR	Mammalian target of Rapamycin
Nrf	Nuclear respiratory factor
p62	Sequestosome 1
PCR	Polymerase Chain Reaction

PD	Parkinson’s Disease
PGC- 1α	Peroxisome proliferator-activated receptor gamma coactivator -1 alpha
PINK	PTEN-Induced putative Kinase
PK	Proteinase K
PonA	Ponastrone A
PQ	Paraquat
RFP	Red Fluorescent Protein
ROS	Reactive Oxygen Species
TEM	Transmission electron microscopy
TMRM	tetramethylrhodamine methyl ester
TOM 20	Translocase of outer membrane 20
ULK	uncoordinated 51-like kinase
UPS	Ubiquitin-Proteasome System
α-syn	Alpha-synuclein

1. Background

1.1. Parkinson's disease

Parkinson's disease (PD) is a neurodegenerative disorder with selective and profound loss of dopaminergic neurons in the substantia nigra and is typically diagnosed by cardinal motor syndromes. The primary symptoms include resting tremor, rigidity (stiffness), bradykinesia (slowness of movement) and postural instability, although to date there are over 30 clinical symptoms recognised as fundamental features for the disease (Przedborski, 2017). Identification of the Lewy body, the intracellular lesion composed of proteins such as α-syn and ubiquitin, at post-mortem autopsy, is the primary pathological hallmark of the disease. PD is the second most common neurodegenerative disorder, and an epidemiological study (Dorsey et al., 2007, Dorsey et al., 2006) predicted the number of over 50 year olds with PD will increase to 8.7 million by 2030, doubling the approximate 4.1 million of 2005. PD is known to be primarily caused by damage to the nigrostriatal dopaminergic pathway, yet the pathogenesis of this heterogeneous disease is not fully understood (Blesa and Przedborski, 2014)

It is believed that PD has existed since ancient times, and it made its first appearance in western medical literature in AD175, described as "shaking palsy" by the physician, Galen (Koehler and Keyser, 1997). However, the first collective definition for PD was established in 1817, when a London doctor James Parkinson published an article entitled "An Essay on the Shaking Palsy". In this study, he described the six cases he came across during his own practice and from the neighbourhood. He characterised in detail the symptoms of this medical condition: involuntary tremors, difficulty with balance, and festination ("A propensity to bend the trunk forwards, and to pass from a walking to a running pace") (Parkinson, 2002). It

was not until the 1960s that emerging evidence identified the biochemical change as lower levels of dopamine in PD brains, resulting from the loss of dopaminergic neurons in the *substantia nigra*, as summarised by Fearnley & Lee, which was later confirmed by Damier and colleagues (Fearnley and Lees, 1991, Damier et al., 1999). It was also during this period that Levodopa was first introduced to treat PD patients. Following this discovery, research on PD progressed remarkably over the years, with better understanding of the disease and effective treatments developed to control the symptoms. As more non-motor symptoms are documented, PD is more distinguished from motor parkinsonism, and it is generally considered as a collective term for multisystem neurodegenerative disorders.

Despite the remarkable progress in characterisation and understanding the disease, to date, there is no neuroprotective or neurorestorative treatment available. Five decades on since its introduction to PD treatment, Levo-Dopa (L-Dopa) remains the best and most common treatment despite the side effects including hypotension, abnormal involuntary movements, and problems with long-term treatment(Barbeau, 1969). Better understanding of the pathogenesis process and finding potential new therapeutic treatments remains an important need.

1.1.1. **Sporadic and familial PD overview**

The topic of PD pathogenesis is complicated by the variations in clinical symptoms and disease pathology. Multiple risk factors have been identified, with ageing standing out as the number one risk factor for people over fifty. Although it would be easier to consider PD as ‘acceleration of ageing’, the difference in age-associated dopamine loss between individuals cannot be explained (Cannon and Greenamyre,

2013). In the early 1980s, a meperidine homolog called 1-methyl-4-phenyl-1,2,3,6-tetrahydropyridine (MPTP), was found to induce severe parkinsonism in drug addicts (Davis et al., 1979, Langston et al., 1983). The culprit was its metabolite 1-methyl-4-phenylpyridinium (MPP^+), a mitochondrial complex I inhibitor. This link and other neurotoxins and pesticides discovered later allowed researchers to look more closely into certain pathways that facilitate disease formation and progression. Meanwhile, the discovery of genetic mutations, especially those linked to early onset of the disease, implicated gene involvement that could be independent from ageing. All PD cases can be generally divided into two categories, those clearly linked to genetic mutations are recognised as familial PD and the rest termed as sporadic PD.

Sporadic PD. Idiopathic PD or sporadic PD refers to all the disease conditions where no evident genetic mutation is found. About 90% of PD cases are sporadic, the remaining cases are caused by genetic mutations (Dawson and Dawson, 2010) , Efforts to better understand the aetiology of the disease have yielded a wide range of potential causes. However, the lack of direct evidence has prevented conclusive consensus being reached and therefore further investigation is required.- Nevertheless, environmental factors, such as exposure to certain organic compounds and heavy metals have been proposed to play a major role. Following the discovery of MPTP, decades of epidemiological study have identified a certain group of pesticides and other herbicides associated with PD including rotenone and paraquat (PQ) (Giasson and Lee, 2000, Priyadarshi et al., 2001, Tanner et al., 2011b). Relevant to these observations, rural living has been associated with higher PD risk (Gorell et al., 1998). It's well known that exposure to high dose of pesticides, even just once, could have lethal toxicity; however the link discovered between

chronic low dose exposure and PD development (Baldi et al., 2003) remains to be further explored.

Rotenone, for instance, is a mitochondrial complex I inhibitor commonly used as insecticide and pisticide (kills fish in lakes and reservoirs etc.). Rotenone has been associated with increased risk of developing PD (Tanner et al., 2011a, Kamel, 2013, Tanner et al., 2011b). Experimental rat models of this systemic exposure to the toxin have replicated many pathological features of the disease in humans including bradykinesia, postural instability, and/or rigidity, all linked to loss in dopaminergic neurons (Cannon et al., 2009, Betarbet et al., 2000). Comparing to rotenone, PQ is more well-documented in PD, as stronger links have been demonstrated from case-studies. PQ is a widely used herbicide for weed control, although it is banned in many countries including Europe, restricted usage is still permitted in the US. PQ shares structural similarities with MPTP, however, it does not have a direct inhibition effect on electron transport chain(Richardson et al., 2005) . Instead, it generates reactive oxygen species (ROS) through redox cycling. In addition, heavy metals such as manganese (Mn) and iron (Fe) have been linked to increased risk of developing PD (Fukushima et al., 2010, Dantzig, 2006, Uversky et al., 2001, Quadri et al., 2012, Roth, 2014).

Intriguingly, a common pathway of mitochondrial dysfunction has been identified for many of the environmental toxicants either through direct inhibition such as rotenone, or through indirect disruption such as ROS generation by PQ (Helley et al., 2017b). Although this link, or alleged increased risk, might not serve as direct evidence for PD, several neurotoxin models have successfully displayed nigrostriatal damages and some of the behavioural phenotypes in rodent and primate models (Tieu, 2011, Bové and Perier, 2012). Interestingly, although some individual factors

on their own would not increase the risk by much, the combination with other factors could significantly increase the risk. For example, the combined exposure of PQ and the fungicide, Maneb have been found to increase the risk of PD by 75% in a case-control study in California (Costello et al., 2009). In experimental models, the concurrent exposure of the two toxins have shown to induce significant neuronal loss in non-transgenic mice, and loss was further enhanced in transgenic mice expressing human α-syn (Desplats et al., 2012). Related to this, gene-environment interaction has received much attention in PD. Elevated α-syn levels, aggregation, secretion and spreading have been shown in different neurotoxin models such as rotenone, suggesting higher induction of the protein in response to the toxin exposure (Feng et al., 2006, Pan-Montojo et al., 2012a).

Familial PD. Familial PD is distinguished from sporadic PD by a clear family history of the disease with an identified monogenic mutation. Approximately 30% of the familial and 3–5% of sporadic PD cases are caused by monogenic mutations, while the other remaining cases are classified as sporadic with unknown aetiology (Klein and Westenberger, 2012, Hernandez et al., 2016, Surmeier et al., 2017, Obeso et al., 2017). Familial PD can be caused by either autosomal dominant or autosomal recessive mutations. Although familial PD only makes up less than 10% of all PD cases, to date there are mutations in over 10 genes discovered in PD. The names of some major genes, their functions and mutations linked to PD are summarised in **Table 1.1**.

Table1.1 List of major mutations discovered to be associated with PD and the normal function of respective proteins (modified from (Helley et al., 2017b))

Gene	PARK Locus	Gene Locus	Inheritance	Mutations	Prevalence	Protein function	Minor Allele Frequency//Penetrance	First reference linked to PD
SNCA	*PARK 1/4*	*4q21 -22*	AD	A53T, A30P, E46K, G51D, H50Q, duplications, triplications	Rare, A53T is most frequent but only found in seven families worldwide	Involved in synaptic vehicle trafficking, precise function not clear	85% for the p.A53T mutation, and is reduced and for gene amplification, estimated at 33% in one family with a duplication	Polymeropoulos et al., 1997; Krüger et al., 1998; Singleton et al., 2003; Zarranz et al., 2004; Appel-Cresswell et al., 2013; Lesage et al., 2013
LRRK 2	*PARK 8*	*12q1 2*	AD	>100 missense and non-sense mutations high risk variants, >15 of which are pathogenic	Up to 40% of familial and up to 10% of sporadic cases	Multiple roles including cytoskeletal dynamics, vesicular transport, and autophagy	Differ by populations and by mutation. p.G2019S shows penetrance sometimes estimated to be as low as 24%, the p.R1441 mutation is highly penetrant (95% at the age of 75 yr)	Funayama et al., 2002
VPS35	*PARK 17*	*16q1 1.2*	AD	D620N	1% of familial and 0.2% of sporadic cases	Part of the retromer cargo-recognition complex critical for the endosome-trans- Golgi	High and age-dependent penetrance (onset range: 34-68 years)	Vilarino-Guell et al., 2011; Zimprich et al., 2011
CHCH D2	*PARK 22*	*7q11 .2*	AD	10 mutations (see	Not available	Activates gene involved in forming	Not available	Funayama et al., 2015; Ogaki et

				Koschmidder et al., 2016)		Complex IV of mitochondrial respiratory chain		al., 2015
GBA	*N/A*	*1q21*	AD	>300 mutations, L444P and N370S are most common	Varies in different PD populations but up to 31% in Ashkenazi Jewish PD patients	a lysosomal enzyme that catalyzes the breakdown of the glycolipid glucosylceramide (GlcCer) to ceramide and glucose	7.6% at 50 years and 29.7% at 80 years	Tsuji et al., 1987; Neudorfer et al., 1996
Parkin	*PARK 2*	*1p35 -36*	AR	~147 exonic mutations	77% familial EOPD and 10–20% EOPD in	Mitophagy	Penetrance complete in individuals who have biallelic pathogenic variants	Kitada et al., 1998
PINK1	*PARK 6*	*6q25 .2-27*	AR	>60 mutations,	General >9%EOPD	Mitophagy	Age-dependent, appears to be complete in individuals who have biallelic pathogenic variants	Valente et al., 2004a
DJ-1	*PARK 7*	*1p36*	AR	>10 mutations	1–2% EOPD	Has been proposed to protect cells from oxidative stress	Penetrance for homozygous and compound heterozygous mutation carriers seems to be complete	Bonifati et al., 2003
ATP13A2	*PARK 9*	*1p36*	AR	>10 mutations	Rare (found in 11 families)	5 P-type ATPase polytopic lysosomal membrane protein	variable penetrance	Ramirez et al., 2006; Di Fonzo et al., 2007
FBXO7	*PARK 15*	*22q12-13*	AR	R378G, R498X, T22M, L34R	Rare	serve as molecular scaffolds in the formation of protein complexes	Not available	Shojaee et al., 2008
PLA2G6	*PARK 14*	*22q13.1*	AR	R741Q, R747W and more	Rare	a phospholipase A2 enzyme	Not available	Paisan-Ruiz et al., 2009

EOPD, Early-onset PD (Age at onset <50 years old); LOPD, Late-onset PD (Age at onset ≥ 50 years old); AD, Autosomal dominant; AR, Autosomal recessive; GW, Genome-Wide

The first mutation discovered was alpha-synuclein (α-syn), before which PD was long considered to be a sporadic disorder. Soon after, mutations in a ubiquitin E3 ligase, Parkin, was reported, in autosomal recessive parkinsonism with early onset.

In 2004, the mutation of a mitochondrial kinase PTEN-induced putative kinase 1 PINK1 (encoded by *PINK1*) was found to induce early-onset PD (Valente et al., 2004). Although PINK1 mutation is rare, accounting for less than 1% of all PD on a population basis with only 1-8% of PD patients (Klein et al., 2007) , the discovery of its mutation is significant. This direct link established the role of mitochondrial dysfunction in PD pathogenesis which has long be suspected since the identification of MPTP (Langston et al., 1983). PINK1, together with parkin, plays a vital role in mitochondrial quality control by mediating mitophagy. It is now a common knowledge that parkin proteins are selectively recruited onto depolarised mitochondria by PINK 1 (Narendra et al., 2008) as an early event of the process. In addition, both PINK 1 and parkin knockout mice have shown reduced mitochondrial respiration capacity in striatum despite no gross morphological abnormalities been observed (Palacino et al., 2004, Gautier et al., 2008). Over the years, other PD-linked mutations including α-syn have been discovered to also have an impact on mitochondria. For example, protein deglycase DJ-1 has also been reported to influence mitochondrial function and mitophagy indirectly through modulation of oxidative stress (McCoy and Cookson, 2011). DJ-1 is a cytosolic protein that belongs to the ThiJ/PfpI protein superfamily, fractionation study and immuno-electron microscopy (EM) have confirmed its mitochondrial localisation (approximately 25% of total DJ-1) (Zhang et al., 2005a).

Leucine-rich repeat kinase 2 (*LRRK 2/PARK8*) is known to be the most commonly seen mutation in familial PD compared to other familial PD-linked genes, especially for certain ethnic backgrounds (Healy et al., 2008). Mutations in this gene are predominantly linked to autosomal dominant cases of PD, although they are also observed, at very low frequency, in other conditions such as AD, mostly as overlapping secondary pathologies observed at later stage of PD (Zhao et al., 2011).

Whilst monogenetic mutations only account for around 10% of all PD cases (de Lau and Breteler, 2006), the pathways affected by each of the mutations, whether shared by other mutations or not, provide insights into key factors that are also possibly disrupted in sporadic PD pathogenesis. With the increased interest in gene-environment interaction, investigating genetic factors holds great value in helping us understanding the aetiology of sporadic cases.

The heterogenicity of PD indicates the complexity of PD pathogenesis. For familial PD cases so far, many different mutations from 18 specific chromosomal regions (known as *PARK*) have been identified, and the most well studied ones include: *SNCA*, *PARK8/ LRRK 2*, *PARK6/PINK1*, *PARK2/parkin*, and *PARK7/DJ-1*. Of these, the first two are accountable for autosomal-dominant forms of PD, whilst the other three are linked to autosomal recessive forms (Klein and Westenberger, 2012). As discussed above, the percentage of monogenic PD (disease caused by a single mutation) is very low, in many cases one mutation alone would not lead to disease pathogenesis, as within the same family carrying a certain mutation, not everyone would develop PD. On the other hand, through genome-wide association studies (GWAS), different mutations have been identified in sporadic PD cases, highlighting the importance of gene environment interaction (Mullin and Schapira, 2015)

In this project I focused on α-syn for evaluating changes in mitochondria and autophagy pathways, as this specific protein is linked to both familial and sporadic PD (Dehay et al., 2015b). This suggests the possible common pathways involved in both familial and sporadic forms. Studying the pathological mechanism of this protein through genetic manipulation (mutation or overexpression) could potentially shed light on understanding disease pathogenesis in sporadic PD.

1.2. Alpha-synuclein (α-syn) and PD pathogenesis

Human α-syn protein is a 14 kDa pre-synaptic protein encoded by *SNCA* gene. Compared to the other two members of synuclein family (β- , γ-), α-syn is widely expressed in different tissues including pancreas, kidney, lung, skeletal muscle and heart, and predominantly in the brain (Lavedan, 1998). The structure of syn proteins is well conserved, with β-syn showing 61% match with α-syn (Goedert et al., 2017). The distinctive difference between these two proteins is the non-amyloid-β component (NAC) region specific to α-syn, which is responsible for the self-assembling of the protein. In fact, only α-syn, not β-syn, is capable of forming aggregates, as shown in neurodegenerative disease models such as PD, Dementia with Lewy bodies (DLB) and multiple system atrophy (MSA). It is highly expressed in the CNS, with specific enrichments at presynaptic nerve terminals. Despite being the first mutation identified in PD, the exact function of this protein remains largely unknown. Nevertheless, it is commonly believed that α-syn is involved in synaptic vesicle trafficking and synaptic release. In 1997, it was found to be one of the main components of Lewy bodies, the intracellular protein lesion recognised as the

pathological hallmark of PD (Spillantini et al., 1997). Approximately at the same time, α-syn mutations were also discovered to be linked to PD, when a large Italian family was identified with a mutation of G209 substitution in the *SNCA* gene, resulting in a change of Alanine to Threonine at position 53. This resulted in an autosomal-dominant form of PD with early onset. This is the first mutation discovered in PD, marking the start of familial PD research. Over the past few decades, as shown in **Table 1.2**, six different point mutations of α-syn have been reported:

Table 1.2 Summary of α-syn mutations

Mutation	Gene Position	Discovery	Clinical features
A53T (Ala53Thr)	G209A	(Polymeropoulos et al., 1997a)	Autosomal dominant early-onset PD
A30P (Ala30Pro)	G88C	(Kruger et al., 1998)	Autosomal dominant early- onset PD
E46K (Glu46Lys)	G188A	(Zarranz et al., 2004a)	Autosomal dominant
H50Q (His50Gln)	T150G	(Appel-Cresswell et al., 2013a)	late-onset parkinsonism/ idiopathic PD
G51D (Gly51Asp)	A152G	(Lesage et al., 2013)	Early-onset parkinsonian-pyramidal syndrome
A53E (Ala53Glu)	C158A	(Pasanen et al., 2014)	Atypical PD

Although the proportion of genetic mutations is low in all PD cases, the presence of wild type protein in Lewy bodies links α-syn with common forms of the disease. In fact, higher levels of wild type α-syn can become toxic, as locus duplication and triplication of α-syn can also induce PD pathogenesis (Singleton et al., 2003a, Chartier-Harlin et al., 2004), with triplication leading to earlier onset and faster disease progression.

The association with both familial and idiopathic PD highlights the important role of α-syn in PD pathogenesis. The accumulation of either mutated or misfolded proteins inhibits autophagy and could lead to protein aggregation. Because α-syn protein is most abundant in the brain, for years it was believed that the aggregation seeds start in the brain. However, recent findings suggest synucleinopathies share a lot of similarity with a prion disease based on the observations that, α-syn aggregation can spread from one cell to another. The misfolded species could act as a 'seed' spreading from the gastrointestinal tract all the way up to the brain(Braak et al., 2006) Although the mechanism of α-syn being transmitted between neurons is not entirely clear, several theories exists and are discussed in the following section. Nonetheless, this ties in well with the Braak Staging concept of the disease progression from brain stem to midbrain and up (Braak et al., 2003). And targeting the propagation of the toxic species might be the key to disease treatment at early stages.

1.3. Pathogenic mechanisms of α-syn

Since its discovery in PD, the role of α-syn in the disease has been studied extensively and different pathogenic mechanisms have been proposed. My study

focuses on mitochondrial dysfunction and impaired autophagy induced by α-syn resulting in neuronal dysfunction and neurodegeneration, as illustrated in **Figure 1.1** and further discussed in more details below.

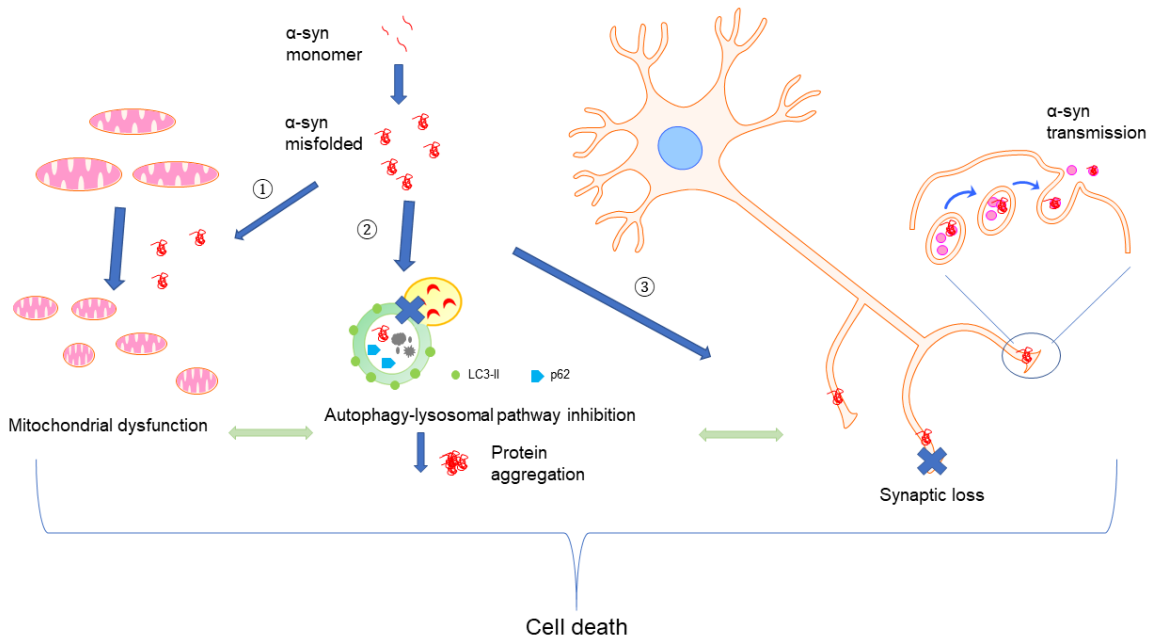

Figure 1.1 Pathogenic mechanisms of α-syn. *When α-syn is misfolded under pathological conditions, this toxic form of the protein would induce 1) mitochondrial dysfunction, 2) autophagy inhibition, and 3) synaptic dysfunction. These three impaired pathways interlink and impact each other, leading to protein aggregation and impaired transmission, and eventually cell death.*

1.3.1. Synaptic dysfunction

The term 'synuclein' originates from the observation of the co-localisation of this protein with both presynaptic terminals and the nuclear envelop, which has been confirmed by subsequent investigations (Yu et al., 2007). Although a certain portion has been found in the nuclear envelop and subcellular organelles, α-syn is mainly cytosolic and predominantly in terminals close to synaptic vesicles. In neurons, the presence of soluble α-syn at pre-synaptic terminals plays an important role in

synaptic plasticity and synaptic vesicle trafficking. It has been proposed that α-syn promotes SNARE complex assembly and regulates transmitter release (Bottner et al., 2015). The absence of α-syn has been shown to induce functional deficits among dopaminergic neurons in mouse model reflected by decreased DA release, whilst overexpression of this protein has also been demonstrated to have negative impact on neurotransmission (Abeliovich et al., 2000, Larsen et al., 2006). Both types of evidence support the theory that α-syn is a negative regulator for neurotransmitter release. However, although α-syn protein aggregation have been extensively characterised, the exact normal physiological function of this protein remains unclear.

1.3.2. Prion theory----α-syn propagation

The theory that α-syn is a prion-like protein is gaining attention in recent years. Although the Braak stage theory remains debatable, the spread of α-syn lesions into different brain regions as PD progresses is observed through post-mortem examinations of patient brains. As characterised by several independent groups, the early stage pathology progresses from caudal to rostral, and in the later stage spreads into limbic and neocortical regions (Braak et al., 2003, Dickson et al., 2010, Parkkinen et al., 2008).

The most direct and strong evidence of α-syn spreading came from post-mortem brain samples of PD patient brains who had gone through embryonic neuron transplantation. Decades after surgery, Lewy body structures were detected in the grafted neurons (Li et al., 2008b, Kordower et al., 2008). This raised the question of what was the mechanism behind the spread of toxic species and would stopping the

spread control disease progression. Ulusoy and colleagues have demonstrated in a rat model that overexpression of human α-syn in the lower brainstem does imitate α-syn pathology in an upward propagation toward rostral regions, in a progressive manner. This long-distance spread recapitulates some disease features, reproducing a PD-like α-syn propagation pattern (Ulusoy et al., 2013).

Cell culture studies have revealed much more detail regarding the process. Emmanouilidou and colleagues have reported that, in cultured SH-SY5Y cells, overexpression of WT α-syn leads to exosome release of the protein, as both oligomeric and monomeric forms are both detected in collected conditional media (Emmanouilidou et al., 2010). On the other hand, nucleation seeds of WT α-syn in the media, once taken up by the cells using transfection reagent, increase intracellular α-syn phosphorylation and protein aggregation (Nonaka et al., 2010).

Several other possible inter-neuronal transmission pathways have also been proposed regarding the 'seeding' of misfolded protein. Apart from exosomal transportation (Danzer et al., 2012), some free-floating protein seeds can also directly travel through the plasma membrane of recipient cells or be taken-up through fluid-phase endocytosis or receptor-mediated endocytosis. Tunnelling nanotubes have also been shown to convey the transport between cells (Abounit et al., 2016). Intriguingly, the transmission has been proved to take place in neuron-to-neuron (Desplats et al., 2009a), neuron-to-astroglia (Lee et al., 2010) and neuron-to-microglia manner (Kim et al., 2013a). The transfer between different cell types highlights the limit of current therapies aimed at targeting dopaminergic neurons alone. Consequentially, a treatment that protects not only this specific cell population could offer greater therapeutic potential.

1.3.3. Protein aggregation and impaired autophagy/lysosome

One of the pathological hallmarks of PD is the formation of Lewy bodies, with α-syn being identified as one of the abundant components. Therefore, it is important to understand the formation of such protein inclusions for better understanding of PD pathogenesis. In cells, two major pathways exist to remove proteins and damaged organelles: the ubiquitin-proteasome system (UPS) which digests proteins through protease hydrolysis and lysosome-autophagy machinery. Both are the major pathways for the clearance of misfolded proteins. The UPS pathway was believed to be the dominant way of α-syn digestion for many years. However, in the past two decades, autophagy, alongside other proteinases including Calpain I, neurosin and metalloproteinases have all be found to be all involved in the protein turnover (Mishizen-Eberz et al., 2003, Kasai et al., 2008, Webb et al., 2003b). Nevertheless, the Greek word ‘Auto-phagy’, meaning self-eating, sums up the degradation system responsible for cleaning up misfolded proteins and dysfunctional organelles inside the cells. Theoretically, the term of autophagy is a collection of three different sub-types: macroautophagy, microautopahgy and chaperone-mediated autophagy (CMA). While in a more general sense, autophagy is commonly used to describe macroautophagy, the most well-characterised type. In this study, I focused on the study of macroautophagy, due to the following reasons: first, the lack of evidence linking microautopahgy and α-syn; second, CMA only degrades monomer and dimer forms of α-syn, and third, above all, macroautuopahgy is the most prevalent form of autophagy. In addition, macroautopahgy has been reported to be impaired by α-syn (Winslow et al., 2010a), which could be potentially linked to α-syn release (Poehler et al., 2014). Macroautophagy (hereafter referred to autophagy), involves targeted

protein/organelles being engulfed by autophagasomes, the cytosolic vesicles that will fuse with lysosome at a later stage to complete the process.

As illustrated in **Fig. 1.2**, autophagy flux involves the nucleation and elongation process of a membrane structure that forms vesicles termed autophagosome. In mammalian cells, this process involves a sequential activation cascade of a series of complexes. One of the main signalling pathways starts with mammalian target of rapamycin (mTOR), the master regulator of cell growth and proliferation. mTOR negatively regulates autophagy by binding the uncoordinated 51-like kinase (ULK)complex and inhibits its function(Hosokawa et al., 2009). Upon certain cellular stress such as starvation, mTOR function is blocked, ULK would then activate the Beclin1/PI3K complex. And this would lead to the membrane nucleation, forming autophagophore. Autophagophore then undergoes the elongation process which involves two important ubiquitin-like conjugations: ATG12 firstly conjugates to ATG5, then binds to ATG16 non-covalently (Kuma et al., 2002); the second is the LC3 cleaved by ATG4 (becoming LC3-I), then conjugates to PE mediated by several proteins including the ATG12-ATG5-AGT16 complex (Walczak and Martens, 2013). Successful elongation leads to the double-membraned autophagosome. The autophagosome then goes on and fuse with lysosomes to form autolysosome, inside which waste proteins, toxins, and faulty organelles will be degraded by the enzymes within the lysosome.

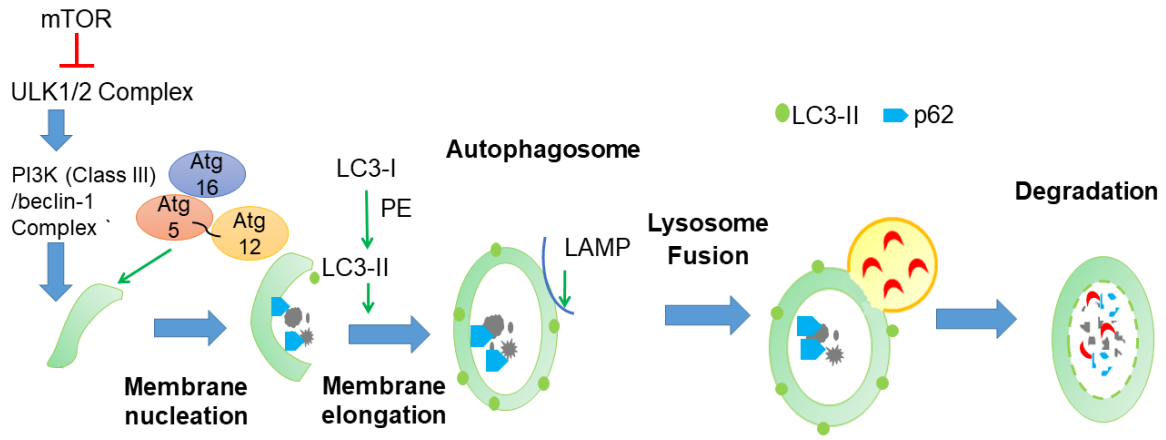

Figure 1.2 Simplified diagram of autophagy flux. *Autophagy process contains three overall steps: autophagosome synthesis (induction), autophagosome-lysosome fusion and cargo degradation (completion). mTOR negatively regulates autophagy, and upon its inhibition, signal is sent to the ULK complex to initiate autophagosome formation. This activates the PI3K (Class III) /beclin-1 complex, which would then generate PI3P for nucleation. Through nucleation, the pre-autophagic structure is formed, which then undergoes elongation. Membrane elongation process involves two ubiquitin-like conjugation complexes: ATG12-5-16L1 and the LC3-PE conjugate (LC3-II). The latter remains on the membrane when autophagosome biogenesis is completed, and therefore is commonly used as a autophagosome marker. Autophagosomes are then shuttled to lysosomes for autophagosome-lysosome fusion. After which lysosomal enzymes degrade the vehicles and cargos including receptor proteins such as p62, releasing amino acids for recycling, and the autophagy flux is completed.*

In yeast, autophagy serves primarily as a starvation response, whilst in higher eukaryotic cells, it is involved in different physiological and pathological processes, and it's dysfunction contributes to pathogenesis of many diseases (Lynch-Day et al., 2012). Autophagy levels vary between different cell types. In neurons, autophagy levels are relatively low yet vital to cellular function, with highly efficient progression from vesicle formation to degradation (Button et al.). Developments of PD pathogenesis research in the past two decades revealed the important role of autophagy dysfunction (Lynch-Day et al., 2012).

It is now well established that α-syn inhibits autophagy (Winslow and Rubinsztein, 2011) through the inhibition of lysosomal function. The same group also demonstrated that α-syn dislocates Atg9, a potent protein involved in autophagosome formation and lysosome trafficking (Winslow et al., 2010a). With two different processes inhibited by α-syn, it is possible that the mechanism might be more complicated than what have been revealed in literature. Nevertheless, the inhibition of autophagy would contribute to an accumulation of misfolded proteins building up leading to aggregation. Additionally, higher levels of α-syn would have a further inhibitory effect upon autophagy, forming the negative feedback loop.

Additional relevance to this study is the observation that autophagy has been shown to modulate the mitochondrial fission protein Dynamin related protein 1 (Drp1) turnover, with autophagy knockdown cells having higher Drp1 levels (Purnell and Fox, 2013). Therefore, in a model where autophagy is reduced, it is possible that there would be a change in the level and activity of Drp1, which potentially could be linked to excessive mitochondrial fission. On the other hand, autophagy has been discovered to be involved in synaptic formation in *Drosophila* (Shen and Ganetzky, 2009). And because of the connections and similarities shared between endosome and lysosome, investigation into autophagy function could potentially find a link with synaptic vesicle trafficking, providing more insights on how α-synuclein interferes with multiple cellular pathways involving double lipid membrane systems.

Mitochondrial autophagy, commonly known as mitophagy, refers to the selective elimination of mitochondria through autophagy. As mentioned previously, upon mitophagy, Parkin are recruited by mitochondrial kinase PINK1 onto depolarised mitochondria, although the mechanism behind this selectivity is not entirely clear, with recent studies showing that PINK1 is capable of inducing mitophagy

independent of Parkin through ubiquitination (Lazarou et al., 2015). Although the exact factors marking the mitochondria for mitophagy remains unclear, enough evidence has shown that this process is selective instead of random. Scorrano *et al* demonstrated that to escape engulfment during autophagy, mitochondria elongates through Protein Kinase A (PKA)-mediated Drp1 inhibition (Gomes et al., 2011), suggesting size is one of the factors. In accordance with this, it is widely acknowledged that fragmented mitochondria being cleared up by mitophagy serves an important role in mitochondria turnover, and this is vital for maintaining a healthy population of mitochondria. Different from normal mitochondrial fission that increases mitochondrial mobility and serves important physiological functions, excessive fragmented mitochondria are linked to mutation and dysfunction, this could be compensated via functional complementation (as discussed in later section) but only to a certain extent. When the threshold is reached, fusion of dysfunctional mitochondria with healthy mitochondria would only have a negative outcome, and therefore their segregation and removal prevent them from contaminating healthy mitochondria. Therefore, it is critical to maintain mitophagy within a certain range that would balance with mitochondrial dynamics and biogenesis, insufficient or excessive amounts would damage the balance. In pathological conditions where there is an excessive amount of mitophagy, whether as a result of mitochondria fragmentation or potentially altered selectivity, this will give rise to a loss of mitochondria, and could eventually leading to cell death (Choubey et al., 2011). Interestingly, on the other hand, in PD models with PINK1 or Parkin deficiency, different laboratories have reported accumulation of fragmented and dysfunctional mitochondria (Cui et al., 2010a, Lutz et al., 2009). Therefore, the key is to maintain a healthy population of

mitochondria through selectively eliminating dysfunctional mitochondria before the ratio of dysfunctional ones reaches a threshold.

α-syn has been shown to induce mitochondrial fragmentation in multiple models *in vitro* and *in vivo,* and different theories have been proposed regarding the involvement of fission/fusion machinery in this process (Kamp et al., 2010, Nakamura et al., 2011, Gui et al., 2012). Fractionation study has confirmed the co-localisation of α-syn with mitochondria (Shavali et al., 2008), and, more recent studies have revealed that α-syn binds to both inner membrane and outer membrane compartments (Robotta et al., 2014, Di Maio et al., 2016) that could potentially interfere with mitochondrial function. Point mutation G51D has been shown to increase membrane binding potential aside from the tendency for aggregation (Fares et al., 2014). α-syn has been reported to preferentially bind to the inner membrane of mitochondria (Kamp et al., 2010, Robotta et al., 2014), which would impact on the cristae structure and therefore mitochondrial respiration. Natural distribution of α-syn does not display specific enrichment on mitochondria, however, cytosolic acidification induced by oxidative or metabolic stress has been shown to significantly increase α-syn translocation onto mitochondria (Cole et al., 2008). Although the purpose of this stress-responsive phenomenon is inconclusive, many studies have shown that increased α-syn translocation is linked to increased mitochondrial dysfunction and mitophagy.

1.3.4. Mitochondrial dysfunction

Mitochondria are well known to be the ‘powerhouse’ of a living cell, yet they serve many other important roles involved in cell function and survival. A good example is

calcium (Ca^{2+}) buffering, which is essential for maintaining the electrophysiological microenvironment. In neurons, the communication between mitochondrial and endoplasmic reticulum (ER) is vital to synaptic function, as has been shown in AD model, the dysregulation of mitochondria with ER is linked to loss of synaptic function, mitochondrial dysfunction, and neuron cell death (Pera et al., 2017). In addition, it is the only organelle inside the cell carrying its own DNA outside nuclei. The mitochondrial DNA(mtDNA) contains about 16,500 base pairs of DNA consisted of 37 genes. 13 out of these 37 encode enzymes essential for oxidative phosphorylation in the electron transport chain complexes. Unlike nuclear DNA, mtDNA does not contain histone and lacks the proof-reading system during replication. As a result, mtDNA is more prone to mutation and damage.

The interest in mitochondrial involvement in PD has been increasing since the MPTP incident, as discussed in **section 1.1.1** (Langston et al., 1983). The active metabolite of MPTP upon oxidation, MPP+, was found to be a mitochondrial complex I inhibitor. As the largest macrocomplex in the electron transport chain (ETC)(illustrated in **Figure 1.3**), mitochondrial complex I has 46 subunits among which 7 are encoded by mtDNA. These 7 hydrophobic units, together with another 7 nuclear-encoded subunits, are believed to form the “minimal essential” catalytical-active composite (Keeney et al., 2006). Impaired catalytic activity of mitochondrial complex I has been identified in various tissues in sporadic PD patients despite the relatively selective cell death of neurons in substantia nigra (Parker and Swerdlow, 1998). Another significance of the finding is that it supported the theory of inheritable mtDNA mutation (Wooten et al., 1997), and the non-Mendelian inheritance pattern displayed could potentially produce a more sporadic occurrence pattern of the disease. Over the years, the role of mtDNA mutation in PD was further explored by

multiple groups (Coxhead et al., 2016, Latsoudis et al., 2008, Hudson et al., 2013, Lin et al., 2012) and mtDNA deletion was also brought to attention by the studies of two separate studies (Kraytsberg et al., 2006, Bender et al., 2006).

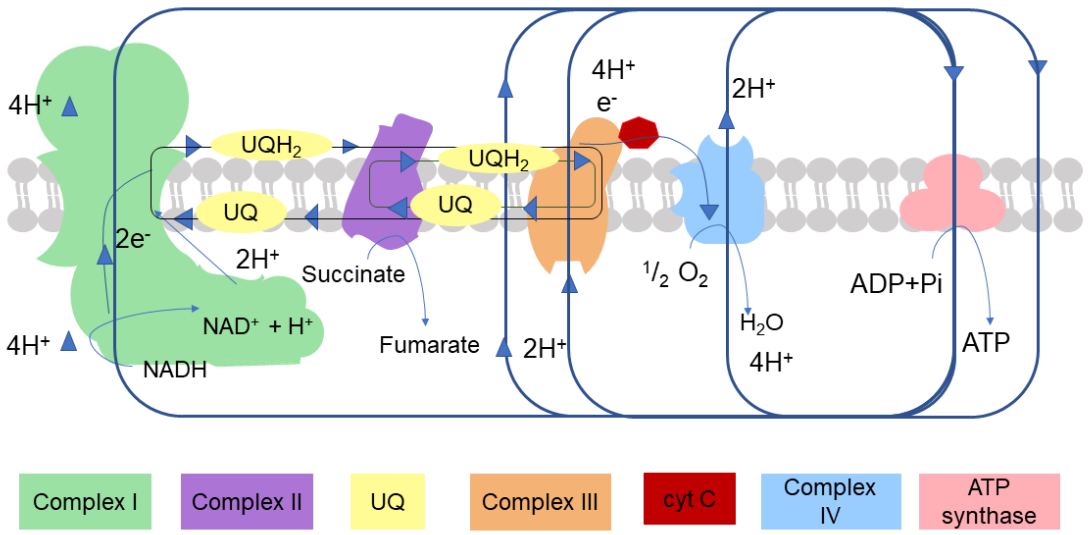

Figure 1.3 Mitochondrial Electron transport Chain. *Mitochondrial electron transport chain consists of five complexes. Complex I: NADH dehydrogenase (NADH-CoQ reductase), Complex II: Succinate dehydrogenase, Complex III: $CoQH_2$-cytochodrme C reductase, Complex IV: Cytochrome C oxidase, and ATP synthase. ATP synthesis is driven by a protonmotive force. The three proton translocating complexes (I, III and IV) act in parallel, generating proton current, whilst complex II reduces UQ to UQH_2 without translocating protons. The proton current is utilised by ATP synthase, proton leak and several secondary processes, completing the proton circuit. ROS is generated as a result of the inability of ETC to completely reduce oxygen to water and the high oxygen consumption at the same time. Inhibition in complex I &III would significantly increase ROS generation and reduce ATP production, as in these situations the 'leakage' of electrons would lead to subsequent oxygen reduction to superoxide.*

Since then a certain group of neurotoxins have been identified to inhibit mitochondrial respiration either through direct (Rotenone) or indirect inhibition (Paraquat). Together with mutations discussed in previous sections, mitochondrial dysfunction is linked to both environmental factors and genetic models of PD,

implicating the common pathways in the disease development of both familial and sporadic PD (Parker et al., 1989, Exner et al., 2012, Helley et al., 2017b).

Over the years, many different groups have investigated how α-syn impairs mitochondrial function and contributes to pathogenesis in different disease models of PD. The mechanisms investigated can be summarised and assigned to three aspects:

I. ETC inhibition;

II. Reduction in mitochondrial biogenesis;

III. Imbalanced mitochondrial fission and fusion.

The first two theories are well known and widely studied, whilst in recent years, there is an accumulation of evidence suggesting altered mitochondrial fission/fusion could be another mechanism.

1.3.4.1. ETC inhibition

The role of mitochondrial ETC dysfunction in PD has been extensively studied since the 1980's, as reduced mitochondrial complex I activity observed in PD patients (Parker et al., 1989, Schapira et al., 1990, Janetzky et al., 1994). Although α-syn is a cytosolic protein, many studies have shown a small fraction of the protein found inside mitochondria, and the binding is enhanced when cytosolic acidity increases (Cole et al., 2008). This small amount of α-syn predominantly resides on inner membrane and has a direct impact on the electron transport chain. In addition, oligomeric forms of the protein has shown to preferentially permeabilise membrane

system modelling mitochondrial membranes rather than plasma membranes (Stefanovic et al., 2014). The accumulation of wild-type α-syn has been reported to be linked to reduced mitochondrial complex I activity, increased ROS production and depolarise mitochondria, especially the misfolded and aggregated forms (Devi et al., 2008, Reeve et al., 2015). Mutations that facilitate protein aggregation, such as A53T, A30P, could possibly accelerate the process. This inhibition effect could relate to toxin inhibition of mitochondria that have been reported previously (Parker et al., 1989, Janetzky et al., 1994, Chinopoulos and Adam-Vizi, 2001, Sherer et al., 2007).

1.3.4.2. Reduction in mitochondrial biogenesis

The peroxisome proliferator-activated receptor-γ coactivator-1α (PGC-1α) is a transcriptional coactivator which regulates energy metabolism. PGC-1α was first found in brown adipose tissue, which showed elevated expression upon cold induction as part of thermogenesis process (Puigserver et al., 1998). Soon after that it was found to stimulate mitochondrial biogenesis through uncoupling protein 2 (UCP-2) and nuclear respiratory factors (Nrfs) (Wu et al., 1999), and is also highly expressed in other mitochondrial enriched tissues such as heart and skeletal muscles (Lehman et al., 2000, Lin et al., 2002). PGC-1α is a master regulator of many cellular pathways including mitochondrial biogenesis. The expression of PGC-1α elevates the expression of Nrf 1 & 2, and PGC-1α would co-activate Nrf1 to trigger the expression of mitochondrial transcription factor A (mt TFA, commonly known as tFam). tFam will translocate from nuclei to mitochondria and activate mitochondrial DNA transcription and replication. In addition, PGC-1α protects mitochondria against oxidative stress by increasing Superoxide dismutase 1 (SOD1) and uncoupling (UCP) proteins.

In 2010, a GWAS study conducted using 6.8 million raw data collected from nine genome-wide expression studiesPGC-1α gene expression was found to be supressed in PD patients, indicating a reduced number of mitochondria. Using an *in vitro* model, they found PGC-1α overexpression to be protective against A53T- α –synuclein toxicity (Zheng et al., 2010). Although it should be noted that PGC-1α is the master regulator of several important pathways, for examples the SOD1 proteins also reduces ROS at cellular level which directly offers protection in many disease models, therefore the benefit of overexpressing PGC-1α cannot be simply credited to the improvement of mitochondrial function alone.

1.3.4.3. Imbalanced mitochondrial fission and fusion

Mitochondrial dynamics (refers to fission, fusion and movement) has been long been suspected to occur and was confirmed in 1990s with the combination of light microscope and fluorescent probes (Bereiter-Hahn and Voth, 1994). In recent years, the link between mitochondrial dynamics and α-syn has become a central question.

Mitochondria are highly dynamic organelles, whose many functions are determined by, and reliant upon, their size, structure and distribution. Increasing evidence suggests that α-syn affects mitochondrial morphology, which is linked to increased mitochondrial fragmentation and mitophagy (Choubey et al., 2011, Xie and Chung, 2012, Gui et al., 2012). These processes would eventually lead up to failure of energy metabolisms and neuronal cell death.

Maintaining mitochondrial morphology largely relies on the balance between fusion and fission. Fusion results in larger mitochondria and promotes energy production, it also rescues stress by sharing mitochondrial components, known as

functional complementation. This is very beneficial toward maintaining mitochondrial function, until the dysfunction reaches a threshold level of 80% (Youle and Van Der Bliek, 2012). Above this threshold, fusion between functional and dysfunction mitochondria results in the contamination of healthy mitochondria with unhealthy once, leading to the loss of function. Fission on the other hand can combat this problem by segregating highly damaged mitochondrial for mitophagy, which is vital toward mitochondrial quality control (Youle and Van Der Bliek, 2012). It is also needed to increase mobility of mitochondria, as it is much easier for shorter mitochondria to be transported to different cellular compartments and during cell division. Together, the fission/fusion dynamics ensures mitochondrial homogenisation(Mishra and Chan, 2014). In addition, the natural balance reached between continuous fission and fusion controls the size and number of mitochondrial tailored to the needs of the cell, determines mitochondrial intracellular connection and distribution. This plays a vital role toward bioenergetics, mitochondrial axonal transport in neurons and apoptosis.

Many different factors can affect mitochondrial fission/fusion, yet a key set of proteins have been identified as regulators for each of the processes, as illustrated in **Figure 1.4.**

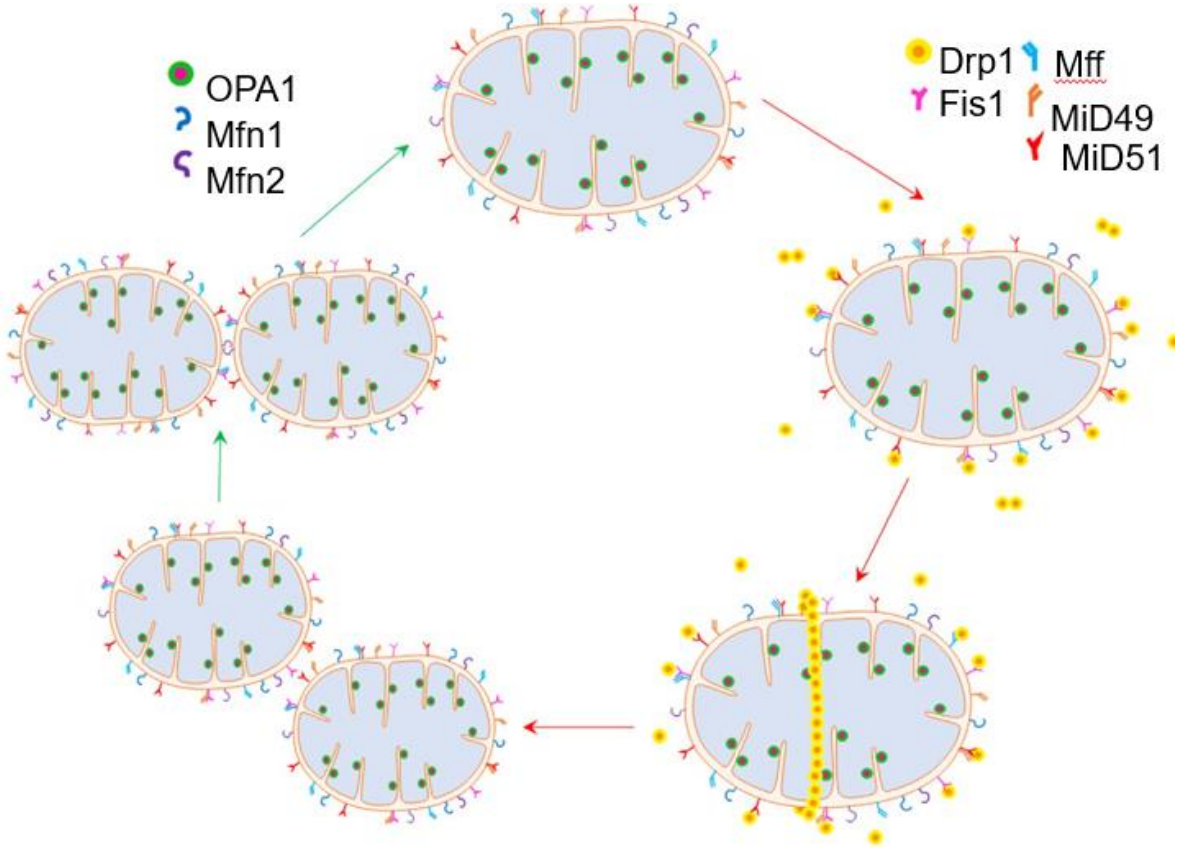

Figure 1.4 Mitochondrial dynamics controlled by mitochondrial fission and fusion proteins *(modified from review paper(Helley et al., 2017b, Tieu, 2014)) Mitochondrial fusion starting with the outer membrane fusion anchored by Mitofusin 1/2 (Mfn1/2), followed by inner membrane fusion mediated by Optic Atrophy 1 (OPA-1). Upon fission, the cytosolic protein Dynamin-related protein 1 (Drp1) is recruited onto mitochondria, a process that can mediated by fission protein 1(Fis1), mitochondrial fission factor (Mff), and mitochondrial dynamics proteins of 49 and 51 kDa (MiD49 /51). All those anchor proteins are located on mitochondrial outer membrane. Through GTP hydrolysis, the GTPase Drp1 forms a oligomeric ring structure that provides restriction force to divide mitochondria.*

In mammalian cells, mitochondrial fusion starts with the outer membrane fusion, mainly controlled by GTPases Mitofusin (Mfn) 1 and Mfn 2, followed by inner membrane fusion, directed by Optic Atrophy 1 (OPA-1). The location of these proteins is reflected by their function. On the other hand, upon fission, cytosolic Drp1 is recruited by Mitochondrial fission 1 protein (Fis 1) and (Mitochondrial fission factor)

MFF, and mitochondrial dynamics proteins of 49 and 51 kDa (MiD49 /51) on the outer mitochondrial membrane and translocate onto mitochondria. Drp1 on mitochondria can assemble into dimers, tetramers and then form into an oligomeric ring-like structure. Drp1 is a GTPase, and GTP hydrolysis provides the main driving force for mitochondrial membrane constriction (Ingerman et al., 2005). As the only non-mitochondrial member among the key fission/fusion machinery, any factors that influence the translocation of Drp1 could effectively alter mitochondria morphology without necessarily changing the protein level or inducing mutation. In addition, Drp1 inhibition has proven to be more effective at blocking Drp1-mediated fission as Fis1 or Mff inhibition does not completely stop Drp1 translocation, especially since the discovery of new anchor proteins Mid49/51 recruiting Drp1 in the absence of Fis1/Mff. (Palmer et al., 2013, Osellame et al., 2016, Palmer et al., 2011), Therefore, Drp1 has been a target for disease models such as neurodegenerative disorders, which involve mitochondrial dysfunction with enhanced fission. Drp1 is the primary target in my study.

Drp1

Drp1 is a cytosolic GTPase involved in mitochondria fission regulation in mammalian cells (its yeast homolog is Dnm1). Drp1 and Dnm1 both contain four functional domains: An N-terminal GTPase domain, a dynamin-like middle domain, Insert B domain, and a GTPase effector domain (GED) located at the C-terminal.

Figure 1.5 Functional domains of Drp1 protein *Drp1 contains four functional domains. The N-terminal GTPase domain (responsible for GTP hydrolysis during mitochondrial fission), the middle domain supports GTPase domain function, insert B/variable domain, and the C-terminal GTPase effector (GED) domain is essential for intra- and intermolecular domain interactions of Drp1, stimulating GTPase activity.*

The GTPase domain is responsible for GTP hydrolysis and self-assembly of Drp1. As GTP hydrolysis results in Drp1 spiral decrease, this is generally considered to provide the driving force for mitochondria constriction during fission. The middle domain works together with the GTP domain which modulates intramolecular and intermolecular interactions of Drp1 proteins, enabling them to assemble into dimers, tetramers and higher structures. A dominant negative missense mutation A395D reported in a human case study has shown to interrupt mitochondrial fission, and *in vitro* investigation revealed that although they retained the ability to form tetramers, the A395D Drp1 failed to form higher structures and subsequent stimulation of GTPase activity. Moreover, Chang et al demonstrated that this mutation impairs the ability of the protein to co-localise onto mitochondria (Chang and Blackstone, 2007). The new-born who carried this mutation displayed abnormal brain development, optic atrophy, and dead at 37 days of age. Fibroblasts deprived from the patient displayed elongated mitochondria morphology (Waterham et al., 2007). The insert B domain is known as the variable domain, as it is less conserved among organisms. The exact function of this domain is not entirely clear, it's known that Drp1 binds to

cardiolipin via GTPase domain, and Sesaki *et al* proposed that this insert B domain could provide specificity for the sites of Drp1-mitochondria binding during apoptosis (Sesaki et al., 2014). In addition, researchers have discovered that Drp1 is a substrate for reaction with nitric oxide (NO) species, and a recent study has shown MPP+ treatment elevates Drp1 level and it's pro-fission phosphorylation at Ser616, both linked to NO production (Zhang et al., 2016).

Post translational modifications of Drp1 and mitochondrial fission Unlike other key fission/fusion proteins, Drp1 is primarily a cytosolic protein with only approximately 3% colocalising with mitochondria as revealed by a percoll gradient fractionation study (Smirnova et al., 2001a). However, this small fraction on mitochondria is responsible for controlling mitochondrial fission, and factors regulating Drp1 distribution such as post translational modifications affect Drp1 function and have an important impact on mitochondria fission.

Phosphorylation One of the phosphorylation sites of Drp1 is Serine 367 in the GED domain (Chang and Blackstone, 2007). This phosphorylation by cyclic AMP-dependent protein kinase (PKA) reduces Drp1 GTPase activity by blocking intramolecular interaction, and reducing Drp1 translocation onto mitochondria.(Chang and Blackstone, 2007). In addition, the overexpression of a phospho-mimetic mutation S637D resulted in elongation of mitochondria (Cereghetti et al., 2008). Yet this elongation effect is less prominent than the overexpression of a well characterised mutation K38A, which depletes GTPase activity to undetectable levels (Chang and Blackstone, 2007). S367 phosphorylation is reversed by calcineurin, a Ca^{2+}-dependent phosphatase, which facilitates Drp1 translocation onto mitochondria.

In contrast to S367 phosphorylation, Erk-mediated phosphorylation at Serine 616 increases Drp1 translocation onto mitochondria and facilitates mitochondrial fission. This phosphorylation has been shown to be induced upon cold exposure or by oncogene Ras in cancer models. Interestingly, when researchers tested its mimetic mutation S616D, GTPase activity was not affected and mitochondrial morphology remained normal. This is the outcome of unaltered GED domain interactions with GTP-binding/middle domain, suggesting Ser616 phosphorylation affects Drp1 function through other mechanisms (Taguchi et al., 2007). Other post-translational modifications include: ***SuMOylation,*** which is a transient and reversible process led by an enzyme belongs to the ubiquitin family called small ubiquitin-like modifier 1 (SUMO 1). Prudent and colleagues have discovered that MAPL-dependent SUMOylation stabilises Drp1oligomeric assembly on mitochondria during apoptosis (Prudent et al., 2015). ***Ubiquitination*** is generally considered as a protein interaction motif that targets protein for proteasome degradation. Parkin, the E3 ubiquitin ligase involved in mitochondrial autophagy (mitophagy), has been shown to promote Drp1ubiquitination for proteasomal degradation (Wang et al., 2011a). ***S-nitrosylation*** refers to the reversible process of NO forming S-nitrosothiols (SNO) with cysteine residues of target proteins through redox reactions. Reactive nitrogen species (RNS) is one of the main sources of oxidative stress commonly seen in neurodegenerative diseases. Cho and colleagues have demonstrated, in an AD model, the role of s-nitrosylation of Drp1 on β-Amyloid linked neuronal injury linked to mitochondrial fission (Cho et al., 2009a).

Apart from regulating mitochondrial fission as part of fission/fusion machinery, another function of Drp1 is in apoptosis. Mitochondrial fragmentation is one of the features for apoptosis. As in healthy cells, functional mitochondria elongate through

increased Drp1 inhibition at Ser637 to bypass mitophagy (Gomes et al., 2011), whilst the fragmented ones are engulfed by autophagy machinery. Upon apoptosis, however, Drp1 translocates onto mitochondria binding to Bax, inducing Bax/Bak-mediated mitochondrial membrane permeabilisation and triggering cytochrome c release.(Cassidy-Stone et al., 2008). Moreover, a recent study has shown that through MAPL SUMOylation, Drp1 also stabilises ER/mitochondria contact and signalling, facilitating Calcium flux and remodelling of cristae structures required by programmed cell death(Prudent et al., 2015)

In short, any dysregulation in Drp1, whether through expression, post-translational modification, or other mechanisms that impact protein distribution and/or activity, would disrupt mitochondrial homeostasis, and further impact cell function and viability.

Role of Drp1 and mitochondrial dynamics in neurodegenerative diseases

Compared to other cell types in the brain, neurons are more susceptible to mitochondrial deficits due to their high energy demand, complex cell morphology and specialised functions including synaptic activity. Synaptic loss occurs before cell death and is now recognised as early event in neurodegenerative disorders including PD. Synaptic formation and plasticity are linked to Ca^{2+} buffering and ATP production by mitochondria being transported to the terminals.

Drp1 is essential for synaptic formation both *in vitro* and *in vivo* (Ishihara et al., 2009, Li et al., 2008a), however hyperactivation of Drp1 has been shown to induce neuronal damage (Nakamura et al., 2010). Indeed, aberrant mitochondrial dynamics has been observed in different neurodegenerative disease models PD, Alzheimer's

disease (AD), and Huntington's disease (HD) and Amyotrophic Lateral Sclerosis (ALS) (Cho et al., 2009b, Burte et al., 2015). Excessive fission associated with Drp1 has been implicated in both cell culture and animal models of PD (Filichia et al., 2016b, Rappold et al., 2014, Wang et al., 2011b, Cui et al., 2010a, Bido et al., 2017b), AD (Wang et al., 2009, Manczak et al., 2011), HD (Shirendeb et al., 2011, Song et al., 2011, Manczak and Reddy, 2015), and ALS (Song et al., 2013, Xu et al., 2010).

In PD, studies have been done in both genetic mutations and environmental toxin models targeting Drp1. For instance, *in vitro*, our laboratory described in a PINK 1 mutation model the protective effect of blocking Drp1 with the putative inhibitor mdivi-1, Drp1-knockdown and dominant negative (K38A) transfection (Cui et al., 2010a). Qi and colleagues applied a Drp1 peptide inhibitor P110 to demonstrate the protection against MPP^+ (Qi et al., 2013b).

There are also emerging *in vivo* studies showing neuroprotection offered by inhibition of Drp1. Our laboratory reported in 2014, as a follow-up study to the *in vitro* work, blocking Drp1 showed significant protection in both PINK1-/- and MPTP mice(Rappold et al., 2014)

α-syn and mitochondrial dynamics, is Drp1 the key? Some studies have shown that α-syn induces mitochondrial fragmentation, although several different theories exist regarding the process. Using model membrane system, Kamp and co-workers reported that α-syn inhibits membrane fusion. Co-expression of wild-typ PINK1, wild-type parkin, wild-type DJ-1, but not the mutations linked to PD, showed protection (Kamp et al., 2010).The authors claimed the fragmentation is independent of the

fission/fusion machinery, despite the fact that they observed less fragmentation induced by α-syn when promoting fusion or inhibiting fission. In 2011, Nakamura and colleagues raised the theory that α-syn drives mitochondrial fission through direct interaction with mitochondrial membrane. In a similar vein as the previous study, they reached the conclusion that this is independent of Drp-1 mediated fission even though they reported less mitochondrial fragmentation with Drp1-K38A transfection.(Nakamura et al., 2011). A year later, Gui et al showed that α-syn induced mitochondrial fragmentation is linked to Drp1 through ERK pathway, and blocking Drp1 was protective(Gui et al., 2012).

Drp1 has been studied in many different disease models and has become a topic of great interest for targeting mitochondria fission, as blocking Drp1 is the more direct and efficient way. This is because Fis1, Mff and MiD49/51 are receptor proteins that act as anchor proteins for Drp1 recruitment (Osellame et al., 2016, Palmer et al., 2013). Blocking Drp1 function is upstream of these proteins and therefore more efficient.

Although debate remains whether blocking Drp1 acts protectively through mitochondria in α-syn models. Previous studies proposed that α-syn induced mitochondrial fragmentation independent of fission/fusion machinery (Kamp et al., 2010, Nakamura et al., 2010). However, these investigators failed to discuss that there was a clear attenuation in fragmented mitochondria induced by α-syn in cells with Drp1 inhibition compared to those overexpressing α-syn alone (Kamp et al., 2010). In contrast to the above studies, other laboratories reported that mitochondrial fragmentation induced by α-syn is mediated by Drp1 (Gui et al., 2012, Choubey et al., 2011) . In collaboration with another laboratory, we recently reported that blocking Drp1 using mdivi-1 is highly protective in a rat model of α-syn-A53T

mutation (Bido et al., 2017c). We demonstrated that mdivi-1 attenuated neurodegeneration, protein aggregation and locomotor impairment. However, some critical questions remained from that study. First, mdivi-1 was used to block Drp1 function (Bido et al., 2017a). Although this inhibitor has been widely reported to produce effects consistent with blocking mitochondrial fission and GTPase function of Drp1 (Smith and Gallo, 2017b, Manczak et al., 2019), questions have been raised whether this inhibitor blocks Drp1 function (Bordt et al., 2017a). Second, α-syn-A53T mutation was used to model PD. Given that this missense mutation is rare and responsible for a very small fraction of PD cases, the significance of that study in relation to sporadic PD needs to be validated in models with wild-type (WT) human α-syn. Third, to date, Drp1 is commonly referred to as a “mitochondrial fission” protein. However, as mentioned previously, most of Drp1 resides not on mitochondria, but elsewhere in the cell. Indeed, a previous study estimated that only about 3% of Drp1 is localized to mitochondria under normal physiological condition (Smirnova et al., 2001b). Although under pathological condition, post-translational modifications such as phosphorylation of Drp1 at S616, would induce its translocation to mitochondria, a significant portion most likely still remains in the cytosol. It is critical to investigate additional protective mechanisms of this protein. My project was designed to address these three issues

1.4. Project hypothesis and aim

Rationale: It is well established that mitochondrial dysfunction plays a role in PD. α-syn point mutation and overexpression are both linked to mitochondrial dysfunction, which contributes to synucleinopathy. Despite being the first protein identified to be associated with PD and therefore being studied for many years, a great deal remains to be understood regarding how α-syn impairs mitochondria function. As discussed in the introduction, several mechanisms have been proposed regarding how α-syn mutation/overexpression facilitates PD formation. However, these pathways are not mutually exclusive, and one key element that potentially links all these mechanisms together is mitochondrial function (Helley et al., 2017b), as illustrated in **Fig.1.6** below. Understanding how α-syn leads to mitochondrial dysfunction could have high clinical potential.

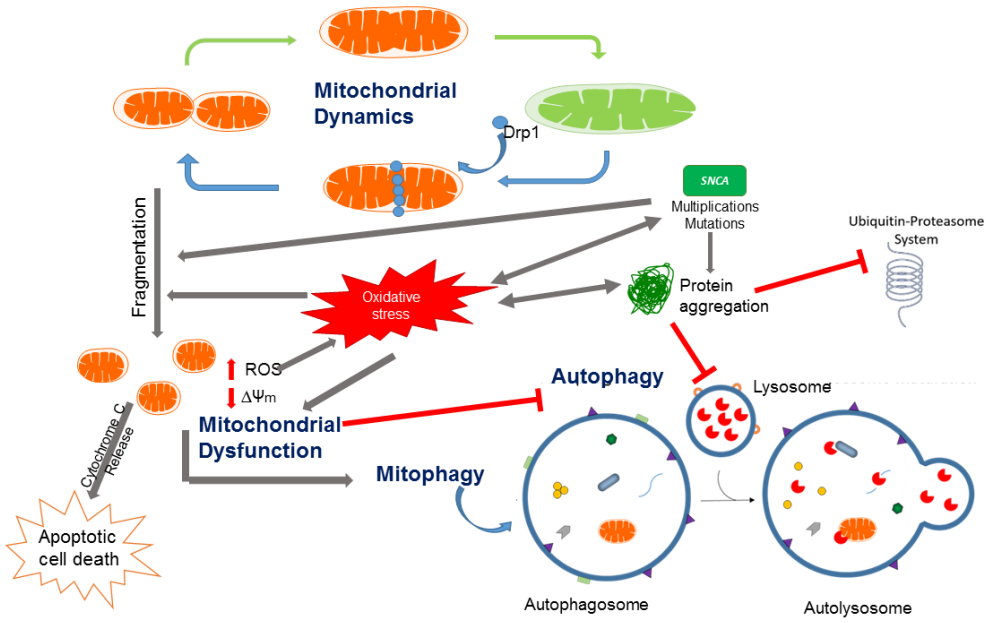

Figure 1.6 Common pathogenic mechanisms induced by *α-syn* .
Mitochondrial dysfunction, induced by α-syn multiplications or mutations, results in a cascade of interconnected cellular dysfunction. Increased mitochondrial fission and fragmentation can initiate apoptotic cell death by inducing cytochrome C release. ATP-dependent processes such as autophagy would be impacted, resulting in reduced autophagic clearance of damaged proteins and organelles. This process is also sensitive to ROS. The multiplications and mutations of α-syn can also lead to increased ROS, which has the capacity to promote the formation of toxic oligomers and protein aggregates, impair ubiquitin proteasomal system function. ROS can also impair mitochondrial function, which in turn produces high mitochondrial ROS and further increases oxidative stress. In addition, increased ROS facilitates protein aggregation which further inhibits autophagy and Ubiquitin-Proteasome system. As illustrated, all these mechanisms cross-talk and culminate in neurodegenerative processes in PD. (Modified from (Helley et al., 2017b)

The overall hypothesis of this project is that α-syn overexpression induces mitochondrial fragmentation and dysfunction through excessive fission, results in oxidative stress, impair autophagy flux, and protein aggregation. Furthermore, blocking Drp1 is protective.

The following three aims were designed to test this hypothesis:

1. Determine the effects of α-syn on mitochondrial morphology and function, oxidative stress, protein aggregation and autophagy mediated through mitochondrial fission.

2. Evaluate the effects of blocking Drp1 on mitochondrial fragmentation and dysfunction induced by α-syn.

3. Assess the impact of Drp1 inhibition on autophagic impairment and accumulation of aggregated protein induced by α-syn.

.

2. Materials and Methods

2.1 Experimental models

Several cell lines were selected in this study to address specific questions, a rat model is also used for investigating synaptosome function as part of a related project. All models discussed in this thesis are summarised in the table below:

Table 2.1 Summary of different experimental models used in this study

Model	Origin	Purpose	Reference
N27 cells with inducible human α-syn expression	E12 rat mesencephalic tissue, immortalised with SV40 vector. Inducible cell line was generated by stable transfection of ecdysone inducible system containing *SNCA*	Study the effects of α-syn expression over time in a more controlled manner	N27 cell line (Prasad et al., 1994) Inducible system method (Cui et al., 2010a)
Luhmes cells	human mesencephalic-derived cell line MESC2.10. immortalized with v-myc retroviral vector.	complementary model for rat dopaminergic cells	(Lotharius et al., 2002)
HeLa autophagy reporter cells	Derived from cervical cancer cells of Henrietta Lacks	Monitor autophagy flux by providing autophagosome and autolysosome levels	HeLa cell line (GEY, 1952)
Sprague Dawley rats	An outbred multipurpose breed of albino rat, first came from Sprague Dawley farms in 1979	As an in vivo model for studying the effect of α-syn via AAV-delivery. Rats provide more striatal synaptosomes than mice.	(White WJ, 1998)

N27 cells with inducible human α-syn expression. Inducible α-syn expression cell line was generated by stably transfecting rat dopaminergic neural cell line N27 with ecdysone inducible system (Agilent, Complete Control Inducible Mammalian Expression System) containing human α-syn (see **Figure 4** below) in the same manner as described in our previous publication (Cui et al., 2010a). α-syn inducible expression is stimulated by the addition of Ponastrone A (PonA), an ecdysone homolog compound.

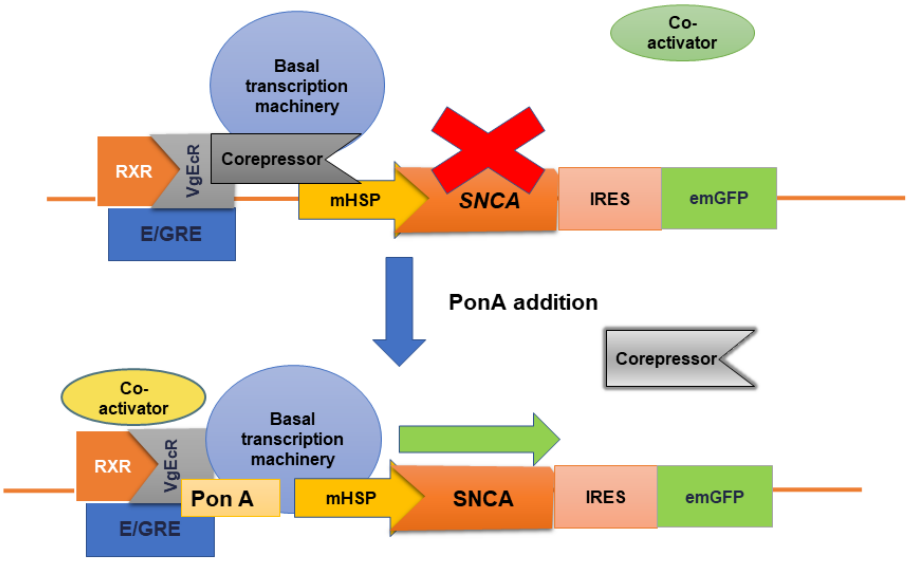

Figure 2.1 Inducible expression of human α-synuclein in rat dopaminergic N27 neuronal cells. *The expression of SNCA is suppressed by co-repressors at VgEcR. Upon PonA induction, co-repressors are released, and coactivators are recruited, resulting in gene activation via the minimal heat shock promoter (mHSP).*

The ecdysone-inducible system consists of two vectors: the receptor vector pERV3 and the expression vector pEGSH modified from The Complete Control® Inducible Mammalian Expression System (Stratagene, LaJolla, CA). As illustrated in **Fig. 2.1**, the pERV3 vector contains an expression cassette from which the VgEcR and RXR proteins are constitutively expressed, and a neomycin-resistant gene for selection.

The pEGSH vector is inserted with the gene of interest, and in this case, *SNCA* (gene encoding α-syn), which is controlled by PonA-inducible expression cassette. Cells were firstly transfected with pERV3 receptor vector, selected by the addition of G418, and cells stably expressing pERV3 were then transfected with pEGSH vector containing full-length human SNCA gene and selected with Hygromycin B.

To select cells with high expression of α-syn, stable cells were incubated with SMARTFLARE human SNCA-Cy3 mRNA probe (Millipore, SF-1254) overnight. This non-toxic probe was taken up by living cells through endocytosis, it recognised and bound to α-syn mRNA produced inside the cells. And when this occurs, the fluorescence quenching sequence was released and Cy3 signal was activated. For sorting, cells were treated with PonA (or ethanol as control) for 24h, with probe (200nM) added 16h prior to sorting. On the day of sorting, cells were trypsinised, centrifuged (X1000g, 3min) to pellet, and re-suspended in sorting buffer containing PBS+1%FBS+20U/ml DNase I + 25mM HEPEs (1ml sorting buffer were used for 2-3million cells). The suspension was then run through a cell strainer snap cap with polystyrene tube attached (BD Falcon™ 352235) by gravity. The tube was then carefully loaded to a FACSAria II, and sorted using FACS Diva 6.1.3 software channel PE-A. Two cell populations were collected: P1 (small fraction of cells with high α-syn expression) and P2 (larger inducible population with lower α-syn expression). Cells were collected in a tube pre-loaded with 1ml RPMI+20%FBS. The collected solutions were diluted into 10ml RPMI+20%FBS+P/S, span for 5min at 1000rpm, and the pellets were then re-suspended in RPMI+20%FBS+P/S, transferred into a T25 tissue culture flask, incubated at 37°C overnight to attach. At least 48hrs were allowed for cells to recover before being changed back to complete medium. Inducible cells were labelled by human α-syn mRNA, as SMARTFlare live

mRNA probes (Millipore) tagged with Cy-3 that specifically recognises human α-syn mRNA were used. Probe up-take was confirmed by confocal microscopy with phase contrast (shown in **Fig 3.1**)

Cells were maintained in RPMI 1640 +10% FBS+G418 (500µg/ml) + hygromycin B (200µg/ml) (complete medium). α-syn expression upon PonA induction was confirmed by immunostaining and western blot. The level was characterised at different time points with different PonA doses for comparison (see result section), with 20µM PonA and 48h chosen for the assessment of mitochondria morphology and function.

N27 cell differentiation development. To test whether the N27 cells could be differentiated into functional dopaminergic neurons, a few differentiation conditions were tested by adding different concentrations of Dibutyryl cyclic-AMP (dbcAMP, Sigma) and/or DHEA (sigma). Cells were differentiated up to 5 days, during which time the survival and morphology of the cells was tracked, and light contrast pictures were taken using a Leica microscope (see Appendix). The expression of synaptic markers (synapsin 1 and PSD 95) were tested using immunocytochemistry.

LUHMES cells. The Lund human mesencephalic LUHMES cell line (ATCC® CRL-2927™) were purchased from Millipore. It is a subclone of the tetracycline-controlled, v-myc-overexpressing human mesencephalic-derived cell line MESC2.10. Differentiated LUHMES cells expresses mature dopamine-like neuron features both morphologically and biochemically.

Cells were maintained in complete growth media containing DMEM/F-12 +1% N-2 supplement (Gibco-Invitrogen 17502-048) + 40 ng/ml b-FGF (basic recombinant human Fibroblast Growth Factor; Gibco-Invitrogen 13256-029), with b-FGF always added fresh right before use. All cell culture surfaces were sequentially pre-coated with 50 µg/mL poly-L-ornithine at room temperature overnight (Sigma, P-3655), and then with 1 µg/mL Human Fibronectin (Sigma, F-0895) at 37°C for 3 hours. Three rinses with ddH_2O were used in between to wash away excessive coating reagents, and all surfaces are left in hood to dry. Coated cell culture vessels were either used right away or stored in fridge (4°C) for up to a week before used. Cells are subcultured every 2-3 days.

For differentiation, bFGF in complete growth medium were replaced with tetracycline (1µg/ml, diluted 1:1000 from 1mg/ml stock), GDNF (glial cell line-derived neurotrophic factor, 2ng/ml, diluted 1:1000 from 2µg/ml stock), and db-cAMP (1mM, diluted 1:100 from 100mM stock). Cells were differentiated up to 10 days and were plated for experiment at Day 2 of differentiation to control the cell number.

HeLa autophagy reporter cells. A stable autophagy-monitoring cell line generated from Hela cells was kindly provided by Dr Shouqing Luo (Plymouth University). These cells were stably transfected with ptfLC3 plasmids, expressing rat LC3 fused to mRFP and EGFP (addgene) as indicators for autophagy flux. Stable cells were maintained in DMEM + 10%FBS + G418 (100µg/ml) + 1%P/S (Penicillin/Streptomycin).

2.2 Cell transfection and treatments

Plasmid transfection. For all cell lines culture experiments apart from the LUHMES cells, plasmid transfections were carried out using either Lipofectamine 3000 or jetPRIME™ DNA and siRNA Transfection Reagent (Polyplus transfection), optimised following the guidance of manufacture's protocol. For 24-well plate, 0.3ug of plasmid were used and for 6-well plate 0.75ug plasmid were used per well.

For lipofectamine transfection, an equal volume of Opti-MEM was used to mix with DNA plasmid and Lipofectamine Reagent, incubated 5min separately before being mixed together for another 15min of incubation. The mixture was then added to cells (in Opti-MEM) in a dropwise motion. 200µl of Opti-MEM complex was added per well for 6 well plates and 50µl for 24 well plates.

For the jetPRIME system, plasmids were diluted into jetPRIME Buffer (50 µl for 24 well plate and 150 µl for 96 well plates), followed by 10s of vortexing to mix and a quick spin to collect everything at the bottom. Then jetPRIME Reagent (2X of plasmid amount v/w) was added to the complex, mixed by vortexing and incubated at room temperature for 15min. The complex was then added in a dropwise motion to cells maintained in normal culture media without antibiotics.**Drp1 knockdown (siRNA).** Pre-designed siRNA against rat *dnm1l* and human *DNM1L* (gene encoding Drp1) were purchased from Dharmacon Research, Inc. SMARTpool: siGENOME Rat *Dnm1l* siRNA was used for the N27 cells and SMARTpool: siGENOME Human *Dnm1l* siRNA was for HeLa cells. Each of this product is a mixture of four individual siRNA duplexes that target four separate sequences of the gene to maximize efficiency of gene silencing. To enhance transfection efficiency, an "in-tube" transfection procedure (Cui et al., 2010b) was used with the following modifications: Cell suspension (80,000-100,000cells/ml) were mixed with jetPRIME™ DNA and siRNA Transfection Reagent (Polyplus-transfection®SA). For every 500µL of cell suspension (RPMI +10% FBS), 50

µL of jetPRIME buffer and 2 µL jetPRIME reagent were used. Cells were plated and left in transfection medium overnight, then media was changed the following day. Gene silencing efficiency was confirmed using western blot, with 10nM of siRNA achieving 75-90% knockdown compared to scrambled control (siGENOME Non-Targeting siRNA Control Pools, Cat# D-001206, Dharmacon Inc) after 48h.

Mdivi-1 treatment. For blocking mitochondrial fission through pharmacological approach, the putative Drp1 inhibitor 3-(2,4-Dichloro-5-methoxyphenyl)-2,3-dihydro-2-thioxo-4(1H)-quinazolinone (mdivi-1) was applied. mdivi-1 (stock prepared in DMSO) was diluted in cell culture media to a working concentration of 10 µM.

2.3 Cell viability assessment

MTT cell viability assay. Cells were plated in 96-well plate at 5000/well-10,000/well depending on the treatment time and incubated overnight for attachment. Cells were treated with PonA the next day and incubated for up to 72h. On the day of assay, 25µl of MTT (3-(4,5-Dimethylthiazol-2-yl)-2,5-Diphenyltetrazolium Bromide) was added into each well, incubated in the dark at 37°C for 3 hours, followed by the addition of 100µl of MTT lysis buffer. The plate was then left overnight for the crystals to dissolve. Plate reading was done the following day after confirming that all the crystals were dissolved, and optical density at 562nm was measured using a Genois one plate reader.

Calcein AM cell viability assay Calcein, AM (Invitrogen,1mg/ml in DMSO) was purchased from Thermo Fisher Scientific. . Working solution (2µg/ml) was made up

in PBS each time prior to experiment. N27 cells were grown in flat bottom 96-well plates. Upon assay, cells were washed with warm dPBS by replacing half the volume of media with dPBS and leave 50µl PBS in each well.100µl Calcein solution was then added to each well and the plate was incubated in dark at room temperature for 1 h. Fluorescence signal was quantified using Synergy H1 Hybrid Reader (Ex/Em 494/520).

.

2.4 Immunostaining, Imaging and Immunoblotting

Immunofluorescence. For imaging, cells were grown on borosilicate cover slips pre-coated with poly-D-lysine (0.1mg/ml in PBS, at room temperature overnight). The plating density varied between 50,000 and 100,000, depending on different treatment time points. Upon fixation, cells were incubated with 4% Formaldehyde (Thermo Scientific™ Pierce™ 28028, 1 in 3 diluted into warm cell culture media from 16% solution) at 37°C for 20 min. The fixative was then washed away by 3 x 5min washes with PBS, after which the samples proceed to blocking with PBS containing 4% normal goat serum and 0.1% Triton-X. Samples were incubated with primary antibody solution (please refer to **Table 2.2** for a list of antibodies and dilutions used) overnight at 4°C on a slow shaker. The next day, primary antibodies were recycled. Samples were washed with 3 x 5 times PBS, followed by secondary antibody solution containing Alexa Fluor® (350/488/586/633) conjugate secondary antibody (Molecular Probes) (1:500 -1:1000 dilution) + 2% normal goat serum in PBS incubation at room temperature for 1h in the dark. Secondary antibodies were washed away with PBS, and slides were mounted with Prolong™ gold anti-fade mountant with or without DAPI (Molecular Probes). Regular epifluorescence imaging was done by Nikon Eclipse TE2000-U Fluorescent microscope. Confocal images

were captured with Leica LAS SP8 or Olympus FV-1200 confocal microscope (software FV10-ASW Version 4.3) with 60X Objective. All images were exported in TIFF format and analysis were done using Image J.

Table 2.2 Primary and secondary antibodies used in immunostaining

Marker	Primary antibody-species and dilution	Company and catalogue number	Secondary antibody species and dilution	Company and catalogue number
α-synuclein	1:500 Mouse monoclonal,	BD Biosciences, #610787	1:1,000, Goat anti-Mouse IgG (H+L) Highly Cross-Adsorbed Secondary Antibody	Life Technologies, Alexa Fluor #A11029 or #A11031 or #A11045
Drp1	1:500 Mouse monoclonal,	BD Biosciences, #611113	1:1,000 goat Goat anti-Mouse IgG (H+L) Highly Cross-Adsorbed Secondary Antibody	Life Technologies, Alexa Fluor #A11031 or #A21052
α-synuclein	1: 2000 Rabbit polyclonal ,	EMD Millipore (Millipore Sigma) #AB5038	1:1,000 Goat anti-Rabbit IgG (H+L) Highly Cross-Adsorbed Secondary Antibody	Life Technologies, Alexa Fluor #A11034
p62	1: 500 Rabbit polyclonal (SQSTM1)	MBL International Corporation #PM045	1:1,000 Goat anti-Rabbit IgG (H+L) Highly Cross-Adsorbed Secondary Antibody	Life Technologies, Alexa Fluor #A21071

HA	1:300 Mouse monoclonal (12CA5)	Roche #11 583 816 001	1:500 Goat anti-Mouse IgG (H+L) Highly Cross-Adsorbed Secondary Antibody	Life Technologies, Alexa Fluor #A11045
TOM20	1:1000 Rabbit polyclonal	Santa Cruz	1:1,000 Goat anti-Rabbit IgG (H+L) Highly Cross-Adsorbed Secondary Antibody	Life Technologies, Alexa Fluor #A11011
TH	1:1000 Mouse monoclonal	Sigma #T2928	1:1,000, Goat anti-Mouse IgG (H+L) Highly Cross-Adsorbed Secondary Antibody	Life Technologies, Alexa Fluor #A11029

Transmission electron microscopy (TEM) Cells used for TEM imaging were grown in tissue culture treated 6-well plates and treated with PonA. Upon harvesting, cell culture media was aspirated and cells were washed briefly with 2 ml of pre-warmed wash buffer (0.1 M sodium cacodylate, 0.1 M sucrose, 3 mM CaCl2).Then wash buffer was replaced with 2ml pre-warmed fixative (2.5% glutaraldehyde in 0.1 M sodium cacodylate, 0.1 M sucrose, 3 mM CaCl2), plates were incubated at RT for 20min, followed by 4°C incubation for an additional 1h40min. Cells were then quickly rinsed with wash buffer, and scraped off of the culture surface into 1ml fresh wash

buffer per well. Collected cells were then transferred into a 1.5ml Eppendorf protein low-bind tube centrifuged at 2000 x g for 5 min (note: It's very important to use low-bind tubes in order for fixed cells to pellet properly). Wash buffer was then replaced with 1 mL 1% osmium tetroxide in 0.1 M sodium cacodylate and incubated at RT for 1 h. The pellet was then washed 2 x 10 min in 0.1 M sodium cacodylate and 1 x 10 min in dH2O. After which cells were sequentially dehydrated in an increasing concentration of ethanol (30%, 50%, 70%, 90%, 3 x 100%) for 10 min each. Cells were then gradually infiltrated with increasing concentrations of resin (30%, 50%, 70%, 2 x 100%), diluted in 100% ethanol, for at least 5 hours per concentration.

Samples were then polymerised within their original 1.5 mL tubes for 12 hours at 60 °C. Polymerised samples were then sectioned at 70 nm on ultra-microtome and subsequently stained with 0.5% uranyl acetate and 3% lead citrate. Processed samples were imaged with JEM-1400 TEM (From polymerisation every step was conducted at Plymouth University Electron Microscopy Centre, by Dr. Martin Helley and Jay Rees).

Western Blot. Cultured cells were rinsed in PBS and then scraped off and collected in 1.5ml or 2ml Eppendorf tubes. The tubes were then centrifuged at 1000g for 3min, after which the supernatant was discarded, and pellets were either frozen down in -80°C or processed immediately. For total cytosolic fraction, cell pellets were re-suspended in RIPA buffer containing 1X Halt Protease and Phosphatase Inhibitor (Thermo Scientific), 75µl of buffer was used for a confluent T25. The suspension was then transferred to a 1ml glass homogeniser, dounced for 20 -30 times, and collected in 1.5ml Eppendorf tubes. The tubes were then centrifuged at 13,000rpm for 15 min at 4°C. Supernatants were collected for protein estimation using

bicinchoninic acid assay (BCA assay). Samples were mixed with 2X or 6X Laemini buffer, boiled at 98°C for 5-8min, and run through 12% or 15% Tris-bis gel (tris-glysine system by Bio-rad), with 30-45ug of protein loaded into each well depending on the abundance of the target protein. Samples were then transferred to a PVDF membrane and probed with antibodies as listed in **Table 2.3** below:

Table 2.3 Primary and secondary antibodies and dilutions for western blot.

Marker	Primary antibody-species and dilution	Company and catalogue no.	Secondary antibody	Company	Dilution
α-synuclein	Mouse monoclonal 1:1000	BD 610787	Goat anti-mouse/ rabbit HRP conjugated secondary antibody Or IRDye 800CW goat anti-mouse /IRDye 680RD goat anti-rabbit secondary antibody	Bio-rad/ Li-COR	1:10,000
Drp1	Mouse monoclonal 1:1000	BD 611113		Bio-rad/ Li-COR	1:10,000
α-synuclein	Rabbit Polyclonal 1: 2000	EMD Millipore AB5038		Bio-rad/ Li-COR	1:10,000
LC3B	Rabbit Polyclonal 1:1000	Novus NB100-2220		Bio-rad/ Li-COR	1:10,000
p62	Rabbit Polyclonal 1:1000	MBL PM045 (SQSTM1)		Bio-rad/ Li-COR	1:10,000
β-Actin	Mouse monoclonal 1:10,000	Sigma A5441		Bio-rad/ Li-COR	1:15,000
Tom 20	Rabbit Polyclonal 1:4000	Santa Cruz		Bio-rad/ Li-COR	1:10,000

After HRP-conjugated secondary, blots were incubated in SuperSignal West Pico Chemiluminescent Substrate for 3 min. The blots were then exposed to X-ray films and developed in dark room. Films were scanned with Epson Perfection V800 scanner and optical density of target bands were quantified using ImageJ. For fluorophore-conjugated secondary antibodies, blots were washed 3X with TBS and scanned with Li-Cor Odyssey Clx scanner and fluorescence intensity of target bands were quantified with Image Studio Ver 5.0.

2.5 Functional analysis

Mitochondrial membrane potential. N27 α-syn cells were plated into 24-well plates and grown to approximately 85% confluency by the time of the assay. To measure mitochondrial membrane potential (ΔΨm), cells were trypsinised for single cell suspension and washed with warm phosphate buffered saline before being stained with 50nM tetramethylrhodamine methyl ester (TMRM) for 20 min at 37 °C. Fluorescent signal was analysed by BD Accuri C6 flow cytometer using FL-2 channel. Cells were treated with 20 μM carbonyl cyanide 4-(trifluoromethoxy) phenylhydrazone for 20 min to collapse ΔΨm, and the obtained TMRM fluorescence was used to set the threshold. Data were expressed as the percentage of cells with signal above this threshold value as previously described (Cui et al., 2010a). Of note, TMRM was chosen for my study because it is one of the least problematic dyes for measuring ΔΨm due to its high selectivity and minimal effects on mitochondrial bioenergetics. It is less hydrophilic and more sensitive than R123, another commonly used tool for the same purpose.

Cellular Oxidative stress. Dihydroethidium (DHE, Invitrogen) was applied to measure oxidative stress by quantifying reactive oxygen species (ROS) in cells. Cells were grown in 24-well plates and treated accordingly. Upon assay, 10μM DHE were added to cell culture media, incubated for 20 min at 37°C, 30mM H_2O_2 was used as a positive control. The dye was then washed away with PBS, and cells were detached by tryspin, re-suspended in PBS+2%FBS, and analysed by flow cytometry. Data were expressed as the percentage of cells with signal above threshold set by H_2O_2.

Mitochondrial oxidative stress. To identify the source of ROS, mitochondrial oxidative stress was assessed using MitoSOX red (M36008, Molecular probes). Cells were plated in 96-well plate (for plate-reading) and coverglass in 24-well plate (for imaging), treated with PonA and different fission/fusion modulators. 48h of Rotenone (50mM) treatment was used as a positive control for mitochondrial ROS.

Upon assay, cells were washed two times with warm HBSS, followed by 2.5 μM of MitoSox working solution (in HBSS) incubated at 37C for 20min. Cells were then washed 2X with PBS to remove MitoSOX residue, and fixed with 4%PFA. (20min at 37°C).

For plate-reading, cells were washed with PBS 3X times and the fluorescence was measured using Spec at Ex/Em 510/595. After which cells were washed with 2X PBS, incubated with DAPI (5ug/ml) in dark at room temperature for 10 min. 3X PBS washes were repeated to wash away excessive DAPI, and DAPI signal was also quantified through plate reading (Ex/Em 358/461).

Mitochondrial Respiration. Mitochondrial function in live cells was assessed using a Seahorse XFe 96 Analyser (Seahorse biosciences Inc). Cells were grown in XFe 96 tissue culture plate, and standard Mito Stress test (**Figure 2.2**) were carried out for real-time assessment of mitochondria function. Briefly, on the day of experiment, cell culture media was replaced with 175ul serum free assay medium (Dulbecco's Modified Eagle's Medium with -5.5mM Glucose, 1.0mM Sodium Pyruvate, 4mM Glutamine, 2mM HEPES, pH 7.4),.incubated in a 37°C non-CO_2 incubator for at least 30min before being loaded into the analyser. Mitochondrial respiration was measured using the Mito-Stress Test (Seahorse Biosciences Inc) as instructed by the manufacturer. Oligomycin (1µg/ml), FCCP (0.5µM), rotenone (1µM) and

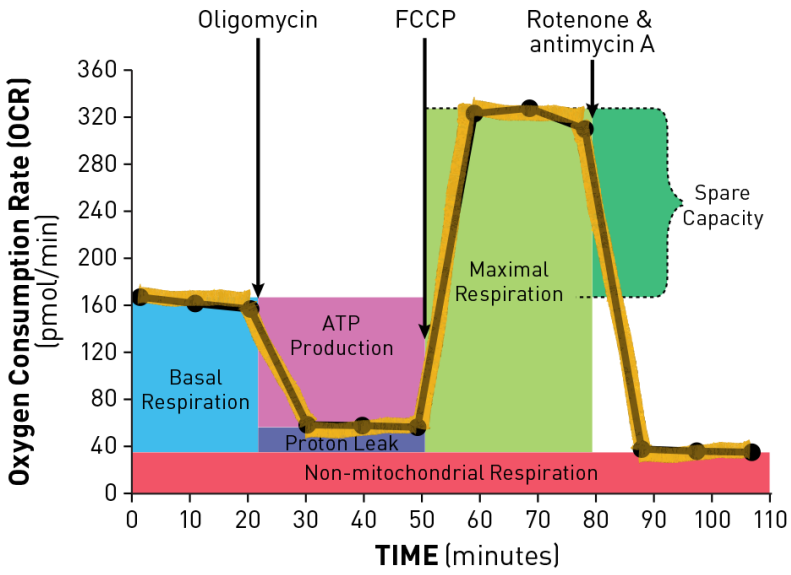

Figure 2.2 Mito Stress Test kinetic profile with assay parameters. *The standard Mito Stress test consists of three sequential injections of Oligomycin (ATP synthase inhibition), FCCP (remove proton restriction, stimulating maximal respiration) and Rotenone& antimycin-A (shutdown ETC). non-Mitochondrial Respiration is the minimum rate after Rotenone/antimycin-A injection. Basal Respiration=(Last measurement before Oligomycin injection) – (non-Mitochondrial Respiration). Maximal Respiration = (Maximum rate after FCCP injection) - (non-Mitochondrial Respiration). Spare Respiratory Capacity%= (Maximal Respiration) / (Basal Respiration) × 100. Coupling Efficiency ATP Production Rate) / (Basal Respiration Rate) × 100*. (Permission to reproduce this image has been granted by Agilent Technologies, Inc.)

antimycin A (1μM) were sequentially added to cells to determine mitochondrial respiration. Each oxygen consumption rate data point refers to the mean rates during each measurement cycle, which consisted of a mixing time of 30 s followed by a data acquisition period of 3 min. Three data points were acquired after each injection, and four data points were recorded for basal respiration. For normalization, cells were fixed with 4% PFA, followed by incubation of DAPI (80μl of 5μg/ml in PBS) for 10 min. The plate was then washed 3 time with PBS, and fluorescent signal DAPI for was quantified at Ex/Em 358/461 nm using the Biotak Synergy H1 Hybrid Reader.

Autophagic vesicles analysis. The analysis of autophagy flux in HeLa cells was performed in a similar way as described by (Button et al., 2014) Green vesicles are considered to be autophagosomes, as when the autophagosome fuses with the lysosome, the pH sensitive GFP signal is quenched by the acidic environment. Red vesicles are made up of both autophagosomes and autolysosomes. The number of autolysosomes was achieved by subtracting the number of green vesicles from that of the red vesicles. For analysis, cells were imaged with an Olympus Fluoview with 60x time objective, autophagosomes and autolysosomes from at least 50 cells per treatment group were counted using ImageJ.

For N27 cells, autophagy blockage was assessed either through western blot analysis of LC3-II (autophagic membrane protein) and p62 (autophagy substrate) level, or through quantification of LC3-cherry puncta together with p62 puncta through immunostaining.

2.6 Protein aggregation

Proteinase K digestion for immunocytochemistry (ICC). To determine the formation of aggregation in cells, Proteinase K (PK) digestion was performed. For ICC plates used for PK digestion, freshly fixed cells were washed 3 X 5min with PBS, then treated with PK solution (~0.34U/ml, Sigma P4850) diluted in PBS. The plates were then be incubated in the dark at room temperature for 10min with gentle shaking, followed by 3 X 5min washes with PBS. After washing the plates were ready to proceed to blocking and subsequent ICC staining for α-syn.

Pre-formed fibrils (PFF) treatment. α-syn monomers were obtained from the Michael J. FOX Foundation, and the generation of PFF was performed according to manufacturer's protocol: The frozen aliquot was thawed on ice, spun at 15,000g for 10 min at 4°C with a SORVALL legend micro 21R centrifuge (Thermo Scientific). BCA was then performed to determine the concentration (triplicates at 3 different dilutions), and protein sample was diluted in sterile dPBS (gibco 14190-144) to 5mg/ml in a 1.5ml Eppendorf protein low-bind tube. The sample was quickly votexed and placed in an Eppendorf ThermoMixer C orbital shaker (with thermo top on), shaken at 1,000 RPM for seven consecutive days at 37°C. Sample was then divided into 25µL aliquots and stored at -80°C.

Upon use, an aliquot was thawed at room temperature, diluted into 0.1mg/mL using sterile dPBS (volume 200-400µL), and sonicated with a Fisher Scientific 120 Sonic Dismembrator with CL-18 microtip (30 X1s pulses, 20% power). Sonicated solution was immediately added to Hela cells grown in 6-well plates (10µg/well). Cells were incubated with PFF for 48h, and PFF media was placed with fresh culture

media, and cells were further incubated for 24h before fixation for immunostaining. TEM images were captured by collaborators in Fudan University, China.

2.7 synaptosome isolation and functional analysis

Synaptosome isolation in rats Synaptosomes were isolated from Sprague Dawley adult rats based on a previous publication(Choi et al., 2009b) but with some modifications. Briefly, striata were quickly removed, rinsed with ice-cold sucrose buffer (320 mM sucrose, 1 mM EDTA, 0.25 mM dithiothreitol, pH 7.4).and then homogenized (10-12 strokes) in dounce glass homogenizer containing 1-1.5 mL sucrose buffer. The homogenates were transferred to 2ml Eppendorf tubes, spun at 1000g at 4°C for 10min. The supernatants were collected and then gently layered onto a discontinuous Percoll gradient (2.5ml of 3%, 10% and 23% in sucrose buffer) in 10 mL centrifuge tubes, and centrifuged at 32500 *g* for 10 min at 4°C in a JA-25.50 fixed angle rotor in a Beckman Avanti J-26 X centrifuge. The band between 10% and 23% from striatum was collected for synaptosomes, pelleted and resuspended in ionic buffer (20 mM HEPES, 10 mM D-glucose, 1.2 mM Na2HPO4, 1 mM MgCl2, 5 mM), protein concentration was measured using nano drop 2000.

Mitochondrial function in striatal synaptosomes. Isolated striatal synaptosomes (2ug/well) were plated into an XFe96 cell culture microplate (Seahorse Bioscience Inc.) which was previously sequentially pre-coated with 0.0033% (v/v) polyethyleneimine (Sigma-Aldrich) and Geltrex (Invitrogen). The plate was centrifuged at 3400*g* for 1h at 4 ºC in a Henttich Rotanta 460R centrifuge to facilitate attachment. The ionic buffer was then replaced with 175µL assay buffer (3.5 mM KCl, 120 mM NaCl, 1.3 mM CaCl2,

0.4 mM KH2PO4,1.2 mM Na2SO4, 15 mM D-glucose, 10 mM pyruvate, 0.4% (w/v) fatty acid-free bovine serum albumin, and 10 mM TES (N-[tris(hydroxymethyl)methyl]-2-aminoethanesulfonic acid), pH 7.4). The plate was incubated in a non-CO_2 incubator at 37ºC for 10-15min, then loaded into the XFe96 Extracellular Flux Analyzer (Seahorse Biosciences Inc.) Mitochondrial function in these synaptosomes, as indicated by oxygen consumption rate (OCR), was monitored in real-time throughout the assay. Different parameters of mitochondrial respiration were obtained with sequential injections of 2.5 µg/ml oligomycin, 4 µM FCCP and 2 µM Rotenone/Antimycin. Oxygen consumption rate data points represents the mean rates of each measurement cycle, which consisted of 30 s mixing time,30s waiting time, followed by 3 min of data acquisition. Basal respiration was measured before the first injection (3 cycles), and 3 data points were obtained following each injection (12 data points in total).

2.8 Statistical Analysis

Data represent the mean ± SEM. For all *in vitro* experiments with two groups, student t-test was applied as they all pass normality test. For normally distributed data with more than 2 groups, differences between means were analysed using one-way ANOVA, followed by Newman-Keuls post hoc testing for pairwise comparison. The Newman-Keuls was post hoc analysis method was selected for its intermediate stringency and it's not too conservative. For *in viv*o study and for *in vitro* experiment with 2 variables, Statistical analysis was performed using two-way ANOVA, followed by Tukey multiple comparison test. All statistical analyses were performed by SigmaStat 3.5 software. The null hypothesis was rejected when the p value < 0.05.

3. Inducible α-syn overexpression in N27 cells impairs mitochondrial morphology and function by enhancing fission

3.1. Introduction

As discussed in Section **1.3**, α-syn has been demonstrated to induce neurotoxicity through multiple but non-mutually exclusive mechanisms (Bourdenx et al., 2015b, Dehay et al., 2015a, Franco-Iborra et al., 2016, Helley et al., 2017a), including impairment in mitochondrial and autophagy-lysosomal function – two mechanisms that are relevant to my research. α-syn has been reported to induce mitochondrial dysfunction and fragmentation in experimental models of PD (Chen et al., 2015, Winslow and Rubinsztein, 2011, Kamp et al., 2010, Gui et al., 2012). However, whether α-syn impairs mitochondrial function and morphology through imbalanced mitochondrial fission and fusion ratio is still a topic of debate (as discussed in **Chapter 1, section1.3.4.3**). This is one of the main questions that I would like to address in my study.

To address this issue, I started with a dopaminergic neuronal cell model with inducible human wild-type α-syn expression. The major advantages of a stable inducible cell line comparing to transient transfection and non-inducible stable cell line include:

1. More homogeneous population compared to transient transfection, and therefore results would be more consistent and reproducible.
2. For proteins that could be toxic such as α-syn, a stable cell line with continuous overexpression of the protein would potentially act as a selective factor that would change the properties of the surviving cells. An inducible cell line tackles the problem by controlling the timing and duration of the protein expression.

3. With controlled level and time of protein expression, inducible cell line offers the flexibility to assess the impact of α-syn in a time depend manner and establish the preferred overexpression level via controlling PonA dose and time.

In addition, the flexibility of cultured cell line, comparing to primary culture, allows me to test different genetic approaches to confirm the effect of certain proteins. This is vital for establishing a model targeting certain pathways as small molecule approaches alone does not offer enough specificity. iPSC cells were also considered as an alternative, however, the problem with heterogeneous genetic background at the time became a major concern and this was put on hold. Another immortalised dopaminergic cell line, LUHMES, was also considered for generating the stable cell line. LUHMES have been established to be differentiated morphologically and functionally mimicking primary dopaminergic neurons (Scholz et al., 2011, Schildknecht et al., 2013). Due to technical issues as discussed later in this chapter, I was unable to generate inducible stable LUHMES cells.

My two initial objectives were to first test the effects of α-syn overexpression on mitochondrial morphology and function. Second, determine whether blocking Drp1 would attenuate the negative impacts of α-syn on mitochondria.

3.2. Materials and Methods

3.2.1. Cell culture, differentiation and α-syn induction

Two dopaminergic neuronal cell lines have been used in this Chapter, the stable N27 cells and LUHMES cells. Most studies were done with stable N27 cells due to the

difficulties of generating stable cell line or transient transfection I encountered with LUHMES cells (discussed in **section 3.3**).

Stable N27 cell culture and differentiation To investigate the impact of α-syn overexpression on mitochondria in detail, an inducible cell line was generated by stably transfecting rat dopaminergic neurons (N27) with an ecdysone system containing human *SNCA* gene (see **Chapter 2 Fig. 2.1**). Population of cells with inducible α-syn expression were sorted using an mRNA probe specific to human α-syn (**Fig. 3.1A**). Cells were maintained in selective media containing RPMI +10% FBS+G418+ Hygromycin B. In the beginning of the study, attempts were made to explore the potential of using differentiated N27 cells with more dopaminergic properties. Different concentrations of Dibutyryl cyclic-AMP (dbcAMP, Sigma) and/or DHEA (sigma) were tested out as indicated in **Fig. 3.2.**

α-syn induction To induce α-syn induction, different doses (up to 30 µM) of Ponasterone A (PonA, Enzo, ALX-370-014-M005, 2mM stock in Ethanol) were diluted into cell culture media right before treatment. 10 and 20µM were established as most effective doses and used for subsequent tests. Cells were incubated for 24, 48 and 72h for respective tests.

LUHMES cell culture and differentiation. Lund human mesencephalic LUHMES cell line (ATCC® CRL-2927™) were maintained in complete growth media containing DMEM/F-12 +1% N-2 supplement (Gibco-Invitrogen 17502-048) + 40 ng/ml b-FGF (basic recombinant human Fibroblast Growth Factor; Gibco-Invitrogen 13256-029), with b-FGF always added fresh right before use. All cell culture surfaces were sequentially pre-coated with 50 µg/mL poly-L-ornithine at room temperature overnight (Sigma, P-3655), and then with 1 µg/mL Human Fibronectin (Sigma, F-0895) at 37°C for 3 hours. For differentiation, bFGF in complete growth medium

were replaced with tetracycline (1µg/ml, diluted 1:1000 from 1mg/ml stock), GDNF (glial cell line-derived neurotrophic factor, 2ng/ml, diluted 1:1000 from 2µg/ml stock), and db-cAMP (1mM, diluted 1:100 from 100mM stock). Cells were differentiated up to 10 days and were plated for experiment at Day 2 of differentiation to control the cell number.

3.2.2. Immunoassays and qPCR

Immunocytochemistry. To confirm and characterise the expression of α-syn, antibodies against α-syn (mouse monoclonal antibody BD 610787) (1:500) and rabbit polyclonal antibody AB5038 (1:2000) were used for immunocytochemistry). For autophagy assessment, antibody against p62 (rabbit polyclonal, MBL PM045) was used at 1:500 dilution. For cell differentiation characterisation, antibodies against TH (mouse monoclonal, Sigma T2928, 1:500 dilution) and Tom 20 (rabbit polyclonal, Santa Cruz sc-17764 ,1:1000 dilution) were used. (more details in **Chapter 2, Table 2.2**)

Western blotting. Upon experiments, cell pellets were collected and lysed with RIPA buffer with proteinase inhibitors, homogenised on ice, and supernatants were loaded on to a 12% SDS-PAGE for separation and transferred to a PVDF membrane. After blocking with 2.5% skin milk, membranes were incubated in primary antibody solutions at 4C overnight: anti-a-syn (1:1000, BD 610787), anti-Drp1 (1:2000, BD 61113), anti-β-actin (1:10,000, Sigma A2228). more details in **Chapter 2, Table 2.3**)

qPCR. Cells were harvested after 24, 48 and 72hrs after PonA induction. mRNA was extracted using RNeasy Mini Kit (Qiagen) followingmanufacturer's instructions. The

isolated mRNA concertation was measured by NanoDrop™ 2000 Spectrophotometer, and cDNA were generated using Thermo Scientific RevertAid First Strand cDNA Synthesis Kit. 1µl of cDNA were mixed 1µl of each primer and with Roche LightCycler® 480 SYBR Green I Master. qPCRs were run in LightCycler® 480 Instrument using a 384-well plate with 10 µl reaction volume.

3.2.3. Functional Studies

Mitochondrial membrane potential. Stable N27 cells were treated with PonA for 48h with or without Drp1 inhibition. They were then stained with 50nM tetramethylrhodamine methyl ester (TMRM) for 20 min at 37 °C. Fluorescent signal was analysed by BD Accuri C6 flow cytometer using FL-2 channel. For positive control, cells were treated with 20 µM (FCCP for 20 min to collapse ΔΨm, and the obtained TMRM fluorescence was used to set the threshold. FCCP uncouples the proton current with ATP production, taking away limitation of proton flow(Singleton et al., 2003b), as a result mitochondria membrane no longer have the ΔΨm generated by ETC complex.

Oxidative Stress (cellular). Stable N27 cells were treated with PonA for 48h with/without Drp1 inhibition. Upon assay, 10µM Dihydroethidium (DHE) were added to cell culture media, incubated for 20 min at 37°C, 30mM H_2O_2 was used as a positive control. DHE gets oxidized by superoxide to form ethidum or 2-hydroxyethidium (ex 500-530 nm/em 590-620 nm)(Owusu-Ansah et al., 2008), and the change in red fluorescence can be quantified as indicators for oxidative stress. The dye was then washed away with PBS, and cells were detached by tryspin, re-

suspended in PBS+2%FBS, and analysed by flow cytometry. Data were expressed as the percentage of cells with signal above threshold set by H_2O_2.

Mitochondrial oxidative stress . To identify the source of ROS in stable N27 cells, mitochondrial oxidative stress was assessed using by 2.5 µM MitoSOX red (M36008, Molecular probes). Cells were plated in 96-well plate (for plate-reading), treated with PonA and different fission/fusion modulators for 48h. Rotenone (50mM) treatment for 48h was used as a positive control for mitochondrial ROS because Rotenone induces mitochondrial ROS by directly and selectively blocking mitochondrial complex I(Palmer et al., 1968). Plate reading (Ex/Em 510/595) was done to quantify mitochondrial ROS. Normalisation was done using DAPI (Ex/Em 358/461).

Mitochondrial respiration. N27 stable cells were grown in XFe 96 tissue culture plate and treated with PonA for 24h. On the day of experiment, cell culture media was replaced with 175ul XF assay medium (Dulbecco's Modified Eagle's Medium with 4.5mM Glucose, sodium pyruvate, PH7.4), incubated in a 37°C non-CO2 incubator for at least 30min before being loaded into the analyser. Mitochondrial respiration was measured using the Mito-Stress Test (see **Chapter 2, Figure 2.2**) (Seahorse Biosciences Inc) as instructed by the manufacturer. Oligomycin (1µg/ml), FCCP (0.5µM), rotenone (1µM) and antimycin A (1µM) were sequentially added to cells to determine mitochondrial respiration. For normalization, cells were fixed with 4% PFA, followed by incubation of DAPI (80µl of 5µg/ml in PBS) for 10 min. The plate was then washed 3 time with PBS, and fluorescent signal DAPI for was quantified at Ex/Em 358/461 nm using the Biotak Synergy H1 Hybrid Reader.

Autophagy and protein aggregation assessment. To assess autophagy, N27 cells were transfected with LC3-cherry, a marker for autophagosomes and autolysosome membranes. And an autophagy substrate, p62 was also marked for

quantification. To quantify aggregation in immunostained cells, slides were incubated with 0.34U/ml Proteinase K (PK) solution (in PBS) for 10min at RT before proceeding to blocking. PK is a nonspecific serine protease that degrades many proteins in the native state(Ebeling et al., 1974), and aggregated forms of proteins will survive the digestion. All puncta quantifications were achieved using image J. (see **section 2.7** for more details)

3.2.4. Cell viability assays

MTT cell viability assay. Cells were plated in 96-well plates (5,000/well for 72h). On the day of assay, 25µl of MTT (3-(4,5-Dimethylthiazol-2-yl)-2,5-Diphenyltetrazolium Bromide) was added into each well, incubated in the dark at 37°C for 3 hours, followed by the addition of 100µl of MTT lysis buffer. The plate was then left overnight for the crystals to dissolve. Plate reading was done the following day after confirming that all the crystals were dissolved, and optical density at 562nm was measured using a Genois one plate reader.

Calcein AM cell viability assay. Calcein, AM (Invitrogen,1mg/ml in DMSO) was purchased from Thermo Fisher Scientific. Working solution (2µg/ml) was made up in PBS each time prior to experiment. N27 cells were grown in flat bottom 96-well plates and induced with PonA for 72h with/without Drp1 inhibition. Upon assay, cells were washed with warm dPBS by replacing half the volume of media with dPBS and leave 50µl PBS in each well.100µl Calcein solution was then added to each well and the plate was incubated in dark at room temperature for 1 h. Fluorescence signal was quantified using Synergy H1 Hybrid Reader (Ex/Em 494/520).

3.2.5. Imaging

Regular fluorescence imaging was done by Nikon Eclipse TE2000-U Fluorescent microscope. Confocal images were taken by Olympus FV1000 with X60 Objective. For TEM imaging, cell samples were processed and imaged with JEM-1400 TEM (imaging were conducted at Plymouth University Electron Microscopy Centre, by Dr. Martin Helley and Jay Rees).

3.3. Results

To assess the inducible expression of α-syn in the stable N27 cells, I performed a pilot study by treating cells containing *SNCA* or empty vector control with varying concentrations of PonA for 48h to induce α-syn expression. Immunostaining (**Fig 3.1**) shows that at 5 μM, the expression of α-syn was minimal, but at 10 μM and higher concentrations, immunofluorescent signal of α-syn was high. In contrast, the group of cells with empty vector control treated with 20 μM did not produce a detectable expression.

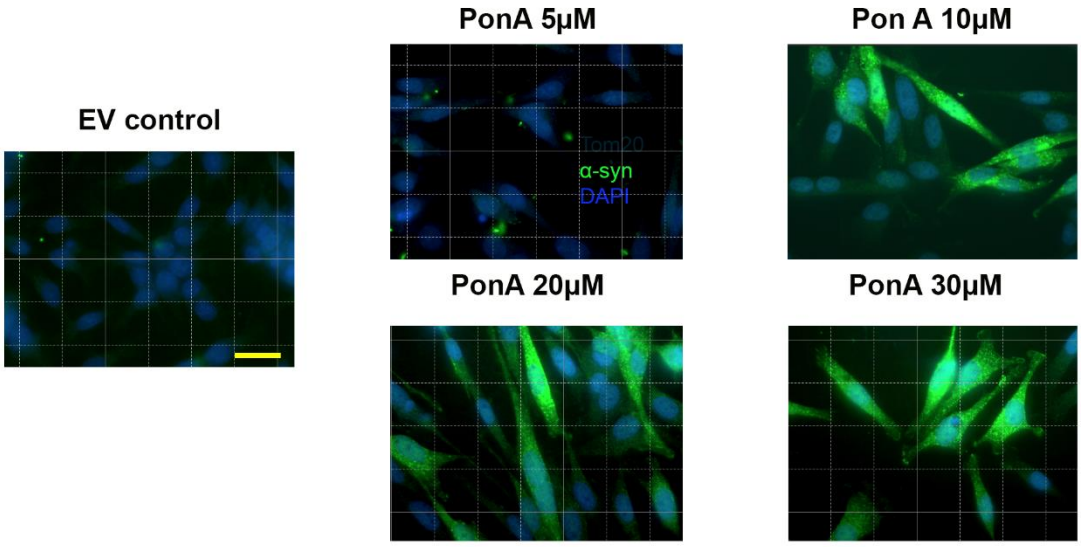

Figure 3.1 Dose-response study of α-syn in stable N27. *Cells were grown on coverslip glass, induced with differing doses of PonA (*5-30 μM*) for 48h before fixation and immunostained for α-syn. Images were captured using Nikon ECLIPSE TE2000-U fluorescent microscope with 60X objective. Scale bar: 30μm.*

Next, to select stable cells with high expression of α-syn, cells with *SNCA* or empty vector control cells were treated with PonA (20μM) for 24h to induce α-syn expression. Cells were then sorted using FACS with an mRNA probe specific to human *SNCA* (**Fig. 3.2A**), the uptake of probe was confirmed by imaging, as shown in the left panel, the probe (red dots) distribution were much higher in some cells. And when quantified by FACS, there was a clear shift to the right (higher fluorescent signal) in the distribution curve after induction. Cell populations in both P1 (lower levels) and P2 (higher levels) gates of induced cells were collected.

Cells with high *SNCA* levels were selected and the inducible expression of α-syn was then further characterised by performing dose-response and time-course studies of PonA treatment. Based on the results obtained from qPCR (**Fig. 3.2B**) and western blotting (**Fig. 3.2C&D**), robust α-syn overexpression was induced as early

as 24 after PonA treatment. Immunoblotting data show PonA at 20 µM for 48h as the most optimal regimen to induce α-syn expression based on protein level; therefore, for subsequent studies, cell were treated with these experimental conditions - unless otherwise specified. Although I could not completely control the exact level of α-syn overexpression by different dose of PonA, the inducible cell line still offers a lot of flexibility and control regarding the time and relative lower levels of expression compared to stable non-inducible cell line and transient transfection.

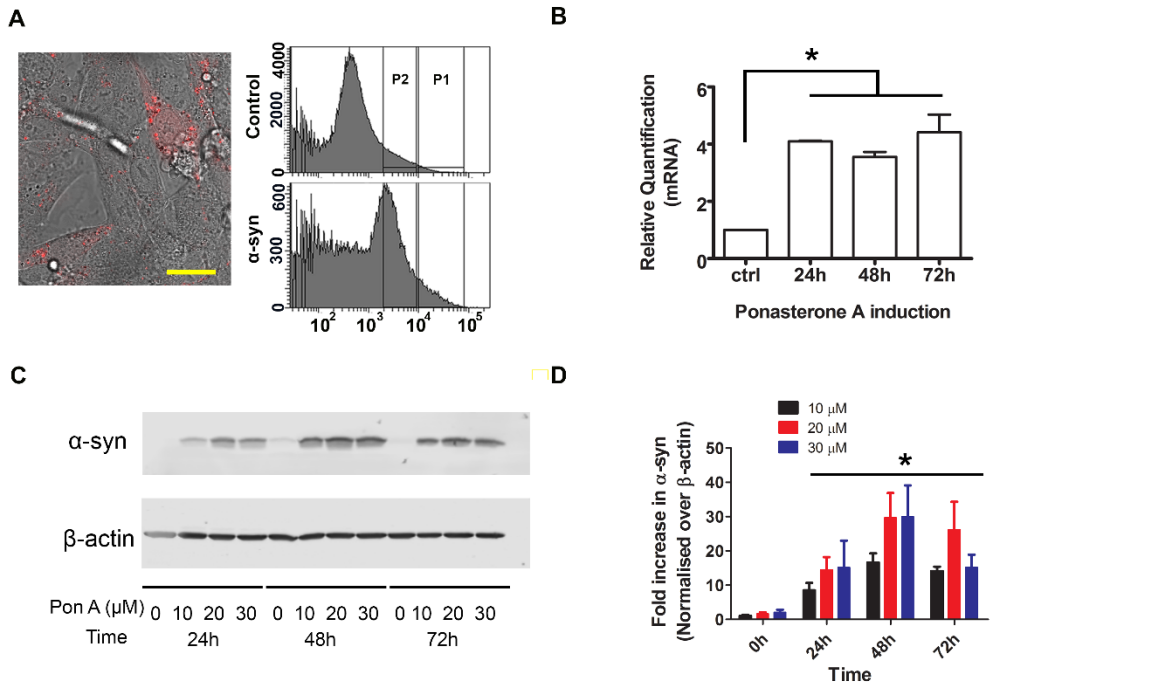

Figure 3.2 Purification and characterisation of stable cells with inducible α-syn. ***(A)*** *Rat dopaminergic neuronal N27 cells transfected with ecdysone-inducible system containing human α-syn were induced with PonA (20μM) for 24h, and then incubated with SMARTFlare Cy3-hα-syn mRNA probe overnight before analysis. Left panel: The uptake of probes was confirmed by confocal imaging using Cy-3 signal (PE Ex/Em 496/578) combined with phase contrast. Right panel: Cell sorting by FACS, Cy-3 signal shift with PonA induction. Two populations (P1 & P2) of cells with α-syn expression levels were collected. P1 (higher expression) population was used for further experiments.* ***(B)*** *qPCR analysis of α-syn expression over different time points. Data presents Mean ± SEM, n=3. p*<0.05 against empty vehicle control.* ***(C&D)*** *Concentrations of 10, 20 and 30 μM of PonA were tested at different time points (24h, 48h & 72h) to determine the optimal conditions for α-syn expression. Western blot analysis of α-syn overexpression in a time and dose dependent manner. Each PonA dose was compared to its respective control using One-way Anova. Data presents Mean ± SEM, n=4. p*<0.05 against empty vehicle control.*

In an attempt to improve the cell culture model to make it more neuronal like, I tried differentiating N27cells (**Figure 3.3**) adapting a protocol previously described(Prasad et al., 1994, Adams et al., 1996) .using Dehydroepiandrosterone

(DHEA) and dibutyryl cyclic AMP (dbCAMP). I tested two concentrations of DHEA and three concentrations of dbCAMP. At day 2, dbCAMP 0.5mg/ml long neurites in these cells were observed at both concentrations of DHEA, suggesting cells started to differentiate. Although this was encouraging, these differentiated cells started to die after day 3. After a few attempts, this low cell viability prevented me from using this cell model for my work.

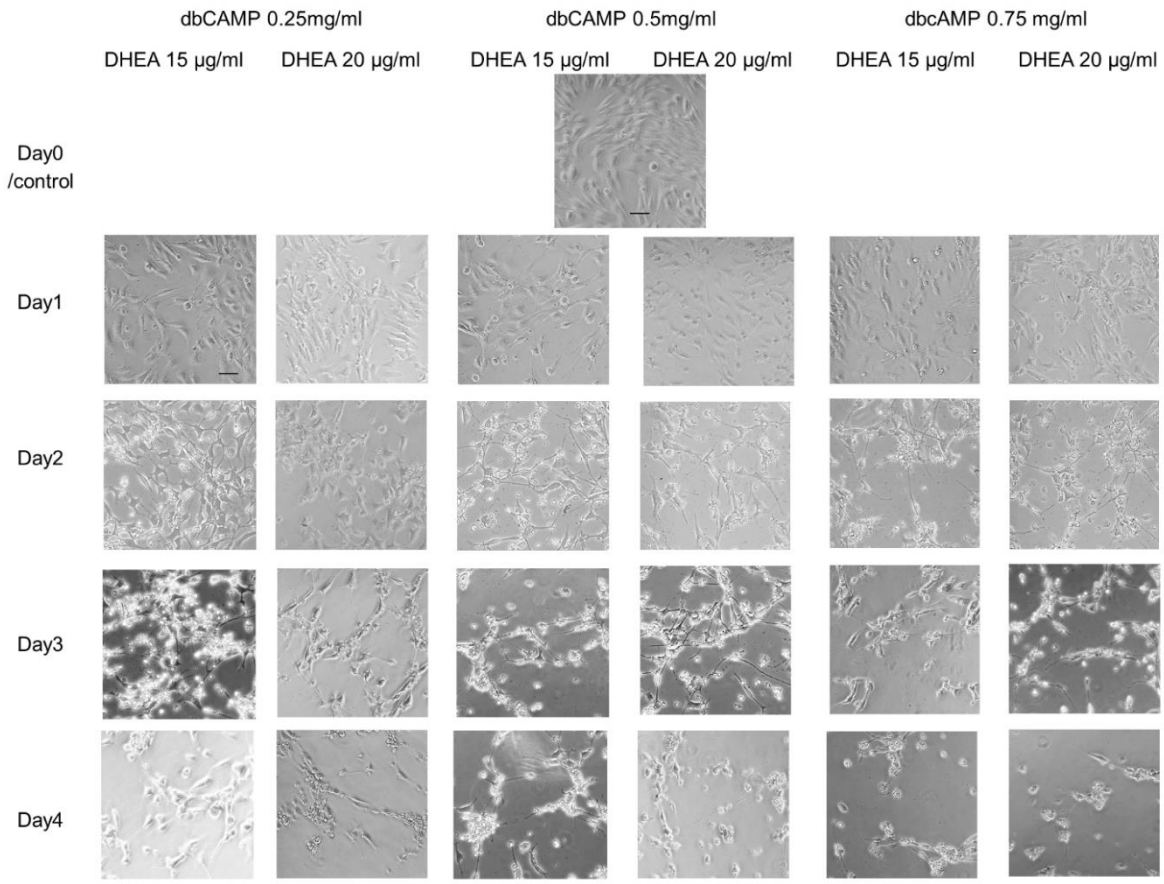

Fig 3.3. N27 differentiation characterisation at different concentrations of DHEA and dbcAMP. *Stable N27 cells were grown on glass coverslips coated with poly-D-lysine. Cells were differentiated for up to 4 days with DHEA + dbcAMP. Different ratios of the two compounds (as indicated) were tested and morphology change was tracked every day with a Leica phase contrast microscope. Representative images were shown. Scale bar: 50µm.*

To complement the N27 cells, which are rat dopaminergic neurons cells, I tried to set up a second model using LUHMES cells, which represent a human mesencephalic-derived cell line (Schildknecht et al., 2013) Based on the cell differentiation protocol of that publication, I differentiated these cells for 10 days and immunostained for tyrosine hydroxylate (TH), a marker commonly used for dopaminergic neurons. As shown in **Figure 3.4A**, the expression of TH was noticeable after day 5 of differentiation. Next, I assessed the response of LUHMES cells to a neurotoxin. As compared to N27 cells, even without differentiation, LUHMES cells showed higher sensitivity to paraquat **(Figure 3.3B**), a pesticide widely used in PD-related studies (Cicchetti et al., 2005, Thiruchelvam et al., 2000). Together, these two observations led me to believe that I could use LUHMES cells to generate a human dopaminergic cell model with inducible α-syn. However, when I started to use these cells to generate an inducible model , I encountered two problems:

1. Low transfection efficiency. Common lipid-based methods like lipofectamine and other chemical transfections resulted in very little transfected cells, electroporation did give higher transfection efficiency, but the aggressive nature of the method resulted in much lower cell viability. According to literature, the common method of LUHMES cell transfection is through lentivirus (Krug et al., 2014), which was not feasible for me to perform at the time.

2. Compatibility with the inducible construct: To generate a stable inducible cell line using the same constructs that I had for the generation of the N27 stable cells, the cells would go through two selection processes with G418 (neomycin) and Hygromycin B. Generated from MESC2.10, LUHMES cells already contains neomycin-resistant gene, which would lead to unsuccessful selection with current

scheme. An alternative construct needs to be designed if I were to generate stable inducible cell line in the future. Given that I had already generated stable N27 cells, I decided to use those stable cells for my study.

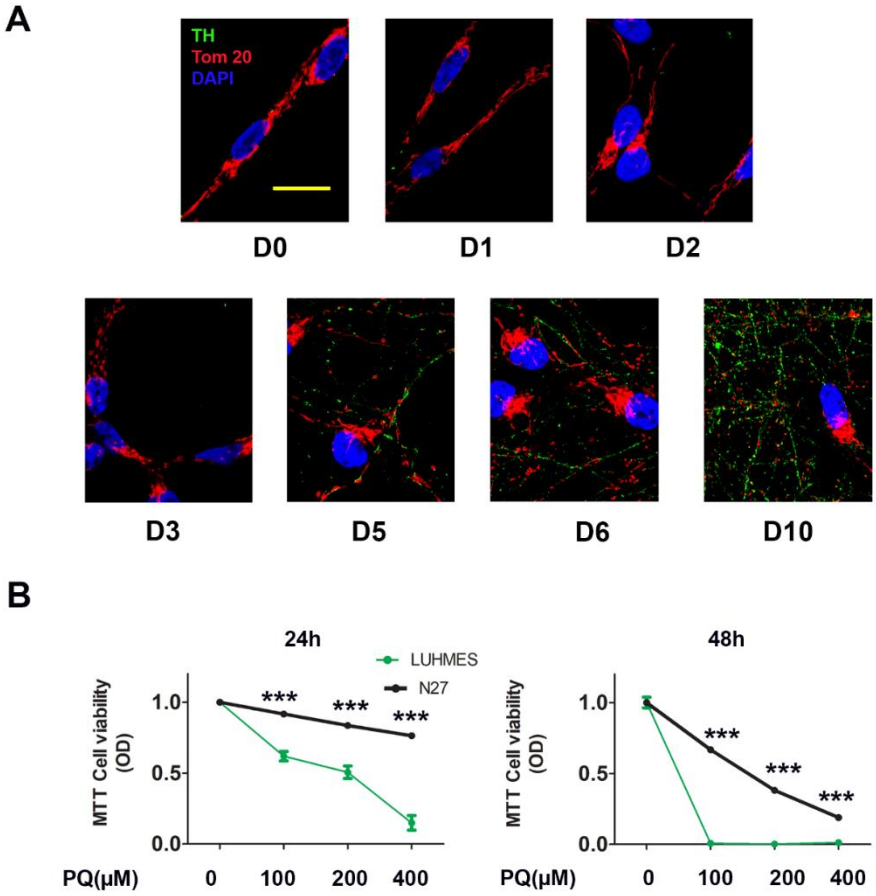

Fig 3.4. LUHMES cell characterisation. (*A*). *Differentiation shows increased TH expression over time. LUHMES cells were grown on coverslip glass pre-coated with poly-L-orthine and fibronectin. Complete growth media was replaced with differentiation medium containing DMEM/F12 + N-2 +Tetracycline + dbcAMP + bFGF, cells were differentiated up to 10 days and fixed at different dates as shown above.* ***(B)***. *Cells grown in 96-well plates were treated with different doses of PQ (as indicated) for 24 and 48h, and 25 µl MTT (5 mg/mL in PBS) were added directly to the wells containing 100 µl media. Optical density was determined by measuring absorbance at end point 560. Data represent the mean ± SEM, n=3-5 independent experiments. Statistical analysis for was performed using two-way ANOVA ***p<0.001)*

3.3.1. α-syn overexpression induces mitochondrial fragmentation and Drp1 translocation to mitochondria

With the inducible dopaminergic N27 cells characterised, I assessed the impact of α-syn on mitochondrial morphology. Cells were transfected with DsRed-Mito to label mitochondria with a red-fluorescent signal. This approach avoids the problems of mitochondrial dyes such as specificity and signal intensity being affected by mitochondrial membrane potential. Cells were then induced with PonA for α-syn overexpression, which as shown in **Fig3.5A**, induced mitochondrial fragmentation with a peri-nuclei distribution after 48h. However, stable cells with empty vector control displayed tubular mitochondria. The observed mitochondrial fragmentation appeared to be mediated by Drp1 because increased levels of this fission protein were observed at the mitochondrial and total levels, as demonstrated using immunohistochemistry (**Fig3.5A**) and immunoblotting (**Fig3.5B**), respectively. Mitochondrial morphology was further quantified using ImageJ and expressed as Roundness and Aspect Ratio (**Fig 3.5C & D)**. Both the values of “roundness” and “aspect ratio” approach 1 as the particle becomes circular.

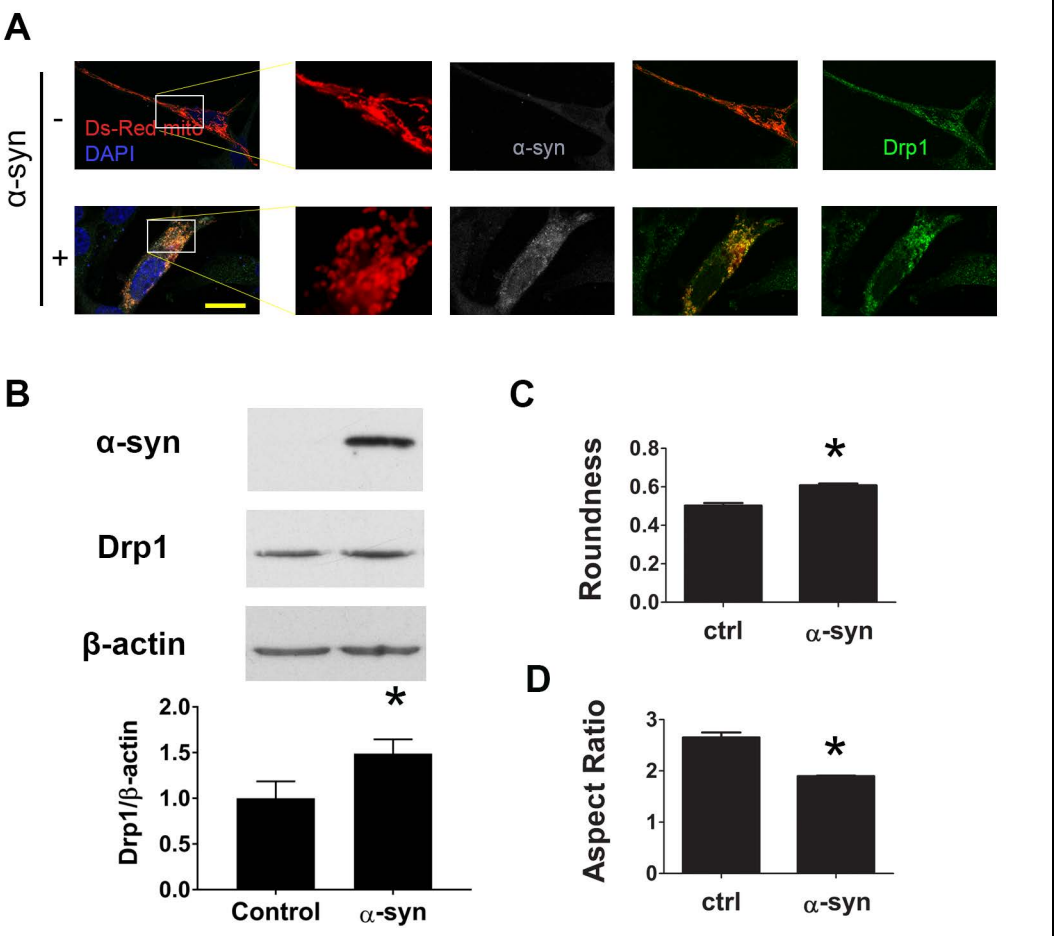

Fig3.5 α-syn overexpression induces mitochondrial fragmentation. **(*A)*** *Stable N27 cells with α-syn or empty vector control were transiently transfected with the mitochondria label Ds-Red-mito and then induced with PonA for 48h. Cells were fixed, stained and imaged using confocal microscopy. Antibodies against Drp1 and* α-syn *were used to label the two proteins. Scale bar: 20μm. (**B)** Stable N27 cells were induced with PonA for 48h, and then harvested, lysed with RIPA buffer and separated with SDS-PAGE. Blots were probed as indicated using antibodies as indicated. Data represent the mean ± S.E, n=4 per group, student t-test * p<0.05. (**C and D)** Quantification of mitochondrial perimeter by ImageJ using ICC images captured with confocal. Data represent the mean ± SEM, n=4 with approximately 50 cells counted per group per experiment, student t-test * p<0.05. Roundness = 4X[Area] / (πX [Major axis]^2). Aspect Ratio = [major Axis]/ [Minor Axis].*

3.3.2. α-syn overexpression impairs mitochondrial function and reduces cell viability

Based on the observation that inducible α-syn impaired mitochondrial morphology, I asked whether mitochondrial function was also impaired in this cell model. Known as the 'powerhouse' of the cell, ATP generation through oxidative phosphorylation is the predominant physiological function of mitochondria. Abnormality in any of the processes that impair oxidative phosphorylation function can cause mitochondrial dysfunction. In this project, I used complementary approaches to evaluate mitochondrial function:

First, I measured mitochondrial membrane potential ($\Delta\Psi_m$), which is established by the electrochemical gradient from redox reactions generated by the mitochondrial electron transport chain (ETC). This gradient is responsible for driving ATP production, and therefore a decrease in $\Delta\Psi_m$ is indicative of unhealthy mitochondria. As shown in **Fig. 3.6A**, after 48h of induction, α-syn significantly reduced $\Delta\Psi_m$ to approximately 50% of the control group without α-syn expression.

Second, oxidative stress is generated from overproduction of free radicals such as reactive oxygen species (ROS). ROS could lead to mtDNA mutations, protein aggregation and have been implicated in cell death and ageing. An impairment in mitochondrial function invariably would lead to free radical production such as ROS. To determine whether such ROS production would originate from mitochondria resulting in a higher total cellular ROS, I quantified MitoSOX Red and Dihydroethidium (DHE) signals to detect mitochondrial superoxide and cellular ROS levels, respectively. Rotenone, a complex I inhibitor, was used as a positive control to generate ROS from the ETC blockade. Consistent with its inhibitory effect on

mitochondrial function, α-syn increased ~30% mitochondrial and 400% cellular ROS levels (**Fig 3.6B-C**).

Third, to measure mitochondrial function more directly and to gain more insights into the kinetics of mitochondria respiration impaired by α-syn, I quantified mitochondrial oxygen consumption using the Seahorse XFe96 Extracellular Flux Analyzer. **Fig 3.7** shows that α-syn specifically reduced mitochondrial spare respiratory capacity (SRC), which represents the ability of mitochondria to provide substrate supply and electron transport in response to an increase in energy demand.

The three parameters above were chosen because each of them provides a different but complementary aspect of mitochondrial health. The simultaneous drop in $\Delta\Psi_m$, spare respiratory capacity and increase in ROS consistently indicates mitochondrial dysfunction. Taken together, these three mitochondrial studies support the negative effects of α-syn on the mitochondrial function.

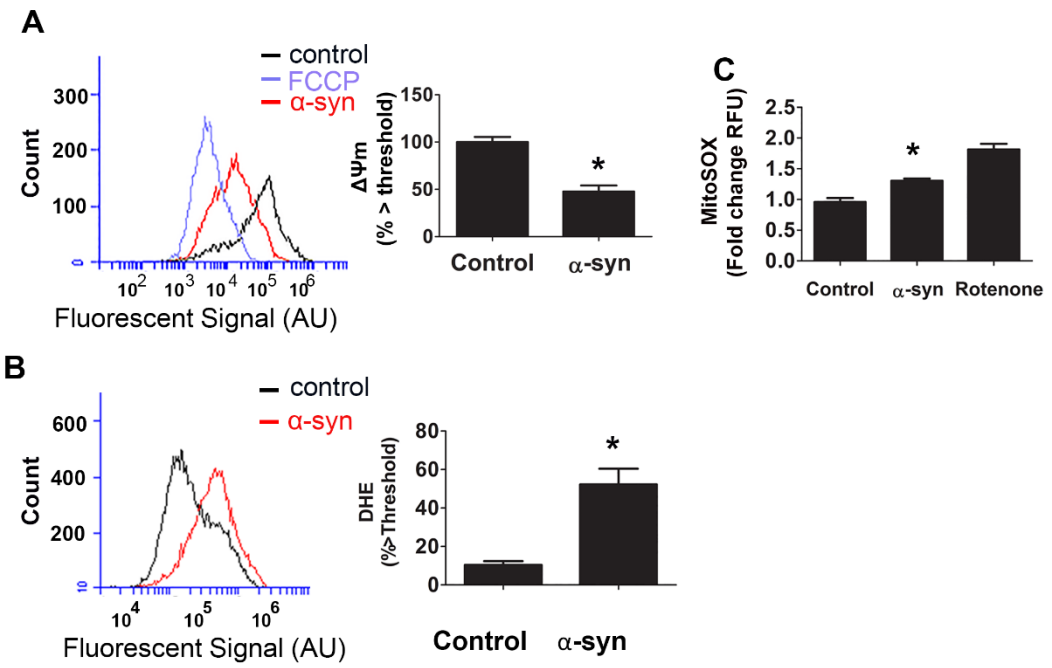

Fig3.6 α-syn overexpression collapses $\Delta\Psi_m$, increases both cytosolic and mitochondrial ROS. (*A*) *Stable N27 cells with α-syn or empty vector control were incubated for 20min at 37°C with 50nM TMRM, and 20μM uncoupler FCCP were added as positive control to collapse membrane potential, a value that served as a threshold for subsequent quantification. Cells were run through a flow cytometer and $\Delta\Psi_m$ signal was recorded. Data are expressed as % above threshold, arbitrary units (AU).* ***(B)*** *Cellular ROS was measured by incubation with 10 μM DHE for 20min at 37°C and analysed by flow cytometry. Data expressed as % above threshold.* ***(C)*** *MitoSox red signal was measured by incubation cells with 2.5 μM working solution of the dye for 20 min and analysed by fluorescent plate reader (Ex/Em 510/580nm). For normalization, cells were fixed and subsequently stained with DAPI (Ex/Em 385/461 nm) for cell density, and relative fluorescence units (RFU) were calculated by dividing mitosox intensity against DAPI. Rotenone was used as a positive control because it produces ROS by blocking mitochondrial function. Data represents Mean ±SEM, n=4 independent experiments, student t-test. *p<0.05.*

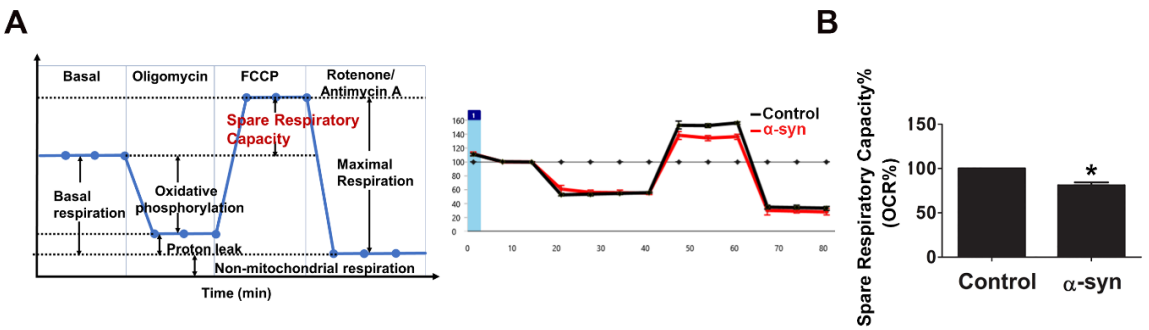

Fig 3.7 α-syn overexpression reduces mitochondrial spare respiratory capacity. (*A*) *Kinetic illustration of mito-stress assay. Three sequential injections of Oligomycin (to inhibit oxygen consumption mediated by ATP synthase), FCCP (an uncoupler to induce maximal OCR), and Rotenone/Antimycin (to inhibit complex I and III, respectively) were done after basal respiration measurement* ***(B)*** *Stable N27 cells with α-syn or empty vector control were grown in Seahorse XF96 Cell Culture Microplates were analysed by a Seahorse XFe96 Analyzer. α-syn overexpression impaired spare respiratory capacity% (=Maximal Respiration/ Basal Respiration). Data represents Mean ± SEM, n=4 independent experiments, student t-test. *p<0.05.*

As mitochondrial spare respiratory capacity determines the capability of producing extra energy on demand, it serves as an important indicator for cell survival under stressed conditions. Therefore, cell viability assays were conducted. Although at 24h and 48h (data not shown) no change in cell number was observed, at 72h there was a clear reduction in cell viability as quantified by using MTT (**Fig 3.8A**) and Calcein assay (**Fig 3.8B**)**.** MTT assesses cell metabolic activity as it's reduced to formazan by mitochondrial succinate dehydrogenase. Calcein AM is a non-fluorescent cell-permeant dye that can be converted to green-fluorescent calcein in live cells. The green fluorescence was quantified using a plate reader. Together, these two cell viability assays indicate that cell density is slowly reduced over time when α-syn is over-expressed.

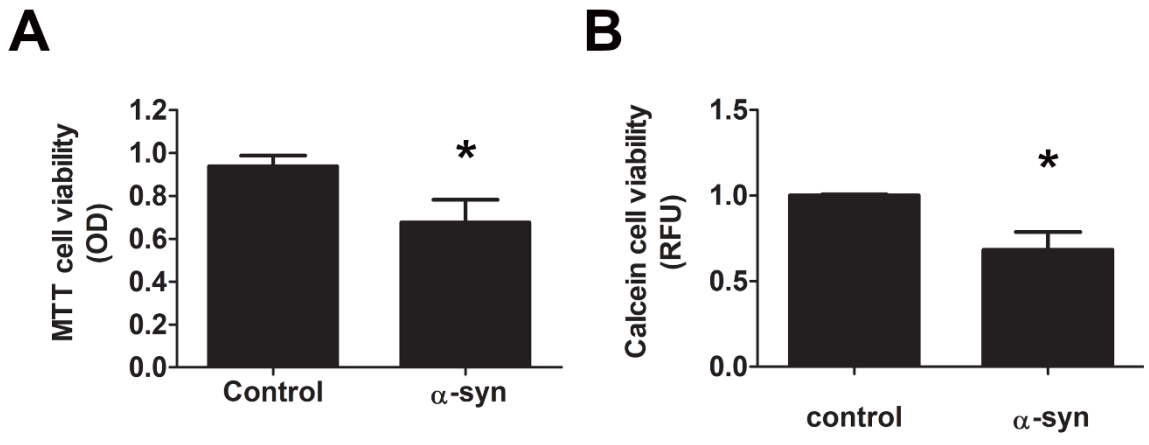

Figure 3.8 α-syn overexpression reduces cell growth. *Stable N27 cells were grown in 96 well plates and treated with PonA for 72h before cell viability was assessed.* ***(A)*** *25 µl MTT (5 mg/mL in PBS) were added directly to the wells containing 100 µl media. Optical density was determined by measuring absorbance at end point 560.* ***(B)*** *Cells were washed with PBS before Calcein AM was added. Fluorescence (Ex/Em* 494/520*) was measured 1h after incubation in dark. Data represent Mean ± SEM, n=3-4 independent experiments, student t-test. *p<0.05.*

3.3.3. 48h α-syn overexpression forms protein aggregation whilst inducing blockade of autophagy flux

Alongside with mitochondrial fragmentation and dysfunction, a distinctive feature of α-syn overexpression is the accumulation of puncta in α-syn staining. To confirm the formation of protein aggregation, proteinase K (PK) digestion was performed. As seen in **Fig 3.9A & B**, 48h after induction, α-syn aggregates(green puncta) were readily detectable in cells with inducible α-syn but not in cells with empty vector control. It's worth noting that the majority of the puncta stain disappeared after PK digestion, suggesting the abundance of soluble oligomeric forms of the protein. Non-soluble aggregation was used in this study as an indicator for insufficient clearance and protein build-up. This is not a suggestion that the soluble oligomers are less

toxic. In fact, studies suggest the soluble forms are more mobile and they promote protein propagation by acting as toxic seeds (Lashuel et al., 2013).

Interestingly, increased numbers of what appeared to be vacuoles were also observed in cells overexpressing α-syn, as highlighted by the yellow arrows (**Fig 3.9C**). To confirm whether these black circular structures were indeed vacuoles, TEM was used. Not only did these EM images reveal vacuoles in these cells (yellow arrows), they also indicated that these structures were part of the machinery of the autophagy process because they contained remnants of organelles, including mitochondria (**Fig. 3.9D**). To further investigate the effects of α-syn on autophagy, N27 inducible cells were transfected with LC3-mcherry (autophagosome membrane marker), and immuno-stained for autophagic substrate p62 (grey) and α-syn (green, **Fig 3.9E & F**). After 48h of α-syn expression, both LC3(red)and p62puncta were increased, indicating a blockade of autophagy flux as both autophagy machinery (autophagosomes) and substrate (p62) were accumulating inside the cells (**E**). The blockade was quantified using Image J (**Fig. 3.9 F**). These data suggest that autophagy-lysosomal pathway is compromised in α-syn-expressing cells, consistent with previous reports (Decressac et al., 2012a, Freeman et al., 2013)

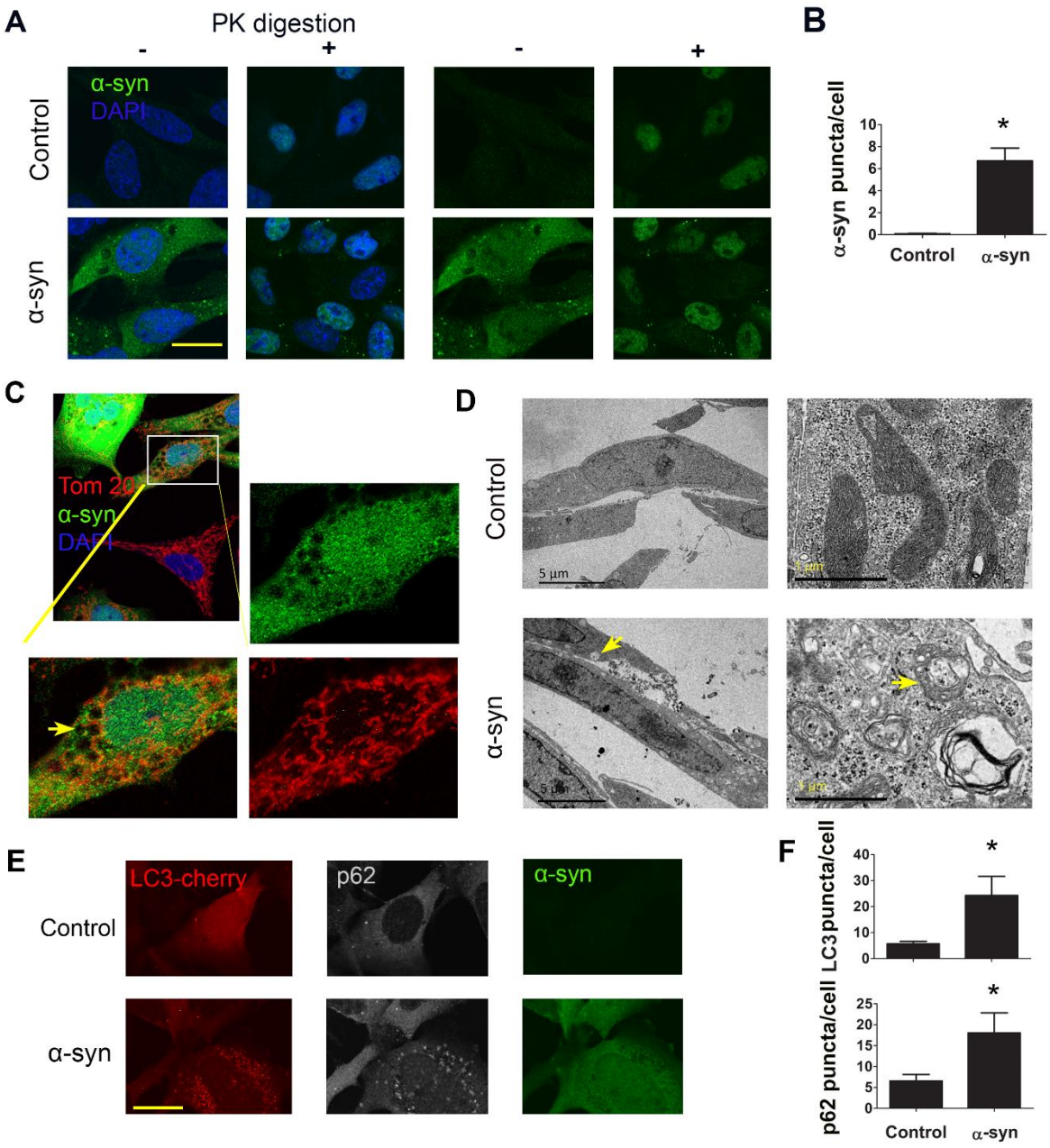

Figure 3.9 α-syn overexpression forms PK resistant aggregates and accumulation of autophagic vesicles. (*A and C)* *Stable N27 cells grown on cover glass were induced with PonA for 48h, fixed and immediately proceeded to PK treatment for 20min at room temperature. Cells were then immunostained for α-syn. Representative ICC images show α-syn (green) overexpression resulted in proteinase K (PK) resistant puncta, which were quantified using Image J with an average of 30 cells were counted for each treatment group per repeat. Data represent mean ± SEM, analysed by student t-test, n=3 independent experiments *p< 0.05.* ***(C)*** *Among the N27 cells without PK digestion, some with α-syn puncta formation (as shown in* ***A****) are accompanied by accumulation of small vesicles appearing as black vacuoles (arrows).* ***(D)*** *Stable N27 cells grown in 6 well plates*

were induced with PonA for 48h and fixed and scrapped off for TEM imaging. Representative EM images taken at different magnifications confirming the accumulation of small vesicles that presented features resembling those of autophagic vesicles. Scale bars as indicated. ***(E)*** *Stable N27 cells were transfected with LC3-mcherry (autophagosome membrane marker), and co-stained for autophagic substrate p62 (grey) and α-syn (green). An increase in both LC3 and p62 puncta were observed in cells with α-syn. (****F****) LC3 and p62 puncta (as shown in panel* ***E****) number per cell upon were quantified using Image J. For quantification, images were captured with a Nikon microscope using X100 Objective. On average 20-30 cells were counted per treatment in each individual experiment, with 4 separate experiments performed. Confocal images were captured with Olympus Fluoview FV1200 X60 Objective. Data represent Mean ± SEM, analysed by one-way ANOVA, followed by Newman-Keuls post hoc test. *p< 0.05 Scale bar: 20μm.*

It's worth noticing that there were less puncta after PK treatment, suggesting some of puncta were soluble oligomeric forms of the protein. Recent literature suggests these soluble misfolded forms are more toxic due to their mobility which could contribute to protein propagation in α-syn pathology. However, in this study, no higher bands were seen in western blot possibly because they were broken down by RIPA buffer during cell lysis.

3.4. Discussion.

Mitochondrial dysfunction and impaired autophagy flux represent two major pathogenic mechanisms in PD. After the discovery of 1-methyl-4-phenyl-1,2,3,6-tetrahydropyridine (MPTP) as the chemical causing parkinsonism(Langston et al., 1983), mitochondrial dysfunction mediated by blockade of the electron transport chain has been quite well-investigated in PD. However, a more recent approach is to understand the impact of mitochondrial fusion and fission, not only for PD but also

other neurodegenerative diseases (Kandimalla and Reddy, 2016, Wang et al., 2016b, Andreux et al., 2013b).

To study the effects of α-syn on mitochondrial function and morphology, I used a rat dopaminergic neuronal cells to generate a model with inducible expression of α-syn. This stable cell model allowed me to observe mitochondrial fragmentation and dysfunction, ROS production, protein aggregation and autophagy blockade in a more controlled and consistent manner as compared to transient transfection. I observed excessive mitochondrial fragmentation and increased Drp1 levels 48h after α-syn induction. Functionally, these cells exhibited lower mitochondrial membrane potential, reduced ATP production and mitochondrial spare respiratory capacity, as well as increased levels of ROS. Both mitochondrial and total cellular ROS levels were quantified in my study. As compared to cellular ROS, the magnitude of ROS originating from mitochondria was less. There might be a few potential reasons for this observation: First, in addition to blocking the ETC resulting in the production of mitochondrial ROS, α-syn also induce ROS production from other non-mitochondrial sources. Second, the sensitivity of detecting ROS by MitoSOX may be lower than by DHE assay. Third, the basal mitochondrial metabolic activity of N27 cells is high and therefore, the “ceiling” of reaching maximal mitochondrial ROS is not very dramatic. Supporting this argument is the observation that rotenone, a specific complex I inhibitor, only induced approximately 1.5-fold higher of mitochondrial ROS as compared to the untreated control group.

In addition to mitochondrial ROS, using the extracellular flux analyser to measure mitochondrial respiration in live cells, I detected a reduction in mitochondrial spare respiratory capacity in cells with α-syn overexpression. Interesting, no other parameters such as basal respiration, proton leak were affected. This observation

could be explained by the slow and chronic effect of overexpressing a wildtype protein at a toxic level as compared to a selective mitochondrial inhibitor such as rotenone. Changes in maximal/spare respiratory capacity are more sensitive indicators of mitochondrial respiration as a drop in any supply to ETC complexes can cause this parameter to decrease. In **Chapter 4**, where I measured the toxicity of a mutant form of α-syn, a more severe drop in spare respiratory capacity was observed, and other parameters such as proton leak started to change. Although at the time I did not get a significance due to the limited experimental animal numbers.

Even though I could not generate those data with differentiated neurons in this study, the cell model used still offered valuable information on α-syn toxicity toward mitochondria and autophagy flux. My findings are consistent with literature investigating the toxicity of α-syn using different *in vitro* and *in vivo* models (Braidy et al., 2014, Tanik et al., 2013, Xie and Chung, 2012). Furthermore, the observations of increased Drp1 translocation and levels suggest excessive mitochondrial fission is involved in the process. Therefore, the next question I asked was whether blocking Drp1-mediated fission would attenuate these abnormal features observed in these cells.

4. Blocking Drp1 is protective against α-syn induced mitochondrial fragmentation and dysfunction

4.1. Introduction

In the previous chapter, I confirmed mitochondrial fragmentation and dysfunction as a result of α-syn toxicity. These observations appeared to be mediated by excessive mitochondrial fission because increased levels of Drp1 was observed at the mitochondrial and total levels. The therapeutic strategy, therefore, is to preserve mitochondrial morphology and function by targeting Drp1. Over the years, researchers have investigated different approaches to alter mitochondrial fission and fusion by targeting the key set of proteins such as Fis1, Mff and MiD49/51. As discussed, it is more effective to block Drp1 function directly rather than these Drp1 receptor proteins individually. In this study, Drp1 silencing via siRNA and dominant negative K38A transfection were both applied as complementary genetic strategies. However, to enhance the translational value of this study, I also used a putative small molecule inhibitor of Drp1, which is further described below.

In a high throughput drug screening study for mitochondrial division inhibitors, a small molecule termed **m**itochondrial **div**ision **i**nhibitor-1 (mdivi-1) was selected out of 23,000 candidates (Cassidy-Stone et al., 2008). The chemical name for mdivi-1 is 3-(2,4-Dichloro-5-methoxyphenyl)-2,3-dihydro-2-thioxo-4(1*H*)-quinazolinone, and at least two structural components of this molecule are vital for its function toward mitochondrial division: an unblocked sulfhydryl moiety on the 2'-position of quinazolinone and limited rotation about the 3'-position nitrogen-phenyl bonds. Even though initially the discovery of GTPase activity was characterised in its yeast homolog Dmn1(Cassidy-Stone et al., 2008), its protective effects consistent with blocking mitochondrial fission has been reported in numerous mammalian cultured cells and mouse models (Cui et al., 2010a, Solesio et al., 2012, Wang et al., 2016c,

Rappold et al., 2014, Manczak et al., 2011, Manczak and Reddy, 2015, Reddy et al., 2017, Grohm et al., 2012). More direct evidence of mdivi-1 blocking mammalian Drp1 GTPase activity has also been reported. For example, a study comparing different compounds with the inhibitory effects on Drp1 has confirmed the efficacy of mdivi-1 inhibiting approximately 50% Drp1 activity at 13μM (Numadate et al., 2014). A more recent study also demonstrated the inhibitory effects of mdivi-1 on the GTPase activity of Drp1 in mammalian cells (Manczak et al., 2019) Nevertheless, these studies does not eliminate the potential off-target effects of mdivi-1, a common observation of chemical treatments. For any study addressing the effect of blocking Drp1, alternative methods such us genetic inhibition of Drp1 as a complementary approach is necessary.

For clinical applications, non-invasive pharmaceutical approaches are more practical and more acceptable by patients, in comparison to gene therapy. However, for research purposes, the genetic approach holds more specificity, and is better for confirming any effects by targeting a specific protein. Therefore, in this study, the two complementary approaches were both applied, side by side, to investigate the protective effect of blocking Drp1. For genetic approach, I used siRNA to knockdown Drp1 as well as a dominant-negative mutation form Drp1-K38A (HA-tagged). This mutation lacks GTPase activity (Smirnova et al., 2001a), and forms characteristic puncta inside the cells attracting wild-type Drp1, which can be used as an indication for transfected cells (Cui et al., 2010a). For pharmaceutical approach, mdivi-1 was used. More details are discussed below in section 4.4.

4.2. Materials and Methods

4.2.1. Cell culture and transfections

Stable N27 cells were grown in RPMI +10%FBS +G418 (500ug/ml) + Hygromycin B (200ug/ml). Plasmid only transfections were carried out using Lipofectamine 3000 and transfections involving siRNA were carried out using jetPRIME following manufacturers' instructions. More details are described in **Chapter 2, Section 2.2.**

4.2.2. Immunocytochemistry

Stable N27 cells were transfected with Ds-Red mito and siRNA / Drp1-K38A plasmid overnight and induced with PonA the next morning. 48h after, cells were fixed with 4% PFA and stained for α-syn (1:2000, AB5038) and Drp1 (1:1000, BD 61113).

4.2.3. Functional studies

Mitochondrial membrane potential. Stable N27 cells were treated with PonA for 24h with/without Drp1 inhibition. They were then stained with 50nM tetramethylrhodamine methyl ester (TMRM) for 20 min at 37 °C. Fluorescent signal was analysed by BD Accuri C6 flow cytometer using FL-2 channel. For positive control, cells were treated with 20 μM carbonyl cyanide 4-(trifluoromethoxy) phenylhydrazone for 20 min to collapse $\Delta\Psi_m$, and the obtained TMRM fluorescence was used to set the threshold.

Oxidative Stress Stable N27 cells were treated with PonA for 24h with or without Drp1 inhibition. Upon assay, 10μM DHE were added to cell culture media, incubated for 20 min at 37°C. H_2O_2 (3mM) was used as a positive control. The dye was then

washed away with PBS, and cells were detached by tryspin, re-suspended in PBS+2%FBS, and analysed by flow cytometry. Data are expressed as the percentage of cells with signal above threshold set by H_2O_2.

Mitochondrial respiration N27 stable s were grown in XFe 96 tissue culture plate and induced with PonA with/without Drp1 inhibition. On the day of experiment, cell culture media was replaced with 175ul XF assay medium (Dulbecco's Modified Eagle's Medium with 4.5mM Glucose, sodium pyruvate, PH7.4), incubated in a 37°C non-CO2 incubator for at least 30min before being loaded into the analyser. Mitochondrial respiration was measured using the Mito-Stress Test (see **Chapter 2, Figure 2.2**) (Seahorse Biosciences Inc) as instructed by the manufacturer. Oligomycin (1µg/ml), FCCP (0.5µM), rotenone (1µM) and antimycin A (1µM) were sequentially added to cells to determine mitochondrial respiration. For normalization, cells were fixed with 4% PFA, followed by incubation of DAPI (80µl of 5µg/ml in PBS) for 10 min. For normalisation, the plate was then washed 3 time with PBS, and fluorescent signal of DAPI was quantified at Ex/Em 358/461 nm using the Biotak Synergy H1 Hybrid Reader. (For more details, see **Chapter 2, Section 2.5**)

4.3. Results

4.3.1. Drp1 inhibition rescues mitochondrial morphology

As shown in the last chapter, α-syn induced multiple abnormal alterations in cells that might be mediated by excessive mitochondrial fission, resulting in observations such as fragmented and donut-shaped mitochondria as my laboratory previously reported in a different genetic model of PD(Cui et al., 2010a) . The decrease in Aspect Ratio and increase in Roundness reflects fragmentation as both of these

values approach 1 as the particle becomes circular. To evaluate whether blocking Drp1 would be protective, I firstly evaluated mitochondrial morphology by performing immunofluorescence. Using DsRed-Mito transfection to visualize mitochondria, I observed that these organelles were fragmented in cells with α-syn overexpression (**Fig. 4.1**). Roundness and Aspect Ratio were calculated with and without Drp1 inhibition. For the genetic approach, Drp1 siRNA (**Fig. 4.1**) and a dominant negative mutation, Drp1-K38A (HA-tagged) (**Fig.4.3**), were applied. For the small molecule approach, mdivi-1 was used (**Fig 4.4**).

As shown in **Fig. 4.1**, Drp1 siRNA blocked mitochondrial fragmentation induced by α-syn efficiently, resulting in the appearance of normal and elongated mitochondria similar to control, while non-targeting scramble control showed mostly round, fragmented mitochondria (**Fig. 4.1A**). I then quantified mitochondrial morphology in a blinded manner using Image J and expressed the values as Aspect Ratio and Roundness (**Fig. 4.1B**).

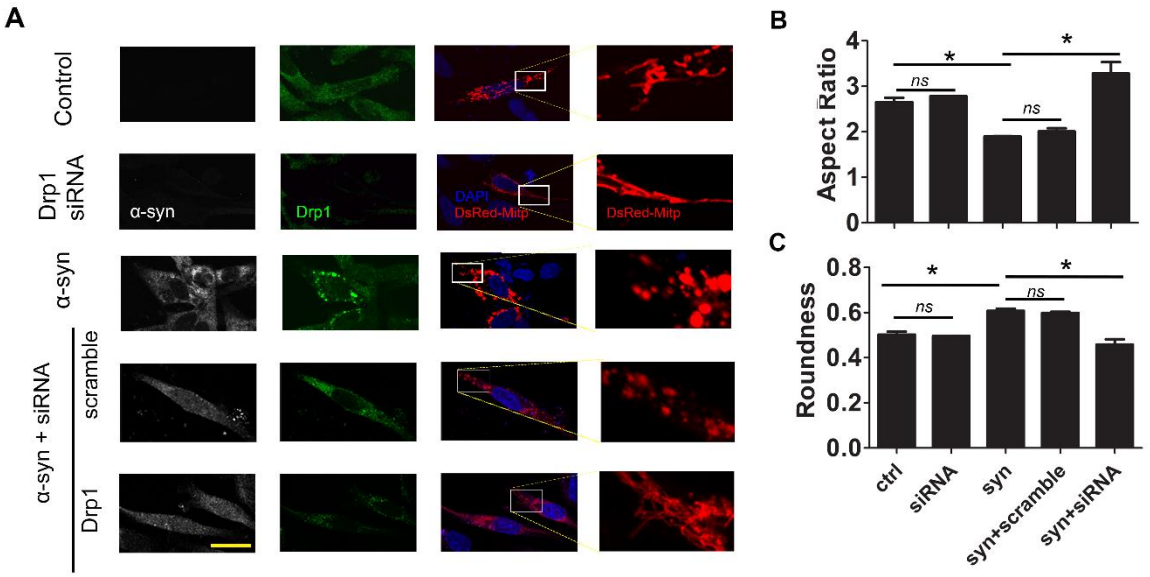

Figure 4.1 Drp1 inhibition via siRNA knockdown reduces mitochondrial fragmentation induced by α-syn overexpression. ***(A).*** *Stable N27 cells were co-transfected with Ds-Red mito and siRNA-Drp1 or scramble control over night, then induced with PonA for 48h. Representative images showing the effect of siRNA versus scramble control.* ***(B &C)****. Quantitative measurement of mitochondrial morphology by Image J. Roundness: 4 × ([Area])/ (π × [Major axis]^2). Aspect Ratio: The aspect ratio of the particle's fitted ellipse. Data represents the mean ± SEM, analysed by one-way ANOVA (n=4 or 5 with >500 mitochondria /group counted for each n), followed by Newman-Keuls post hoc test. *p< 0.05. Scale bar: 20μm.*

Drp1 knockdown efficiency was confirmed using western blot, with 10nM of siRNA achieving approximately 80% Drp1 reduction as compared to scrambled control (**Fig. 4.2**). Drp1 protein levels were quantified using Image J and normalised to housekeeping control β-actin.

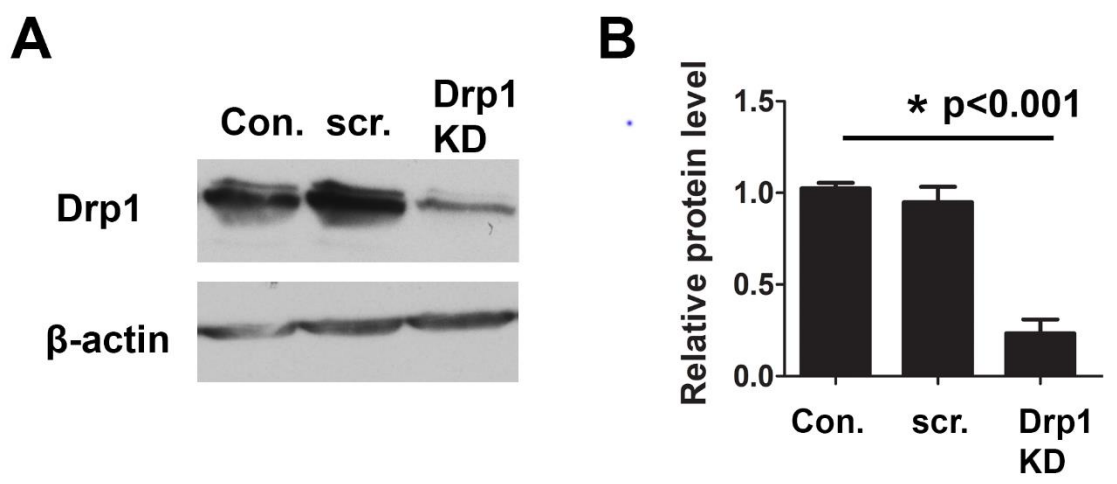

Figure 4.2 Efficiency of *Drp1* siRNA confirmed by western blot. (*A*). *N27 cells were transfected with siRNA-Drp1 or non-targeting scramble control for 48h and then collected for immunoblotting. Representative images of Drp1 levels and the loading control β-actin.* ***(B).*** *Drp1 levels were normalized to β-actin and quantified using ImageJ. Data represent mean ± SEM, analysed by one-way ANOVA, followed by Newman–Keuls post-hoc testing. n = 4 independent experiments*.

Next, I tested dominant negative Drp1-K38A transfection (**Fig. 4.3**). Because this mutant protein was tagged with HA and appears as small aggregates after transfection, I performed HA immunofluorescence to distinguish overexpressed mutant Drp1 from endogenous Drp1 to help identify cells expressing the mutation. Representative images captured using confocal microscopy shown in **Fig. 4.3A** illustrate cells with α-syn overexpression displaying small, fragmented mitochondria (red). However, cells with Drp1-K38A overexpression preserved tubular mitochondrial morphology in cells with α-syn overexpression. Mitochondrial morphology was quantified using using Image J and expressed as Aspect Ratio (**B**) and Roundness (**C**).

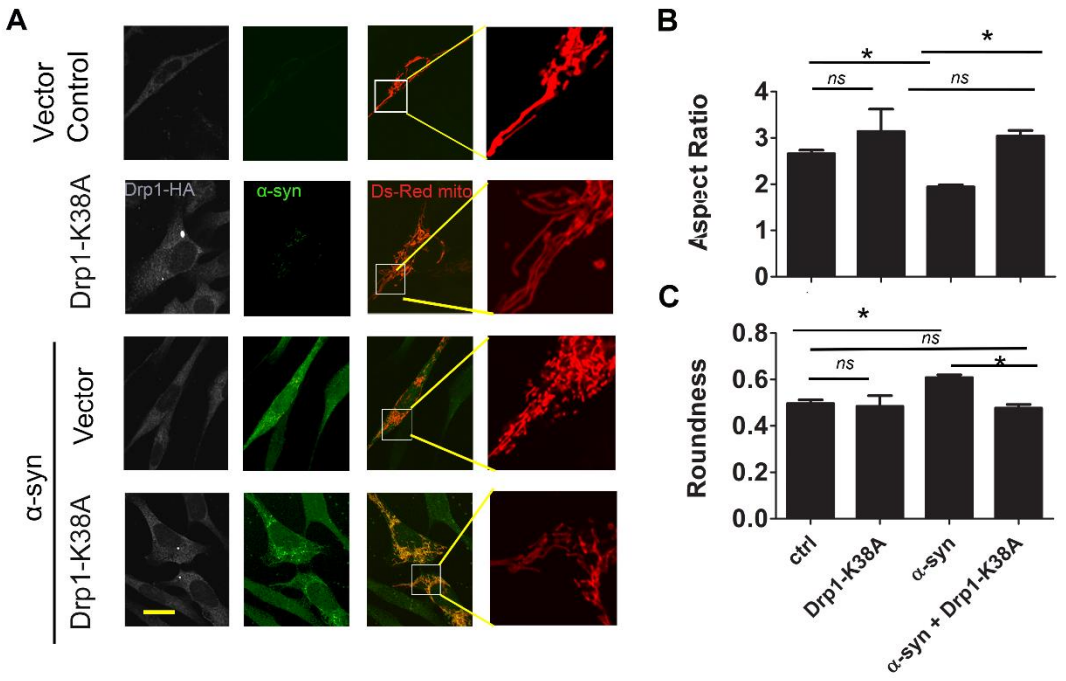

Figure 4.3 Drp1 inhibition through dominant-negative transfection reduces mitochondrial fragmentation induced by α-syn overexpression. ***(A)****Stable N27 cells were co-transfected with dominant-negative mutation Drp1-K38A (HA-tagged) and Ds-Red mito, then induced with PonA for 48h before fixation. HA and α-syn were probed by antibodies. Representative ICC images showing mitochondrial morphology in Drp1-K38A expression (as characterised by Drp1 puncta formation) cells versus α-syn overexpression alone.* ***(B &C)****. Quantitative measurement of mitochondrial morphology by Image J. Roundness: 4 × ([Area])/ (π × [Major axis]^2). Aspect Ratio: The aspect ratio of the particle's fitted ellipse. Data represent the mean ± SEM, analysed by one-way ANOVA (n=4 or 5 with >500 mitochondria /group counted for each n), followed by Newman-Keuls post hoc test. *p< 0.05. Scale bars: 20μm*

Together, consistent with the effects of siRNA knockdown, Drp1 dominant negative mutation also prevented mitochondrial fragmentation induced by α-syn. Lastly, I evaluated the protective effect of the small molecule, mdivi-1. As shown in **Fig. 4.4**, 10 μM mdivi-1 treatment for 48h protected mitochondria from being fragmented by α-syn. In summary, as demonstrated morphologically through images of immunofluorescence and quantitatively by calculating the values of Aspect ratio

and Roundness, all three strategies (genetically and pharmacologically) blocked mitochondrial fragmentation induced by α-syn.

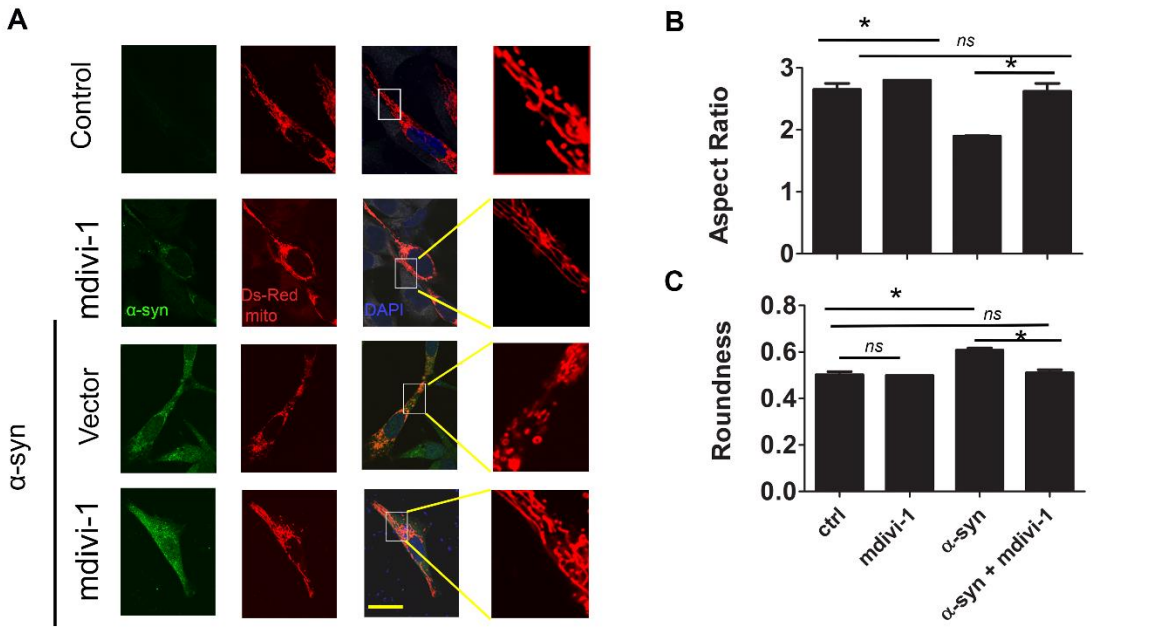

Figure 4.4 Drp1 inhibition by mdivi-1 reduces mitochondrial fragmentation induced by α-syn overexpression. *(A)*. *Stable N27 cells were transfected with Ds-Red mito and induced with PonA with/without mdivi-1 (10μM) for 48h before fixation. Representative ICC images shows that mdivi-1 treatment reduced mitochondrial fragmentation induced by α-syn overexpression.* ***(B &C)***. *Quantitative measurement of mitochondrial morphology by Image J. Roundness: 4 × ([Area])/ (π × [Major axis]^2). Aspect Ratio: The aspect ratio of the particle's fitted ellipse. Data represent the mean ± SEM, analysed by one-way ANOVA (n=4 or 5 with >500 mitochondria /group counted for each n), followed by Newman-Keuls post hoc test. *p< 0.05. Scale bars: 20μm*

4.3.2. Drp1 inhibition rescues mitochondrial function and cell viability

Based on the observation that blocking Drp1 protected mitochondrial morphology against α-syn neurotoxicity, I asked whether Drp1 inhibition would also improve

mitochondrial function. To this end, I evaluated multiple mitochondrial function parameters. The efficiency of plasmid transfection in N27 cells is below 50%, this could dilute the effect of Drp1 inhibition. Therefore, only siRNA knockdown and small molecule inhibition are used in the following experiments with the same cell model. First, I measured mitochondrial membrane potential ($\Delta\Psi_m$). As previously discussed, a decrease in $\Delta\Psi_m$ is indicative of mitochondrial dysfunction. Using flow cytometry, I quantified fluorescent intensity of tetramethylrhodamine (TMRM) taken up by mitochondria in N27 cells. After 48h of induction, α-syn significantly reduced $\Delta\Psi_m$. Drp1 inhibition, either mediated by gene silencing (**Fig. 4.5A)** or the small inhibitor mdivi-1(**Fig. 4.5B**), completely prevented this deficit. An impairment in mitochondrial function invariably would lead to free radical production such as reactive oxygen species (ROS). To determine whether such ROS production would originate from mitochondria resulting in a higher total cellular ROS, I quantified Dihydroethidium (DHE, **Fig. 4.5C&D**) and MitoSOX Red (**Fig. 4.5E&F**) signals to detect cellular and mitochondrial ROS levels, respectively. Rotenone, a complex I inhibitor, was used as a positive control to generate ROS from the electron transport chain (ETC) blockade. Consistent with its inhibitory effect on mitochondrial function, α-syn increased ROS levels, an adverse effect that was blunted by Drp1 inhibition (**Fig. 4.5C-F**). Taken together, these mitochondrial studies support the negative effects of α-syn on the mitochondrial ETC and that blocking Drp1, whether genetically or pharmacologically, is protective.

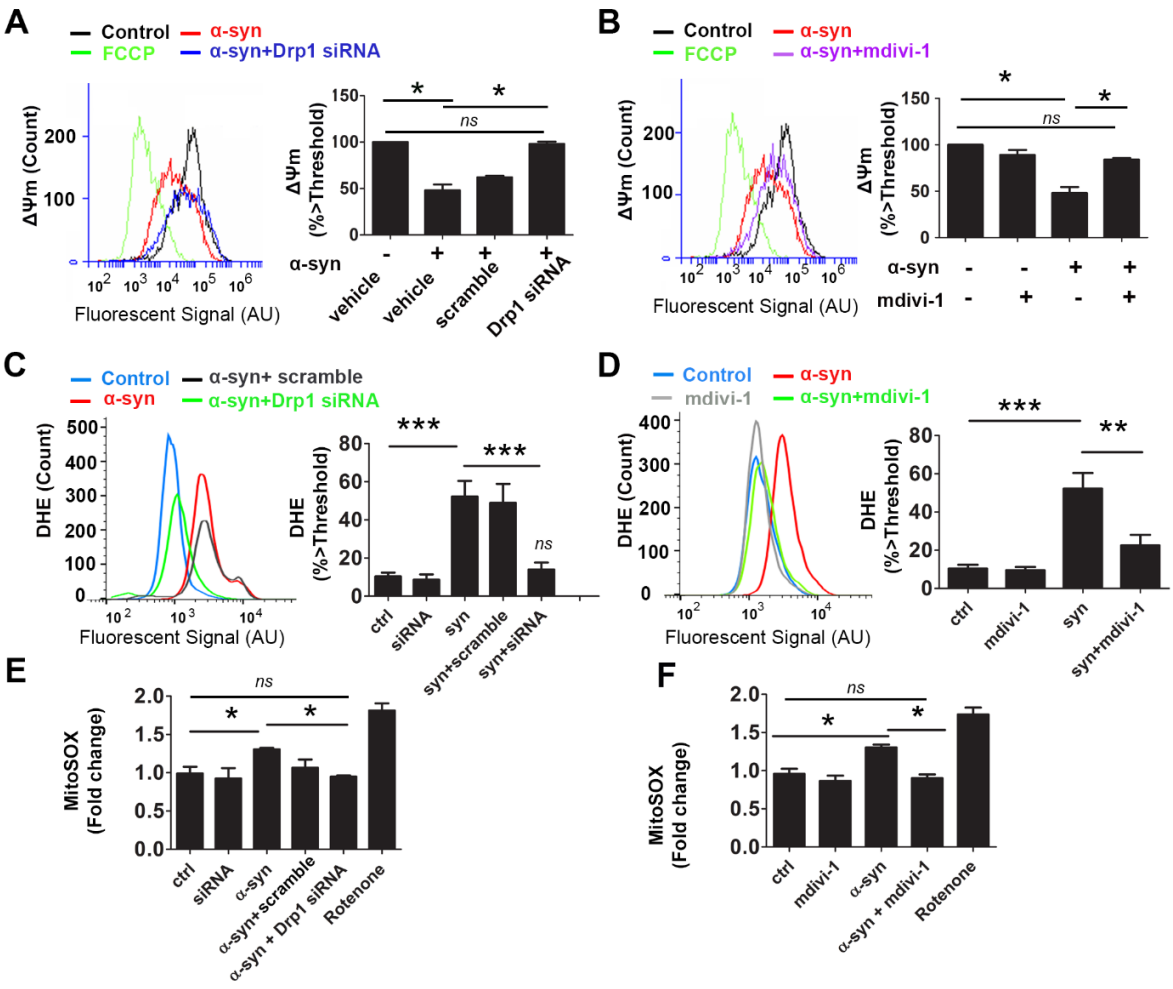

Figure 4.5 Drp1 inhibition restores $\Delta\Psi_m$ and reduces oxidative stress from α-syn overexpression. ***(A&B)*** *Stable N27 cells were incubated with TMRM (50nM), and fluorescence intensity was analysed by flow cytometry for ΔΨm. The uncoupler agent carbonyl cyanide 4- (trifluoromethoxy) phenylhydrazone (FCCP, 20μM) was used as positive control to set up threshold.* ***(C&D)*** *Cellular ROS was measured by incubating cells with 10 μM Dihydroethidium (DHE) and analysed by flow cytometry. Signal intensity (AU, arbitrary unit) was expressed as % above threshold established by FCCP.* ***(E&F)*** *MitoSox red signal was measured by incubating cells with 2.5 μM working solution of the dye for 20min and analysed by fluorescent plate reader (Ex/Em 510/580nm). For normalization, cells were fixed and subsequently stained with DAPI (Ex/Em 385/461 nm), and relative fluorescence units (RFU) were calculated by dividing mitosox intensity against DAPI. Mitochondrial complex I inhibitor rotenone (50nM) was used as positive control to induce oxidative stress. For Drp1 silencing, stable N27 cells were transfected with siRNA-Drp1 or scramble control overnight, followed by PonA induction for 48hs. For mdivi-1 treatment, cells were co-treated with PonA and mdivi-1 (10μM) for 48h. Data represent the mean± SEM ., analysed by one-way ANOVA (n=4), followed by Newman-Keuls post hoc test. *p< 0.05 ** p≤0.02, *** p<0.001*

To directly measure mitochondrial function, I quantified mitochondrial respiration using the Seahorse XFe96 Extracellular Flux Analyzer (**Fig. 4.6**). After 48h of induction of α-syn expression in the stable dopaminergic N27 neuronal cells, I assessed multiple mitochondrial respiration components as illustrated in **Fig. 4.6A**, with or without Drp1 inhibition (both siRNA knockdown and mdivi-1 inhibition). **Fig. 4.6B & D** show that α-syn specifically reduced mitochondrial respiration and siRNA-Drp1 or mdivi-1 blocked this deficit.

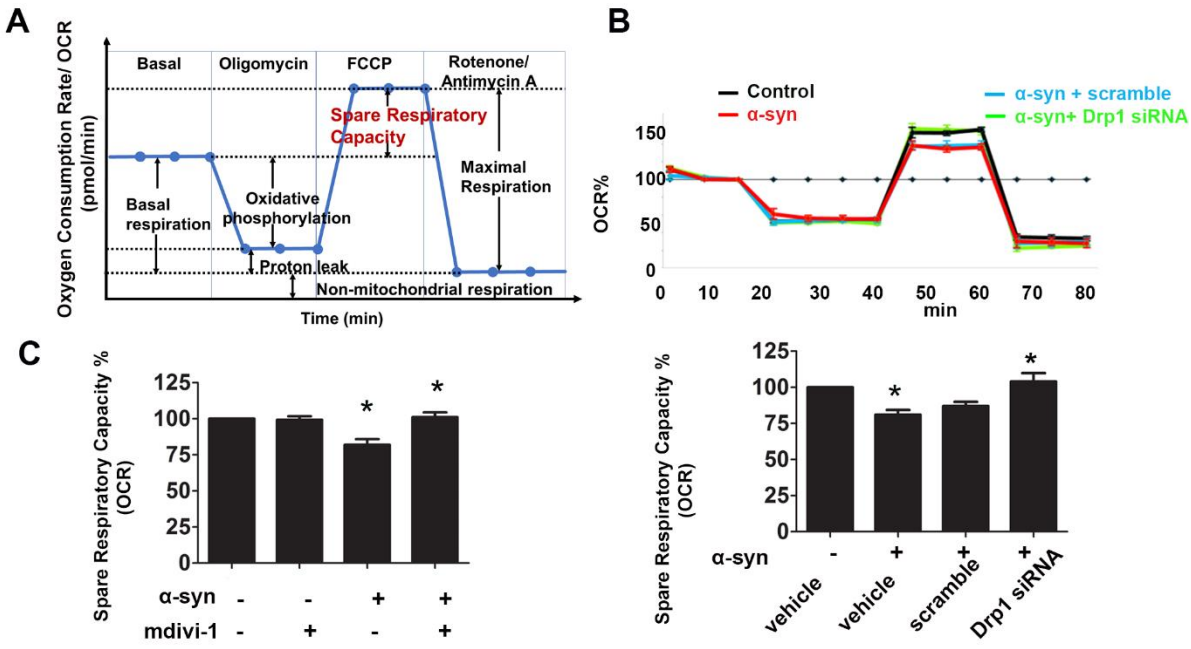

Figure 4.6 Drp1 inhibition is protective toward mitochondrial spare respiratory capacity reduced by α-syn overexpression ***(A)*** *As previously explained in* ***Fig. 3.5****, mitochondrial function in live cells was assessed by measuring oxygen consumption rate (OCR) using the XFe96 Extracellular Flux Analyzer.* ***(A)*** *Sequential injections of oligomycin (to inhibit oxygen consumption mediated by ATP synthase), FCCP (an uncoupler to induce maximal OCR), Rotenone/Antimycin (to inhibit complex I and III, respectively). Spare Respiratory Capacity was calculated as % = (Maximal Respiration) / (Basal Respiration) × 100.* ***(B)*** *Representative kinetic graph showing 48h of α-syn overexpression impairs spare respiratory capacity, and Drp1 knockdown conferred protection. (****C****) Blocking Drp1 function using mdivi-1 was also protective. Data represent the mean± SEM analysed by one-way ANOVA (n=4), followed by Newman-Keuls post hoc test. *p< 0.05*

Corresponding to the improved profiles of spare respiratory capacity, $\Delta\Psi_{m,}$ ROS production and mitochondrial morphology, Drp1 knockdown also attenuated cell loss induced by α-syn 72h after gene induction, as assessed by using calcein assay (**Fig. 4.7**). Calcein AM is a non-fluorescent cell-permeant dye that can be converted to green-fluorescent calcein in live cells.

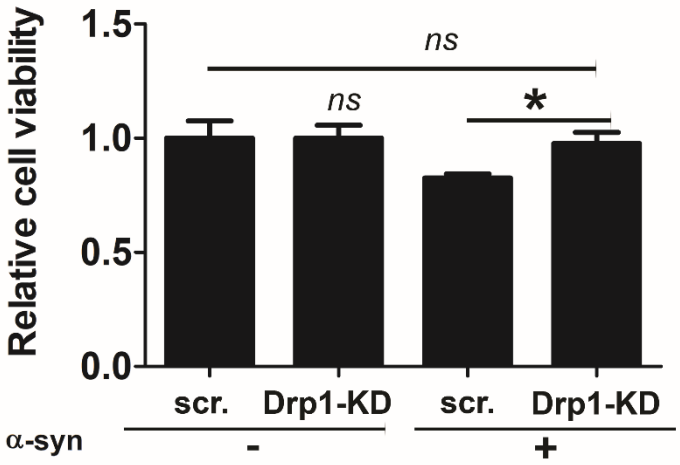

Figure 4.7 Drp1 inhibition prevents cell loss induced by α-syn overexpression *Stable N27 cells were transfected with Drp1 siRNA or scramble control overnight prior to be treated with PonA for 72h to activate* α-syn expression*. Calcein AM was then added to the cells after washing with PBS. The green fluorescence was quantified using a plate reader. Data represent the mean± SEM., analysed by one-way ANOVA (n=4), followed by Newman-Keuls post hoc test. *p< 0.05. ns marked are compared to control level.*

4.3.3. Drp1 inhibition protects synaptic mitochondrial respiration *in vivo*

As demonstrated so far in my project, using the N27 dopaminergic neuronal cells, I evaluated multiple mitochondrial function parameters to determine whether blocking

Drp1 would confer protection against α-syn With this *in vitro* model, I demonstrated that blocking Drp1 function by using siRNA, overexpressing the dominant negative Drp1-K38A, and small molecule mdivi-1 in dopaminergic neuronal N27 cells with inducible α-syn reduced mitochondrial fragmentation (**Fig4.1**), preserved *ΔΨm* (**Fig 4.5A & B**), reduced ROS production (**Fig 4.5C-F**), and protected mitochondrial respiratory capacity (**Fig 4.6**). Furthermore, the improved mitochondrial function reduced cell loss induced by α-syn at a later stage In addition to the above *in vitro* model, I also collaborated in a separate study using a rat model overexpressing mutant α-syn A53T via adeno-associated virus (AAV2). This mutant α-syn also impair mitochondrial function. In general, α-syn has been demonstrated in rodent models to reduce striatal presynaptic dopamine release (Chen et al., 2015, Nemani et al., 2010, Larsen et al., 2006, Burre et al., 2010, Garcia-Reitbock et al., 2010), and impair mitochondrial respiration in the striatum (Subramaniam et al., 2014). Together, these observations are consistent with the critical role of mitochondria in synaptic function(Manczak et al., 2016, Kandimalla et al., 2016). With the promising results from my cell culture experiments, it is important to determine the protective role of Drp1 inhibition against α-syn toxicity *in vivo*. To address whether blocking Drp1 improved mitochondrial function in an animal model, I isolated synaptosomes from the striatum of rats with stereotaxic injection of AAV2 encoding human A53T-α-syn or GFP control with or without i.p. injections of mdivi-1 or vehicle control (surgeries and injections were done by Dr. Martin Helley), One week later, striatal synaptosomes were isolated and measured for mitochondrial function using XFe96 Extracellular Flux Analyzer with a method adapted from a previous study (Choi et al., 2009b). The high sensitivity of this assay format allows measurement of mitochondrial respiration in relatively small quantity and thus facilitates the

assessment in specific brain regions. Of note, prior to the isolation experiments, the delivery and expression of AAV has been verified by immunostaining (performed by Martin Helley, data not shown). As seen in **Fig. 4.8**, one week after gene delivery (an early time point that induces about 50% cell death) (Bourdenx et al., 2015a), A53T-α-syn significantly impaired maximal rate of mitochondrial respiration as compared to the control group, resulting in reduced spare respiratory capacity. This set of data has recently been published (Bido et al., 2017c), in which I served as a co-author.

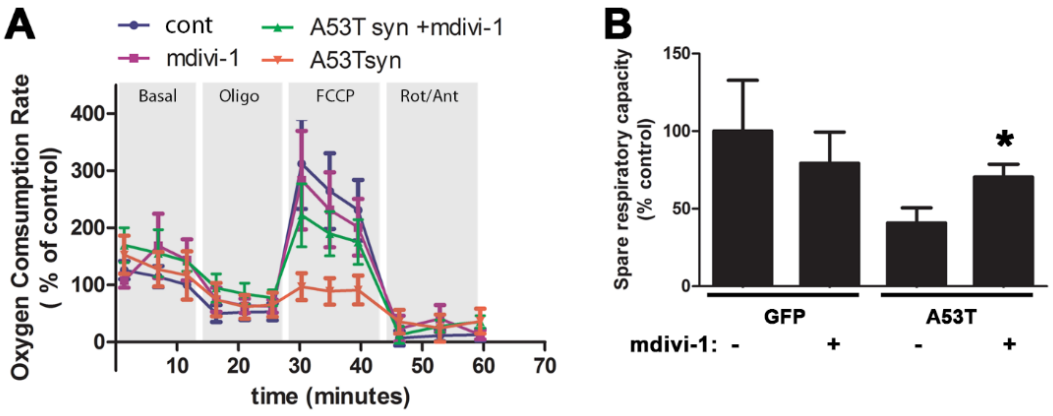

Figure 4.8 Drp1 inhibition by mdivi-1 attenuates mitochondrial dysfunction in isolated synaptosomes *A.* *Adult Sprague Dawley rats (6 weeks old) were stereotaxically injected with AAV2 encoding either human α-syn-A53T or GFP control in the substantia nigra in the absence or presence of mdivi-1 (20mg/kg twice daily i.p. injection). One week after gene delivery, striatal synaptosomes were processed and oxygen consumption rate (OCR) was measured using the XFe96 Extracellular Flux Analyzer. Sequential injections of oligomycin (to inhibit oxygen consumption mediated by ATP synthase), FCCP (an uncoupler to induce maximal OCR), Rotenone/Antimycin (to inhibit complex I and III, respectively).* ***B****.Values obtained from (A) were then used to calculate Spare Respiratory Capacity as a % = (Maximal Respiration)/(Basal Respiration) × 100 Data represent means ± SEM of 5 five animals per group (except for the GFP+mdivi-1 group, n = 3), Statistical analysis was performed using two-way ANOVA, followed by Tukey multiple comparison test (*p < 0.05 compared A53T groups with or without mdivi-1). (Bido et al., 2017c)*

So far in this study, I've been focusing on the effect of Drp1 in s α-syn-induced mitochondrial toxicity. Cell culture results confirmed the hypothesis that α-syn overexpression results in mitochondrial fragmentation and dysfunction and blocking the fission protein Drp1 provides rescuing effect. The collaboration project working with the mutant form of α-syn further confirms the finding in rats. Together, these data highlight the effectiveness of blocking Drp1 via the mitochondrial pathway.

4.4. Discussion

In this chapter, I focused on the protective effect of blocking Drp1. In stable dopaminergic neuronal cells with inducible expression of α-syn, reducing Drp1 function genetically (Drp1 knockdown and overexpression of Drp1-dominant negative) and pharmacologically (mdivi-1 treatment) attenuated the negative impacts of α-syn on mitochondrial morphology and function (membrane potential, reactive oxygen species, respiration and spare respiratory capacity (SRC). As discussed, a reduction in SRC leads to energy crisis when energy demand exceeds the supply ability of mitochondria and SRC has been considered as a major factor that defines the survival of the neuron (Choi et al., 2009a). Together, these results support the hypothesis that α-syn induces mitochondrial fragmentation and dysfunction through, at least partially, a Drp1-dependent mechanism. This topic has been discussed and debated in the field, partly because of some conflicting data between previous studies (Gui et al., 2012, Kamp et al., 2010). A significant difference between my model and those from other laboratories is the utilisation of the inducible cell line to keep α-syn expression at relatively lower and more consistent levels compared to

transient transfection. Additionally, I believe I used multiple complementary approaches to confirm my results. For example, I used two genetic and one chemical strategies to block Drp1 function. I measured multiple parameters of mitochondrial function, in addition to morphology.

Relevant to my project, my laboratory collaborated with another group in France and together we recently published data demonstrating that intraperitoneal injection of mdivi-1 reduced neuropathology induced by α-syn-A53T in rats (Bido et al., 2017a). We reported that mdivi-1 improved locomotor function and reduced nigral dopaminergic neuronal death. Intriguingly, mdivi-1 also significantly reduced α-syn-Ser219, a phosphorylated form which correlates to increased protein aggregation. Consistently with this observation, we also observed mdivi-1 reduced proteinase K-resistant α-syn. Together, these data suggest that blocking Drp1 function results in the reduction of formation of the toxic species of α-syn and protein aggregation. However, the underlying mechanism that provided these observations remained to be established. Because autophagy plays a major role in removing misfolded and aggregated proteins, it is possible that Drp1 inhibition also plays a role in autophagy. Given that I have already demonstrated in my N27 stable cell line that α-syn blocks autophagy (**Chapter 3, Fig. 3.9**), I decided to investigate the effect of blocking Drp1 on autophagy flux and protein aggregation, which is the topic in the next chapter.

5. Drp1 inhibition is protective against impairment of autophagy flux induced by α-syn

5.1. Introduction

Autophagy plays a critical role in removing misfolded proteins, including α-syn (Webb et al., 2003a, Cuervo et al., 2004, Lee et al., 2004). Therefore, impairment in autophagy leads to accumulation of α-syn, which further exacerbating the blockade of autophagy as demonstrated cell culture and animal models (Winslow et al., 2010b, Ebrahimi-Fakhari et al., 2011, Yu et al., 2009, Chen et al., 2015, Bido et al., 2017a), thus creating a bidirectional positive feedback loop of neurotoxicity (Xilouri et al., 2016). Although still a topic of debate, a general assumption is that monomeric forms of α-syn can largely be degraded by the UPS, while the oligomeric and aggregated forms of the protein, like other longer-lived macromolecules, mostly rely on autophagy-lysosome pathway for degradation (Ji and Kwon, 2017). This is based on the functional property and pattern of each pathway. Therefore, the formation of α-syn aggregation could be linked to lack of autophagy, as suggested in recent literature (Winslow and Rubinsztein, 2011, Sato et al., 2018).

In addition to mitochondrial dysfunction, my data in **Chapter 3** indicate that autophagy flux is impaired in my stable N27 dopaminergic neuronal cell model, as evidenced by an accumulation of LC3 and p62 puncta in α-syn overexpressing cells. Additionally, I observed the formation of PK resistant α-syn puncta after 24h of α-syn overexpression in N27 stable cells. My laboratory recently demonstrated that pharmacological blocking of Drp1 dramatically reduced α-syn aggregates in nigral DA neurons of rats overexpressing α-syn (Bido et al., 2017b). However, it was not determined whether such protective effect was mediated through the autophagy pathway. Taken together, therefore, it is critical to investigate whether blocking Drp1,

in addition to preserving mitochondrial function, could also have a protective role towards autophagy.

Commonly, studies use LC3-II, the autophagosome membrane protein, as an indication for autophagy change (Afeseh Ngwa et al., 2011). However, LC3-II level (or the number of autophagosome and autolysosome levels collectively) alone is not sufficient to determine the state of the autophagy flux. As autophagy is a dynamic process, the number of autophagosome is determined by both upper (induction) and lower (degradation) streams of the flux. Therefore, the increase of LC3-II level could be from increased induction or disturbed degradation, or a combination of both. In order to more fully evaluate whether autophagy is blocked, it is important to combine LC3 quantification with an autophagy substrate such as p62 or ubiquitin. In the situation of increased autophagy induction, LC3-II level would increase but not p62, whereas the blockade of lysosomal degradation would result in the increase of both markers. In fact, p62 would be a more reliable marker for quantifying autophagy blockade as the increase in p62 is a direct result from disrupted autophagy. Two cell line models were used in this chapter. The same stable N27 cells were used for direct association of autophagy and puncta formation in the cell, and for correlation of mitochondrial dysfunction and autophagy. To more directly monitor autophagy flux in the present study, I utilized the autophagy reporter HeLa cells with stable overexpression of mRFP-GFP-LC3 (kindly provided by Dr. Shouqing Luo, Plymouth University). These cells were designed to monitor autophagy flux(Kimura et al., 2007). The ratio of autophagosome against autolysosome obtained from the HeLa cells provides information that cannot be measured directly in N27 cells.

5.2. Materials and Methods

5.2.1. Cell culture and transfection

Stable N27 cells were maintained in selective media that contains RPMI +10% FBS + G418 (500 µg/ml, Invitrogen) + Hygromycin B (200 µg/ml)

Hela autophagy reporter cells were maintained in selective media with DMEM+ 10%FBS +G418 (100 µg/ml). This cell line is stably transfected with a construct containing RFP-GFP-tagged LC3 (see **Fig. 5.2A**) and have autophagosome puncta labelled with both green and red signal simultaneously. The GFP signal is pH sensitive whilst the RFP signal is pH stable. When autophagosomes fused with the acidic lysosomes, the low pH quenches the GFP signal, leaving only the red signal. This allows for the distinction between autophagosomes (yellow-GFP and RFP merged), and autolysosomes (red-RFP only), a more detailed and insightful way to monitor autophagy blockade.

Plasmid transfection Stable N27 cells were transiently transfected with LC3-cherry plasmid, and Hela cells were transfected with α-syn plasmid using lipofectamine 3000 following manufacturer's protocol.

Drp1 knockdown 10nM of Dharmacon SMARTpool siGENOME DNM1L siRNA (Rat for N27 cells and Human for Hela cells) or non-targeting scramble control were added to cell suspension upon plating.

5.2.2. PFF treatment

α-syn monomers were obtained from the Michael J. FOX Foundation, and the generation of PFF was performed by shaking at 1,000 RPM for seven consecutive days at 37°C according to manufacturer's protocol (more details can be found in **Chapter 2, Section 2.7**). Upon use, one aliquot was diluted into 0.1mg/mL using

sterile dPBS and sonicated with a Fisher Scientific 120 Sonic Dismembrator with CL-18 microtip (30 X1s pulses, 20% power). 10µg/ml sonicated PFF were added the Hela cells grown in 6-well plates.

5.2.3. Quantification analysis

Puncta quantification For puncta quantification, images taken at 60X for individual channels (in tif. format) were imported into Image J and analysed using objective counter.

Western blot N27 stable cells were induced with PonA for 48h with or without Drp1 inhibition. Upon experiments, cell pellets were collected and lysed with RIPA buffer plus proteinase inhibitors, homogenised on ice, and supernatants were loaded on to a 12% SDS-PAGE for separation and transferred to a PVDF membrane. After blocking with 2.5% skin milk, membranes were incubated in primary antibody solutions at 4C overnight: anti-p62 (1:1000, MBL PM045), anti-Drp1 (1:2000, BD 61113), anti-β-actin (1:10,000, Sigma A2228).

Proteinase K digestion N27 cells were grown on glass coverslips coated with poly-D-lysine. Freshly fixed cells were washed with PBS 2X, and incubated with proteinase K (0.34U/ml) for 20 min at room temperature with shaking. Cells were then washed with PBS and proceeded to immunostaining for α-syn.

5.3 Result

5.3.1 Drp1 inhibition protects autophagy flux in stable N27 cells

As discussed above, autophagy is a primary pathway by which misfolded proteins such as α-syn are removed (Webb et al., 2003a, Cuervo et al., 2004, Lee et al., 2004).

One possible mechanism by which Drp1 inhibition reduced protein aggregation is by improving autophagic flux. Because LC3-II is selectively associated with autophagosomes, LC3-II or LC3-decorated vesicles has been widely used to indicate autophagosome levels or contents in cells (Klionsky, 2005).The levels of p62 as a selective autophagy substrates inversely correlate with autophagic flux (Bjorkoy et al., 2005). To test the hypothesis Drp1 inhibition would attenuate autophagic impairment induced by α-syn, I quantified the levels of LC3-II and p62 levels in the N27 cells with inducible α-syn expression. To achieve this objective, I co-transfected N27 cells with LC3-cherry plasmid plus either siRNA-Drp1 or scramble control (an overexpression of LC3 was necessary to facilitate quantification of autophagy due to low expression of LC3 in these neuronal cells). As seen in **Fig. 5.1A & B**, α-syn significantly increased the number of LC3 puncta, supporting accumulation of autophagosomes. I also observed an increase in p62 puncta levels, indicating a blockade of autophagy (**Fig. 5.1A & B**). The alterations in p62 levels were also assessed using immunoblotting (**Fig. 5.1C**)**.** Together, these data suggest that autophagy-lysosomal pathway is compromised in α-syn-expressing cells, consistent with previous reports (Freeman et al., 2013, Decressac et al., 2012b). The accumulation of these autophagic proteins, however, was significantly attenuated by siRNA-Drp1 (**Fig. 5.1A-C**), suggesting that Drp1 inhibition restores autophagy-lysosomal activity or autophagic flux.

Protein aggregation is a common pathological feature of α-syn. In our cell model proteinase-K resistant α-syn aggregates were detectable two days after gene induction (**Fig. 5.1D & E**). Knocking down Drp1 with siRNA drastically reduced such protein aggregation (**Fig. 5.1D & E**). This genetic approach provided data consistent with our previous publication where α-syn-A53T accumulation in rats was significantly reduced by mdivi-1 (Bido et al., 2017a)

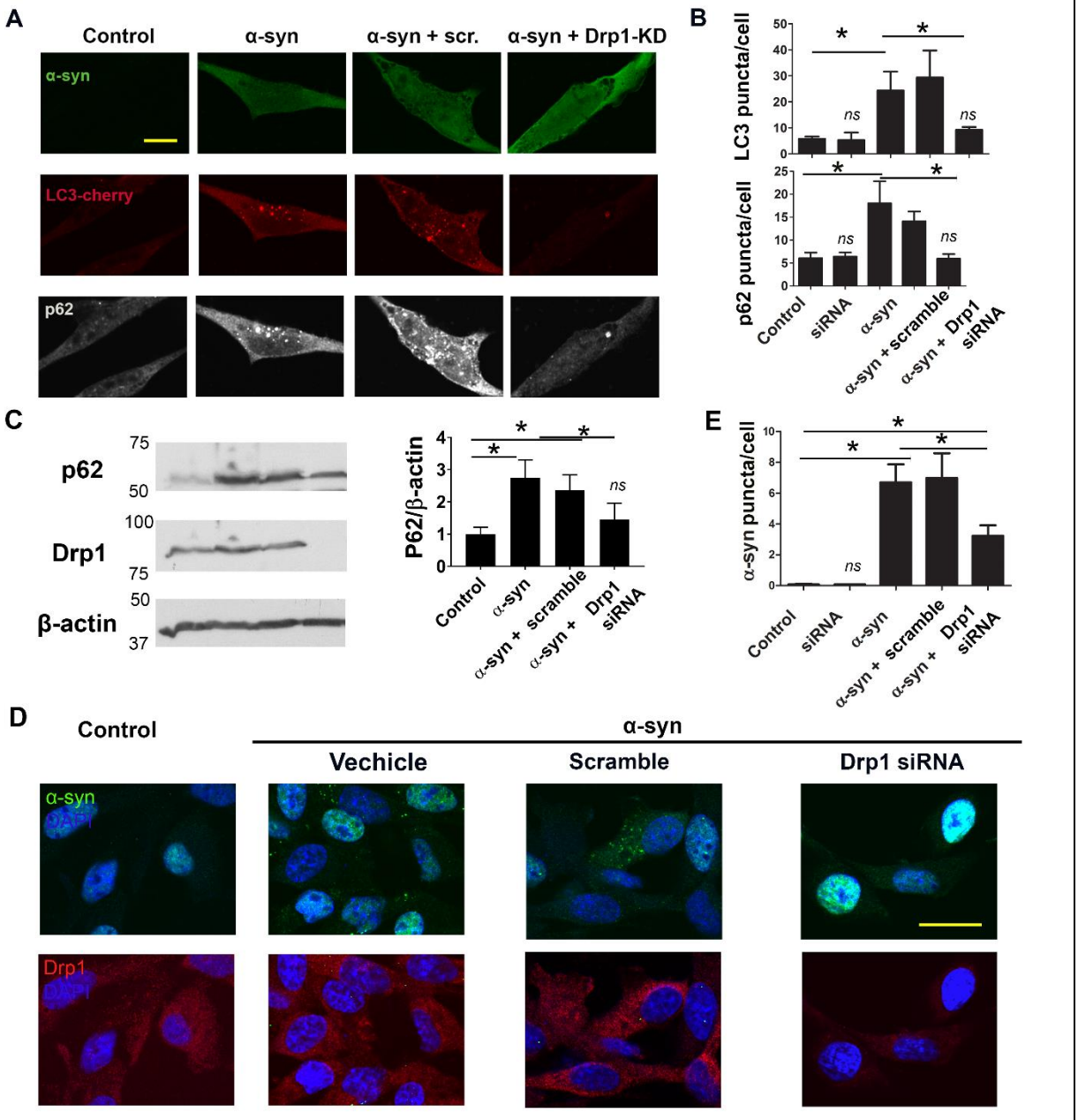

Fig 5.1 Drp1 inhibition attenuates autophagic blockade and protein aggregation in dopaminergic N27 neuronal cells with inducible α-syn. (*A*) *Stable N27 cells were co-transfected with LC3- LC3-cherry with and siRNA-Drp1 or scramble control, then induced with PonA for 48h. Cells were then fixed and immunostained for α-syn and p62. Representative ICC images demonstrate that the effect of Drp1 siRNA (10nM) transfection reduced on both LC3 (red) and p62 (grey) puncta versus cells overexpressing α-syn alone or with siRNA scramble.* ***(B)*** *Quantification of LC3 puncta and p62 puncta (as shown in A) number using Image J.*

Images for quantification were captured using a Nikon ECLIPSE TE2000-U microscope, with 100x objective. On average 20-30 cells were counted per treatment in each individual experiment, with 4 separate experiments performed. ***C*** *Stable N27 cells were transfected with siRNA-Drp1 or scramble control, then induced with PonA for 48h.Cells were then harvested, lysed with RIPA buffer, and separated by SDS-PAGE. Blots were probed as indicated. Data represent mean ± SEM* ***(D)*** *Stable N27 cells were induced with PonA for 48h, fixed and immediately incubated with proteinase-K (PK) for digestion. Drp1 and α-syn were then probed with antibodies. Representative images show protein aggregation upon α-syn overexpression with or without Drp1 inhibition by siRNA. Confocal images captured with Olympus Fluoview X60 Objective.* ***(E)*** *Proteinase-K resistant α-syn puncta number was counted using Image J, on average 30 cells were counted for each treatment group per repeat. Data represent mean ± SEM, analysed by one-way ANOVA, n=3 independent experiments, followed by Newman-Keuls post hoc test. *p< 0.05. Images for quantification were captured with a Nikon ECLIPSE TE2000-U microscope, with 100x objective, on average 20-30 cells were counted per treatment in each individual experiment, with 4 separate experiments performed. Data represent mean ± SEM, analysed by one-way ANOVA, followed by Newman-Keuls post hoc test. *p< 0.05. ns(non-significant) marked are compared to control levels. Scale bar: 20μm.*

5.3.2 Drp1 inhibition protects autophagy flux in HeLa autophagy reporter cells

Although the data presented in **Fig. 5.1** support the role of Drp1 in autophagy, to more directly monitor autophagy flux in my study, I utilized the autophagy reporter HeLa cells. These cells were designed to monitor the process of autophagosome fusing with lysosome during autophagy (as shown in **Fig.5.1Aa**) with stable overexpression of mRFP-GFP-LC3 (**Fig. 5.2Ab**). mRFP-GFP-LC3 vesicle analysis allows me to monitor autophagosome synthesis and autophagosome-lysosome fusion by labelling autophagosomes (green and red) and autolysosomes (red), since the low lysosomal pH quenches the GFP signal. Previously, α-syn was shown to impair autophagic flux with increased autophagosome accumulation and reduced autophagosome-lysosome fusion (Freeman et al., 2013). To investigate whether blocking Drp1 would improve

autophagy flux impaired by α-syn, I co-transfected these autophagy reporter cells with wild type human α-syn in the presence or absence of siRNA-Drp1 or siRNA-scramble control (**Fig. 5.2B**). After 48h, cells were immunostained for α-syn and the number of autophagosomes and autolysosomes were quantified in these immunoreactive cells in a blinded manner. As demonstrated in **Fig. 5.2C & D**, Drp1 knockdown, but not scramble control, significantly attenuated autophagosome accumulation and enhanced autolysosomal levels in the cells with α-syn overexpression, indicating that Drp1 knockdown alleviates autophagic impairment induced by α-syn.

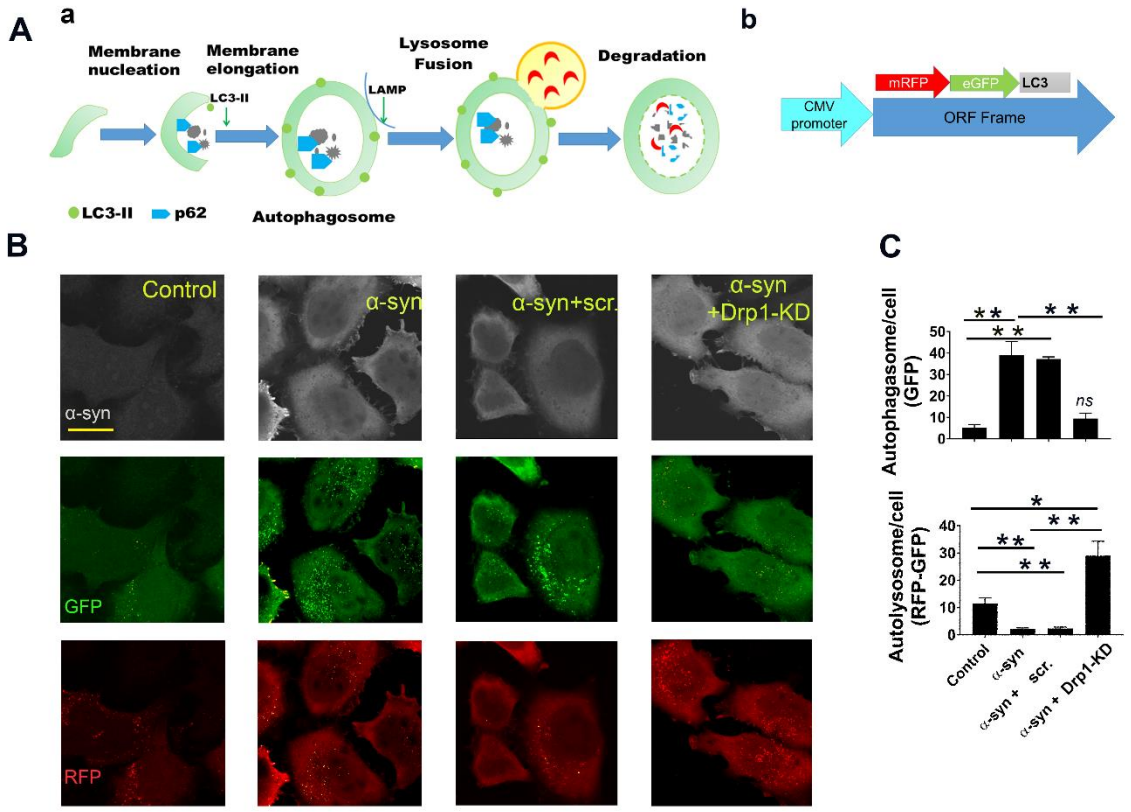

Figure 5.2 Drp1 knockdown prevents autophagy flux impairment induced by transfected α-syn in the autophagy reporter cells.. ***(A)*** *Schematic diagram illustrating the autophagy flux pathway and b the construct used to create the mRFP-GFP-LC3 stable reporter HeLa cells. With this cell model, autophagosomes appear yellow due to the colocalization RFP and GFP signals. Red signal indicates the flux is functional because the green signal is quenched by the acidic environment of the lysosome, which fuses with autophagosome. (**B)** Hela cells were co-transfected with α-syn-wild type plasmid and siRNA-Drp1, using jetPRIME® (Polyplus). **(C)** Quantification of autophagosome and autolysosome number upon α-syn overexpression with or without Drp1 knockdown using ImageJ. The numbers of autophagosomes (green vesicles) and autolysosomes (red vesicles minus green vesicles) were counted and analysed using ImageJ. Glass coverslips were then mounted onto slides with Prolong Diamond anti-fade mounting reagent and imaged with a Leica LAS SP8 using 60x objective. Data represent the mean ± SEM, n=3 independent experiments. Analysis done by one-way ANOVA, followed by the Newman--Keuls post hoc test. *p< 0.05. Scale bar: 20μm.*

Gene silencing efficiency was confirmed using western blot, with 10nM of siRNA achieving over 75% knockdown compared to scrambled control (**Fig 5.3**).

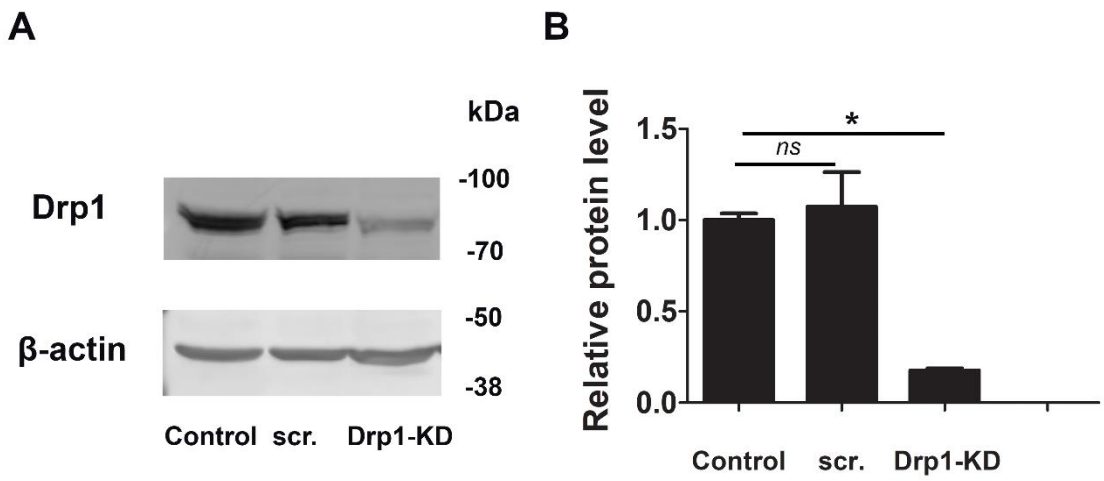

Figure 5.3 Drp1 knockdown efficiency in Hela cells. ***(A)*** HeLA cells were transfected with siRNA-Drp1 or non-targeting scramble control for 48h and then collected for immunoblotting. Representative images of Drp1 levels and the loading control β-actin ***(B)*** Drp1 levels were normalized to β-actin and quantified using ImageJ. *Data represent the mean ± SEM, n=4 independent experiments. Analysis done by one-way ANOVA, followed by the Newman--Keuls post hoc test. *p< 0.05, ns marked are compared to control group.*

Using another genetic approach to reduce Drp1 function, I transfected cells with the mutant Drp1-K38A dominant negative (**Fig. 5.4**). In cells with Drp1-K38A expression as evidenced by immunostaining of the HA-tag, autophagy flux was significantly improved despite the co-transfection of α-syn.

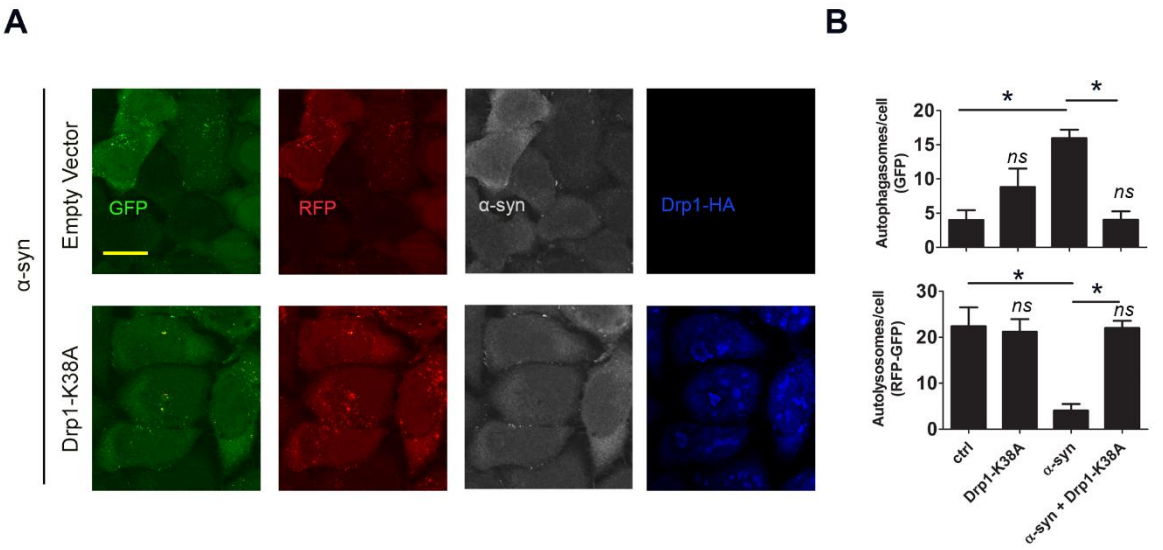

Figure 5.4 Dominant negative mutation Drp-K38A prevents autophagy flux impairment induced by transfected α-syn in the autophagy reporter cells. ***A.*** *As a complementary approach to siRNA knockdown, Hela cells were co-transfected with α-syn-wild type plasmid and HA-tagged Drp1- K38A using Lipofectamine 3000. After 48h, cells were fixed and immunostained with anti-α-syn (Millipore AB5038) and anti-HA (Roche 12CA5) Cover glasses were then mounted onto slides with Prolong Diamond anti-fade mounting reagent and imaged with a Leica LAS SP8 using 60x objective. (Cyan: α-syn, Gray: HA) Scale bar: 20μm.* ***B*** *Quantification of autophagosome and autolysosome number was performed using Image J. Data represent the mean ± SEM, n=3 independent experiments. Analysis done by one-way ANOVA, followed by the Newman--Keuls post hoc test. *p< 0.05, ns marked are compared to control group.*

As a comparison to genetic approaches, I also assessed the effects of the small molecule mitochondrial division inhibitor-1 (mdivi-1) in this study. **Fig. 5.5** demonstrate that mdivi-1 also protected against α-syn-induced autophagy blockade.

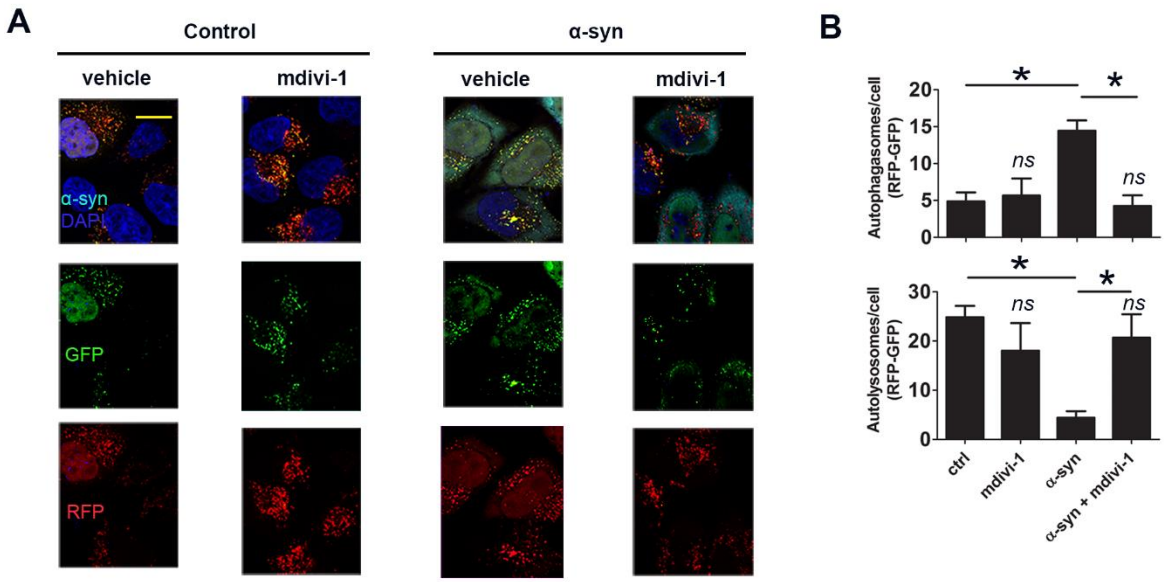

Figure 5.5 Drp1 inhibition with mdivi-1 prevents autophagy flux impairment induced by transfected α-syn in the autophagy reporter cells. (*A*) *Hela cells were transfected with α-syn-wild type as described above and treated with mdivi-1 (10μM) 24h later. Next day, cells were fixed and immunostained for α-syn (Millipore AB5038), followed by Alexa Fluor 633 anti-rabbit secondary. Cover glasses were then mounted onto slides with Prolong Diamond anti-fade mounting reagent and imaged with a Leica LAS SP8 using 60x objective (Cyan: α-syn, Gray: HA, scale bar: 20 μm) Scale bar: 20μm.* ***(B)*** *Quantification of autophagosome and autolysosome number was performed using Image J. Data represent the mean ± SEM, n=3 independent experiments. Analysis done by one-way ANOVA, followed by the Newman--Keuls post hoc test. *p< 0.05, ns marked are compared to control group.*

Human α-syn preformed fibrils (PFF) has been used in recent years to induce the release of exosomes and the spread of α-syn from one cell to another *in vitro* (Freundt et al., 2012, Volpicelli-Daley et al., 2014, Luk et al., 2012) and *in vivo* (Luk et al., 2012). Small seeds of PFF generated from recombinant α-syn can be endocytosed by neurons where it recruits endogenous α-syn to form phosphorylated and insoluble aggregates (Volpicelli-Daley et al., 2014). I obtained α-syn monomers from the Michael J. FOX Foundation and generated PFF according to the accompanying

protocol. With transmission electron microscopy (TEM), I confirmed the morphology and size of PFF and its sonicated form (**Fig. 5.6A**). Using the autophagy reporter HeLa cells, I confirmed that PFF blocked autophagy flux and siRNA-Drp1 attenuated this impairment (**Fig. 5.6B & C**). Furthermore, this treatment also reduced α-syn protein aggregation. In combination, in a human cell model designed to monitor autophagy flux, the genetic and pharmacological data provide strong evidence that blocking Drp1 alleviates the negative impact of α-syn on autophagy flux and therefore supporting a novel protective mechanism of Drp1 inhibition.

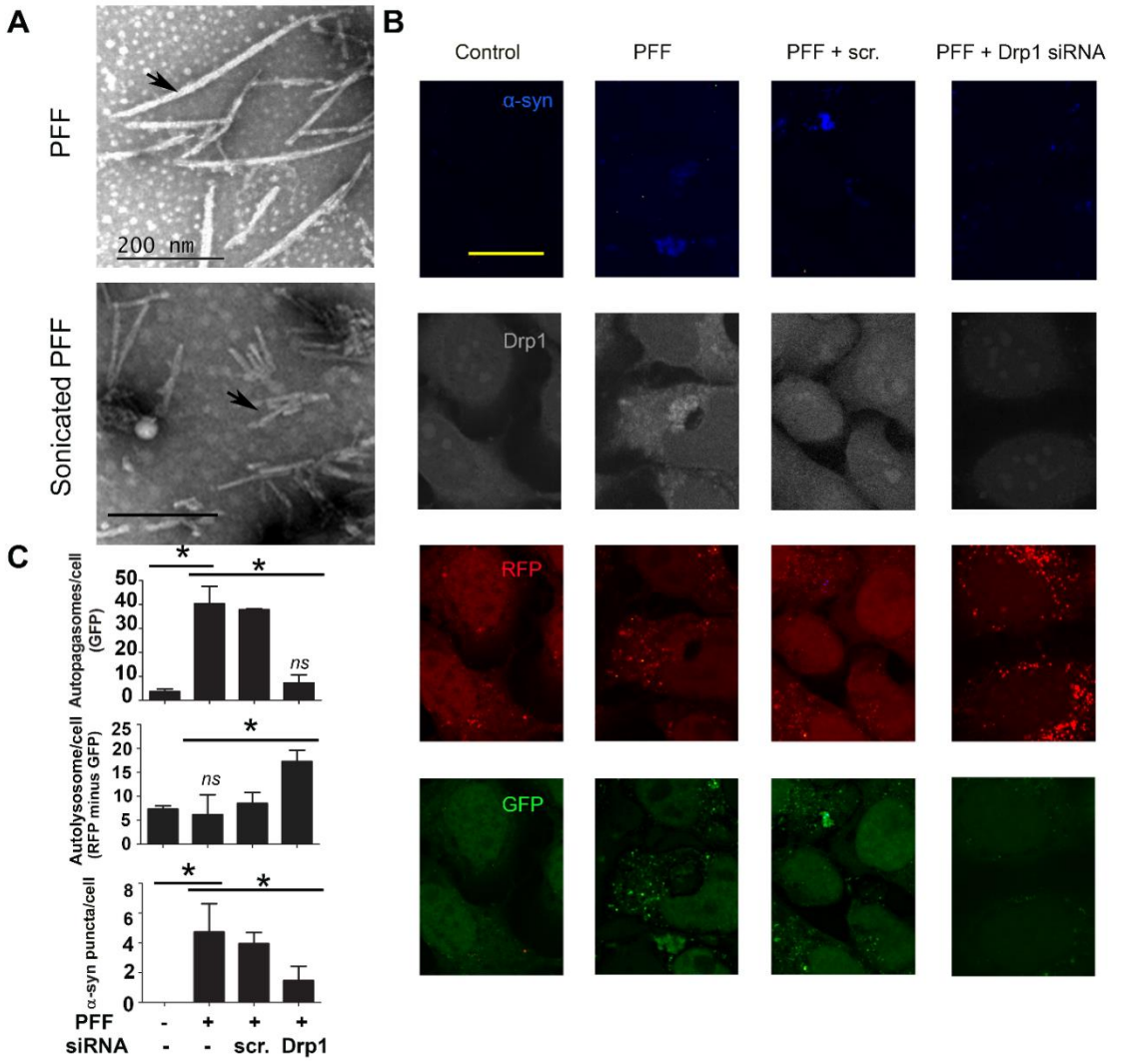

Figure 5.6 Drp1 inhibition prevents autophagy flux impairment induced by pre-formed fibril (PFF) α-syn in the autophagy reporter cells. (*A*) *EM images confirming the formation and sonication results of PFF* ***(B)*** *Sonicated PFF (8 µg/well) was added to HELA cell culture for 72h, cells were then washed thoroughly, fixed and immunostained for α-syn. Representative images showing addition of PFF blocking autophagy flux in Hela cells and siRNA-Drp1 knockdown (10nM) improves autophagy flux. Hela cells were plated onto cover glass in 6-well plates, knockdown using jetPRIME. The next day media was changed and sonicated PFF (8µg/well) was added to the cells and incubated for 72h. Drp1 knockdown in the cells is confirmed by ICC staining using Drp1 antibody (BD 61113).* ***(C)*** *Quantitative analysis of autophagosome and autolysosome numbers along with protein aggregation formation. Puncta numbers were counted using image J. On average 30 cells were counted per treatment group for each repeat. Data represent the mean ± S.E., n=3/4. Analysis done by one-way ANOVA, followed by the Newman--Keuls post hoc test. *p< 0.05. Scale bar: 20µm.*

5.4 Discussion

In this chapter I evaluated the protective effects of Drp1 inhibition mediated through autophagy. Between two cell models, rat N27 dopaminergic neuronal cells with inducible expression of α-syn and human autophagy reporter HeLa cells, reducing Drp1 function genetically (Drp1 knockdown and overexpression of Drp1-dominant negative) and pharmacologically (mdivi-1 treatment) attenuated autophagy flux blockade induced by α-syn.

One major rationale for using the N27 cells for this study was to maintain consistency by using the same neuronal cell model as other studies in chapters 3 and 4. The fact that these are dopaminergic neuronal cells also made them more ideal to model the cell type affected in PD. To monitor autophagy flux in these cells, I quantified the levels of LC3 and p62. However, because the expression of endogenous LC3 N27 cells was low, I had to perform transient transfection of LC3-cherry plasmid. As with other transient transfections, maintaining a consistent level of protein expression between experiments could be challenging and there was a concern that too high level may affect the outcome of the study. The HeLA autophagy reporter cells provided by Dr. Shouqing Luo allowed me an additional opportunity to evaluate the protective effects of blocking Drp1 against impaired autophagy induced by α-syn. With stable overexpression of mRFP-GFP-LC3, these cells were designed specifically to monitor autophagy flux (Kimura et al., 2007). I believe that adding this human cell model to my N27 rat cells would make my study more translational and scientifically more rigorous. The consistent results that I obtained between these two cell lines indicate that the protective effects of blocking Drp1 is reproducible across cell lines, regardless of human or rat origin as well as

neuronal or non-neuronal cells. As a fundamental process for cell survival, autophagy flux is a universal and highly conserved process across different cell types (King, 2012). Although not a neuronal cell line, HeLa cell model is a very quick and useful tool to confirm and provide more information on α-syn induced autophagy blockade. In addition, different cell types have been reported to contribute to α-syn aggregation and propagation in PD models (Braak et al., 2007, Breen et al., 2019), indicating rescuing autophagy blockade in other cell types can also be beneficial. Therefore, confirming the protective effect of blocking Drp1 toward autophagy in a non-neuronal cell line would further strengthen the potential of targeting this protein as a therapeutic strategy.

6. Discussion and Conclusions

6.1. General discussion

Perhaps the most investigated PD-linked gene to date is *SNCA*. While mutation in this gene is rare, the *SNCA* locus is a significant variant factor for PD development(Lill et al., 2012). Missense mutations as well as gene duplications and triplications of *SNCA* have been identified in familial PD (Polymeropoulos et al., 1997b, Appel-Cresswell et al., 2013b, Zarranz et al., 2004b). The fact that increasing the gene dosage of *SNCA* by two to three fold can also cause PD (Singleton et al., 2003b) is significant, because it indicates that elevated wild-type α-syn alone is sufficient to cause the disease. α-syn is also a key factor of idiopathic PD and present in Lewy bodies, which are abnormal proteins commonly observed in PD (Spillantini et al., 1998). Pathogenic mechanisms associated with α-syn have therefore been at the forefront of the PD research and multiple high-profile discoveries have greatly contributed to the understanding of disease pathology. It is not surprising, therefore, that targeting α-syn as a therapeutic strategy for PD has been intensively pursued. Since its discovery as the first familial link to PD over two decades ago, this protein has been associated with multiple neurotoxic mechanisms, such as mitochondrial dysfunction and impaired autophagic flux. These two mechanisms are highly relevant to my project.

Mitochondria are essential to the maintenance of normal neuronal function and viability through regulation of key processes such as energy production, calcium homeostasis, intracellular transport, neurotransmitter release and reuptake (Hollenbeck, 2005, Ly and Verstreken, 2006). Studies in recent years have also highlighted that mitochondria are highly dynamic organelles prompting the term “mitochondrial dynamics”, which refers to the processes of fission, fusion and movement along microtubules that allow mitochondria to relocate to axons, dendrites and terminals (Chen and Chan, 2009). Accumulating evidence indicates that perturbed

mitochondrial dynamics is a pathogenic mechanism in a number of neurodegenerative diseases, and manipulating mitochondrial fission and fusion has been considered as a potential novel mitochondrial therapy in recent years (Wang et al., 2016a, Archer, 2013, Andreux et al., 2013a). Within this context, blocking dynamin-related protein 1 (Drp1) is the most highly pursued strategy to block mitochondrial fission, because Drp1 can bind to multiple downstream fission proteins to sever mitochondria, as illustrated in **Fig. 1.5**. Using the MPTP and Pink1-KO mouse models as in vivo PD models of mitochondrial dysfunction, we have demonstrated that blocking Drp1 genetically and pharmacologically (mdivi-1) is protective against synaptic dysfunction and neurodegeneration (Rappold et al., 2014). In a more recent study, we demonstrated that mdivi-1 improved mitochondrial function and reduced protein aggregation induced by α-syn-A53T in rats (Bido et al., 2017a).

Mdivi-1, as discussed in **Chapter 4**, was discovered in a high throughput drug screening study from a chemical library of 23,000 candidates as an inhibitor of Drp1 (Cassidy-Stone et al., 2008). It is worth noting, however, that a recently study questioned whether this inhibitor was specific for Drp1 and these authors reported that mdivi-1 had a reversible mitochondrial complex I inhibitory property (Bordt et al., 2017b). In that study, Drp1-GTPase activity was assessed using recombinant human Drp1, and no more than 25% of GTPase activity inhibition was achieved using up to 100μM mdivi-1. The results of this study are in contrast with another study (Numadate et al., 2014). This latter study provided direct evidence of mdivi-1 in blocking Drp1 function with a Ki_{50} of 13μM. In addition, many different laboratories have reported a rescue effect of mdivi-1 on mitochondrial fragmentation in different disease models as recently reviewed (Smith and Gallo, 2017a). As pointed out by Smith & Gallo, the dose of mdivi-1 used by Bordt et al. was quite high. Many groups

including our laboratory have seen the protective effect of the molecule at lower doses in different *in vitro* models. In our previous study (Cui et al., 2010a), a clear dose effect of this small molecule was noticed, with a dose as low as 5 μM conferred protection but a neurotoxic effect was observed at 30 μM. To date, more than 100 primary publications (Pubmed search) have reported the protective effect of mdivi-1 in a wide-range of experimental model and the observation of elongated mitochondria is widely observed. Therefore, although more studies are required to provide more direct evidence regarding the link between mdivi-1 and Drp1, available evidence suggests that mdivi-1 does block mitochondrial fission and confers striking protective effects across multiple disease models (Smith and Gallo, 2017a)

Autophagy has been reported to play a critical role in removing misfolded and aggregated α-syn (Webb et al., 2003a, Cuervo et al., 2004, Lee et al., 2004). Inhibition of autophagy flux induced α-syn, therefore, leads to accumulation of this toxic protein, which further exacerbating the blockade of autophagy as demonstrated cell culture and animal models (Winslow et al., 2010b, Ebrahimi-Fakhari et al., 2011, Yu et al., 2009, Chen et al., 2015, Bido et al., 2017a), thus creating a bidirectional positive feedback loop of neurotoxicity (Xilouri et al., 2016). Strikingly, recent data from my laboratory and others show that blocking Drp1 is capable of reducing protein aggregation. Reddy and colleagues, for example, reported than crossing *Drp1*$^{+/-}$ mice with either the AβPP (Tg2576) or the Tau P301L transgenic mouse models of (AD) reduced accumulation of toxic proteins in these animals (Manczak et al., 2016, Kandimalla et al., 2016). We recently demonstrated that pharmacological blocking of Drp1 dramatically reduced α-syn aggregates in nigral DA neurons of rats overexpressing α-synclein-A53T (Bido et al., 2017a). Together, these results suggest

that one possible mechanism by which blocking Drp1 reduces protein aggregation is through an improvement in autophagic function.

Given the well-established function of Drp1 in mitochondrial fission and its potential role in autophagy, my project evaluated the protective effects of Drp1 inhibition mediated through these two mechanisms. I obtained data showing that blocking Drp1 improved both mitochondrial function and autophagic flux in experimental models of α-syn. Using the rat N27 dopaminergic neuronal cells with inducible wild-type human α-syn, I observed excessive mitochondrial fragmentation and increased Drp1 levels 48h after gene induction. Functionally, these cells exhibited lower mitochondrial membrane potential, reduced ATP production and mitochondrial spare respiratory capacity (SRS), as well as increased levels of mitochondrial reactive oxygen species (**Chapter 3**). To evaluate the protective role of Drp1 inhibition, I used three complementary approaches: gene silencing mediated by siRNA, overexpression of Drp1-dominant negative and the small molecule mdivi-1. Both morphological and functional defects induced by α-syn were attenuated by these strategies (**Chapter 4**). Importantly, Drp1 inhibition drastically reduced proteinase K-resistant α-syn in multiple cell models with overexpressing human wild-type α-syn or the treatment of recombinant α-syn (PFF). Based on that observation, I investigated the involvement of autophagy. Through a combination of stable HeLa autophagy reporter cells and immunostaining for LC3 and p62 in N27cells with either α-syn overexpression or treatment of human α-syn PFF, I observed that Drp1 inhibition abolished autophagic impairment induced by α-syn (**Chapter 5**). In combination, my novel observations highlight new insights that Drp1 inhibition confers neuroprotection through both mitochondrial and autophagy-lysosomal pathways as illustrated in **Fig. 6.1**.

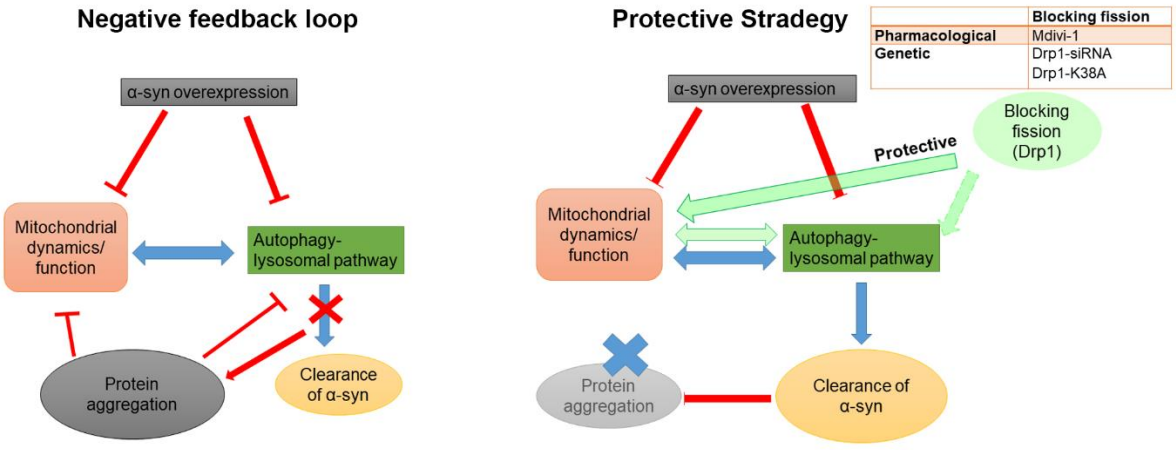

Figure 6.1 Drp1 inhibition breaks the negative feedback loop created by α-syn overexpression. *Left: α-syn overexpression disrupts mitochondrial dynamics, leading to mitochondrial fragmentation and dysfunction. α-syn also inhibits the autophagy-lysosomal pathways. Because autophagy flux is an energy dependent process and autophagy is important for the removal of damaged mitochondrial, these two important processes influence each other's functions. Impaired autophagy reduces the clearance of misfolded α-syn, which accumulates inside the cells, forms aggregates whilst imposing more inhibition on the two mitochondrial and autophagy pathways. Right: Blocking Drp1 breaks the negative feedback loop by restoring mitochondrial function and improving autophagy flux, resulting in enhanced clearance of misfolded protein oligomers and reduced accumulation of protein aggregation. This would in turn pose less inhibition on the mitochondria and autophagy function.*

.

.

6.2. Conclusions and future perspectives

Mitochondrial dysfunction, impaired autophagy flux, oxidative stress and α-syn pathology (aggregation and spread) have all been proposed to play a dominant pathogenic role in PD. Previously, our lab have reported that blocking Drp1 is neuroprotective in both cell (Cui et al., 2010a) and animal models of PD (Bido et al., 2017b, Rappold et al., 2014). A complementary approach using a peptide known as P110 to block the binding of Drp1 to Fis1 has also been shown to be protective in the MPTP models (Qi et al., 2013a, Filichia et al., 2016a). However, all these previous studies only focused on the mitochondrial fission pathway. Using models of α-syn, which is relevant to familial and sporadic PD, my study provides the following novel observation: Drp1 inhibition through multiple approaches (siRNA, dominant negative K38A transfection and mdivi-1) have consistently shown to enhance autophagy flux, pointing to a novel pathway involving Drp1 and autophagy. Together with mitochondrial function, these discoveries highlight new insights that Drp1 inhibition confers neuroprotection through both mitochondrial and autophagy-lysosomal pathways, further strengthening the therapeutic potential of targeting Drp1. Nonetheless further study is needed to address the following questions:

First, how and at what stage of autophagy flux does Drp1 inhibition has an impact on? Since the submission of this thesis, I have performed additional experiments to address this question and have included these data in the manuscript that I recently submitted for publication. Briefly, I transfected the autophagy reporter mRFP-GFP-LC3 HeLa cells with siRNA-Drp1 or scramble control and then treated them with chloroquine to block lysosomal function, which resulted in a reduction in autolysosomes and an increase in autophagosomes. These alterations were

attenuated by Drp1 inhibition, suggesting a partial improvement in lysosomal function. Interestingly, the number of autophagosomes remained relatively high in the cells with higher levels of autolysosomal activity under Drp1 inhibition. This result suggests that Drp1 inhibition might also promote the formation of autophagosomes. Therefore, in theory, Drp1 inhibition enhances autophagy flux by increasing both the levels of autophagosomes and the function of lysosomes. To gain additional mechanistic insights into the observed higher autophagosome levels, I transfected stable N27 cells with siRNA-Drp1, followed by α-syn induction for two days and then cells were collected for immunoblotting to assess mTOR activity (which inhibits autophagy) by quantifying the levels of phosphor-4E-BP1, which is a downstream substrate of mTOR. I observed α-syn activated mTOR, and strikingly, knocking down Drp1 inhibited mTOR activity to an equivalent extent as rapamycin, an mTOR inhibitor (data included in the submitted manuscript). Together, these data provide a highly novel evidence that Drp1 inhibition increases autophagy flux by a combination of increasing the formation of autophagosomes and the function of lysosomes. However, future studies are needed to address: (i) whether Drp1 is localized to the autophagy pathway, (ii) does Drp1 functionally interact at an early or late stage of autophagy (or both), and (iii) whether Drp1 mediates its effects on autophagy through a mitochondrial dependent mechanism.

Second, given that autophagy flux could be affected by mitochondrial function, does Drp1 inhibition have a direct effect on autophagy or through a mitochondrial dependent mechanism? It could be challenging to answer this question as multiple pathways are interlinked and impacted by each other in the cell. The function of mitochondria and autophagy are not mutually exclusive and as a consequence, it would be difficult to distinguish whether or to what extent the effect of Drp1 on

autophagy is mediated through a mitochondrial independent mechanism. A potential approach is to use cells with minimal to no mitochondrial function to study the effect of Drp1 inhibition on autophagy flux. One example of such a cell model is the so called “Rho 0” cells, which are depleted of mtDNA. Although viable, these cells do not have fully functional mitochondria. If blocking Drp1 could still promote autophagy, this would provide evidence that Drp1 affects autophagy via a mitochondrial independent mechanism.

Third, does blocking Drp1 reduce the propagation of α-syn through exosomal release and therefore reduce the spread of α-syn pathology? Blockade of the mitochondrial electron transport chain and autophagy flux has been shown to induce the spread of α-syn inter-cellularly. For example, exposure of enteric neurons to rotenone, a mitochondrial complex I inhibitor, promotes the release of α-syn, which is subsequently taken up by and form aggregates in the recipient neurons (Pan-Montojo et al., 2012b). Emerging evidence indicates that α-syn can spread inter-cellularly through exosome release, primarily because of its ability to impair mitochondria and autophagy (Guo and Lee, 2014, Alvarez-Erviti et al., 2011). Exosomes are small extracellular vesicles with a typical size of 40–100 nm. Because these vesicles carry cargos such as mRNA and proteins, they could play a role in the spread of misfolded proteins such as α-syn (Chistiakov and Chistiakov, 2017). It has been demonstrated that impaired autophagy induces exosome-mediated α-syn spread to other neurons (Alvarez-Erviti et al., 2011), forming aggregates and inducing death in the receiving cell (Desplats et al., 2009b, Hansen et al., 2011). Based on my data, by improving mitochondrial function and autophagy flux, it is likely that blocking Drp1 would reduce exosome release.

Fourth, would neuroinflammation be reduced if Drp1 function is reduced in glial cells such as microglia and astrocytes? The role of activated microglia in causing neuroinflammation by releasing molecules such as TNF-α, IL-1β and IL-6 has been well-documented and proposed to be involved in PD pathogenesis(Kim et al., 2013b, Su et al., 2008, Zhang et al., 2005b). Relevant to my study, lipopolysaccharide (LPS) has been reported to induce mitochondrial fission in microglia leading to neuroinflammation. Using primary microglia (Nair et al., 2019) and the BV2 murine microglial cells (Park et al., 2013), two independent studies show that LPS induces mitochondrial fragmentation and neuroinflammation via a Drp1-dependent mechanism. Blocking Drp1 using shDrp1 and mdivi-1 reduces LPS-induced release of pro-inflammatory molecules. In addition to microglia, astrocytes are capable of causing neuroinflammation (Sarkar et al., 2018) - although to a lesser extent than microglia. In primary mouse astrocytes and the human U373 astrocytes, manganese (Mn) reduces oxidative phosphorylation, increases mitochondrial fragmentation and neuroinflammation - especially in the presence of supplemented aggregated α-syn (Sarkar et al., 2018). The mitochondrial targeted antioxidant mito-apocynin was demonstrated to be highly protective against Mn-induced such alterations in astrocytes (Sarkar et al., 2018), suggesting impaired mitochondria as the cause of neuroinflammation. Together, these studies indicate that enhanced mitochondrial fission in microglia and astrocytes are linked to their production of proinflammatory molecules. It is important to assess the protective effects of blocking Drp1 against neuroinflammation in PD models.

To conclude, my results highlight that Drp1 inhibition confers neuroprotection through both mitochondrial and autophagy-lysosomal pathways. Although additional studies are required to fully understand the mechanism(s) by which blocking Drp1

improves autophagic function, the strong possibility that blocking Drp1 also reduces neuroinflammation and spread of misfolded toxic proteins further strengthens the therapeutic potential of targeting Drp1.

7. Appendices

8 List of References

ABELIOVICH, A., SCHMITZ, Y., FARINAS, I., CHOI-LUNDBERG, D., HO, W. H., CASTILLO, P. E., SHINSKY, N., VERDUGO, J. M., ARMANINI, M., RYAN, A., HYNES, M., PHILLIPS, H., SULZER, D. & ROSENTHAL, A. 2000. Mice lacking alpha-synuclein display functional deficits in the nigrostriatal dopamine system. *Neuron,* 25**,** 239-52.

ABOUNIT, S., BOUSSET, L., LORIA, F., ZHU, S., DE CHAUMONT, F., PIERI, L., OLIVO-MARIN, J. C., MELKI, R. & ZURZOLO, C. 2016. Tunneling nanotubes spread fibrillar alpha-synuclein by intercellular trafficking of lysosomes. *Embo j,* 35**,** 2120-2138.

ADAMS, F. S., LA ROSA, F. G., KUMAR, S., EDWARDS-PRASAD, J., KENTROTI, S., VERNADAKIS, A., FREED, C. R. & PRASAD, K. N. 1996. Characterization and transplantation of two neuronal cell lines with dopaminergic properties. *Neurochemical Research,* 21**,** 619-627.

AFESEH NGWA, H., KANTHASAMY, A., GU, Y., FANG, N., ANANTHARAM, V. & KANTHASAMY, A. G. 2011. Manganese nanoparticle activates mitochondrial dependent apoptotic signaling and autophagy in dopaminergic neuronal cells. *Toxicology and Applied Pharmacology,* 256**,** 227-240.

ALVAREZ-ERVITI, L., SEOW, Y., SCHAPIRA, A. H., GARDINER, C., SARGENT, I. L., WOOD, M. J. & COOPER, J. M. 2011. Lysosomal dysfunction increases exosome-mediated alpha-synuclein release and transmission. *Neurobiol. Dis,* 42**,** 360-367.

ANDREUX, P. A., HOUTKOOPER, R. H. & AUWERX, J. 2013a. Pharmacological approaches to restore mitochondrial function. *Nature Reviews Drug Discovery,* 12**,** 465-483.

ANDREUX, P. A., HOUTKOOPER, R. H. & AUWERX, J. 2013b. Pharmacological approaches to restore mitochondrial function. *Nat Rev. Drug Discov,* 12**,** 465-483.

APPEL-CRESSWELL, S., VILARINO-GUELL, C., ENCARNACION, M., SHERMAN, H., YU, I., SHAH, B., WEIR, D., THOMPSON, C., SZU-TU, C. & TRINH, J. 2013a. Alpha-synuclein p.H50Q, a novel pathogenic mutation for Parkinson's disease. *Mov Disord,* 28.

APPEL-CRESSWELL, S., VILARINO-GUELL, C., ENCARNACION, M., SHERMAN, H., YU, I., SHAH, B., WEIR, D., THOMPSON, C., SZU-TU, C., TRINH, J., AASLY, J. O., RAJPUT, A., RAJPUT, A. H., JON STOESSL, A. & FARRER, M. J. 2013b. Alpha-synuclein p.H50Q, a novel pathogenic mutation for Parkinson's disease. *Mov Disord,* 28**,** 811-3.

ARCHER, S. L. 2013. Mitochondrial dynamics--mitochondrial fission and fusion in human diseases. *N Engl J Med,* 369**,** 2236-51.

BALDI, I., CANTAGREL, A., LEBAILLY, P., TISON, F., DUBROCA, B., CHRYSOSTOME, V., DARTIGUES, J. F. & BROCHARD, P. 2003. Association between Parkinson's disease and exposure to pesticides in southwestern France. *Neuroepidemiology,* 22**,** 305-10.

BARBEAU, A. 1969. L-Dopa Therapy in Parkinson's Disease: A Critical Review of Nine Years' Experience. *Canadian Medical Association Journal,* 101**,** 59-68.

BENDER, A., KRISHNAN, K. J., MORRIS, C. M., TAYLOR, G. A., REEVE, A. K., PERRY, R. H., JAROS, E., HERSHESON, J. S., BETTS, J., KLOPSTOCK, T., TAYLOR, R. W. & TURNBULL, D. M. 2006. High levels of mitochondrial DNA deletions in substantia nigra neurons in aging and Parkinson disease. *Nat Genet,* 38.

BEREITER-HAHN, J. & VOTH, M. 1994. Dynamics of mitochondria in living cells: shape changes, dislocations, fusion, and fission of mitochondria. *Microsc Res Tech,* 27**,** 198-219.

BETARBET, R., SHERER, T. B., MACKENZIE, G., GARCIA-OSUNA, M., PANOV, A. V. & GREENAMYRE, J. T. 2000. Chronic systemic pesticide exposure reproduces features of Parkinson's disease. *Nat Neurosci,* 3.

BIDO, S., SORIA, F. N., FAN, R. Z., BEZARD, E. & TIEU, K. 2017a. Mitochondrial division inhibitor-1 is neuroprotective in the A53T-á-synuclein rat model of Parkinson's disease (in press). *Sci. Rep*.

BIDO, S., SORIA, F. N., FAN, R. Z., BEZARD, E. & TIEU, K. 2017b. Mitochondrial division inhibitor-1 is neuroprotective in the A53T-α-synuclein rat model of Parkinson's disease. *Scientific Reports,* 7**,** 7495.

BIDO, S., SORIA, F. N., FAN, R. Z., BEZARD, E. & TIEU, K. 2017c. Mitochondrial division inhibitor-1 is neuroprotective in the A53T-α-synuclein rat model of Parkinson's disease. *Scientific Reports,* 7**,** 7495.

BJORKOY, G., LAMARK, T., BRECH, A., OUTZEN, H., PERANDER, M., OVERVATN, A., STENMARK, H. & JOHANSEN, T. 2005. p62/SQSTM1 forms protein aggregates degraded by autophagy and has a protective effect on huntingtin-induced cell death. *J Cell Biol,* 171**,** 603-14.

BLESA, J. & PRZEDBORSKI, S. 2014. Parkinson's disease: animal models and dopaminergic cell vulnerability. *Frontiers in Neuroanatomy,* 8**,** 155.

BORDT, E. A., CLERC, P., ROELOFS, B. A., SALADINO, A. J., TRETTER, L., ADAM-VIZI, V., CHEROK, E., KHALIL, A., YADAVA, N., GE, S. X., FRANCIS, T. C., KENNEDY, N. W., PICTON, L. K., KUMAR, T., UPPULURI, S., MILLER, A. M., ITOH, K., KARBOWSKI, M., SESAKI, H., HILL, R. B. & POLSTER, B. M. 2017a. The Putative Drp1 Inhibitor mdivi-1 Is a Reversible Mitochondrial Complex I Inhibitor that Modulates Reactive Oxygen Species. *Dev. Cell,* 40**,** 583-594.

BORDT, E. A., CLERC, P., ROELOFS, B. A., SALADINO, A. J., TRETTER, L., ADAM-VIZI, V., CHEROK, E., KHALIL, A., YADAVA, N., GE, S. X., FRANCIS, T. C., KENNEDY, N. W., PICTON, L. K., KUMAR, T., UPPULURI, S., MILLER, A. M., ITOH, K., KARBOWSKI, M., SESAKI, H., HILL, R. B. & POLSTER, B. M. 2017b. The Putative Drp1 Inhibitor mdivi-1 Is a Reversible Mitochondrial Complex I Inhibitor that Modulates Reactive Oxygen Species. *Dev Cell,* 40**,** 583-594.e6.

BOTTNER, M., FRICKE, T., MULLER, M., BARRENSCHEE, M., DEUSCHL, G., SCHNEIDER, S. A., EGBERTS, J. H., BECKER, T., FRITSCHER-RAVENS, A., ELLRICHMANN, M., SCHULZ-SCHAEFFER, W. J. & WEDEL, T. 2015. Alpha-synuclein is associated with the synaptic vesicle apparatus in the human and rat enteric nervous system. *Brain Res,* 1614**,** 51-9.

BOURDENX, M., DOVERO, S., ENGELN, M., BIDO, S., BASTIDE, M. F., DUTHEIL, N., VOLLENWEIDER, I., BAUD, L., PIRON, C., GROUTHIER, V., BORAUD, T., PORRAS, G., LI, Q., BAEKELANDT, V., SCHELLER, D., MICHEL, A., FERNAGUT, P. O., GEORGES, F., COURTINE, G., BEZARD, E. & DEHAY, B. 2015a. Lack of additive role of ageing in nigrostriatal neurodegeneration triggered by alpha-synuclein overexpression. *Acta Neuropathol Commun,* 3**,** 46.

BOURDENX, M., DOVERO, S., ENGELN, M., BIDO, S., BASTIDE, M. F., DUTHEIL, N., VOLLENWEIDER, I., BAUD, L., PIRON, C., GROUTHIER, V., BORAUD, T., PORRAS, G., LI, Q., BAEKELANDT, V., SCHELLER, D., MICHEL, A., FERNAGUT, P. O., GEORGES, F., COURTINE, G., BEZARD, E. & DEHAY, B. 2015b. Lack of additive role of ageing in nigrostriatal neurodegeneration triggered by alpha-synuclein overexpression. *Acta Neuropathol. Commun,* 3:46. doi: 10.1186/s40478-015-0222-2.**,** 46-0222.

BOVÉ, J. & PERIER, C. 2012. Neurotoxin-based models of Parkinson's disease. *Neuroscience,* 211**,** 51-76.

BRAAK, H., DE VOS, R. A., BOHL, J. & DEL TREDICI, K. 2006. Gastric alpha-synuclein immunoreactive inclusions in Meissner's and Auerbach's plexuses in cases staged for Parkinson's disease-related brain pathology. *Neurosci Lett,* 396**,** 67-72.

BRAAK, H., SASTRE, M. & DEL TREDICI, K. 2007. Development of alpha-synuclein immunoreactive astrocytes in the forebrain parallels stages of intraneuronal pathology in sporadic Parkinson's disease. *Acta Neuropathol,* 114.

BRAAK, H., TREDICI, K., RUB, U., VOS, R. A., JANSEN STEUR, E. N. & BRAAK, E. 2003. Staging of brain pathology related to sporadic Parkinson's disease. *Neurobiol Aging,* 24.

BRAIDY, N., GAI, W.-P., XU, Y. H., SACHDEV, P., GUILLEMIN, G. J., JIANG, X.-M., BALLARD, J. W. O., HORAN, M. P., FANG, Z. M., CHONG, B. H. & CHAN, D. K. Y. 2014. Alpha-Synuclein Transmission and Mitochondrial Toxicity in Primary Human Foetal Enteric Neurons In Vitro. *Neurotoxicity Research,* 25**,** 170-182.

BREEN, D. P., HALLIDAY, G. M. & LANG, A. E. 2019. Gut–brain axis and the spread of α-synuclein pathology: Vagal highway or dead end? *Movement Disorders,* 34**,** 307-316.

BURRE, J., SHARMA, M., TSETSENIS, T., BUCHMAN, V., ETHERTON, M. R. & SUDHOF, T. C. 2010. Alpha-synuclein promotes SNARE-complex assembly in vivo and in vitro. *Science,* 329**,** 1663-7.

BURTE, F., CARELLI, V., CHINNERY, P. F. & YU-WAI-MAN, P. 2015. Disturbed mitochondrial dynamics and neurodegenerative disorders. *Nat Rev Neurol,* 11**,** 11-24.

BUTTON, R. W., LIN, F., ERCOLANO, E., VINCENT, J. H., HU, B., HANEMANN, C. O. & LUO, S. 2014. Artesunate induces necrotic cell death in schwannoma cells. *Cell Death Dis,* 5**,** e1466.

BUTTON, R. W., LUO, S. & RUBINSZTEIN, D. C. Autophagic activity in neuronal cell death. *Neuroscience bulletin,* 31**,** 382-394.

CANNON, J. R. & GREENAMYRE, J. T. 2013. Gene-environment interactions in Parkinson's disease: specific evidence in humans and mammalian models. *Neurobiol Dis,* 57**,** 38-46.

CANNON, J. R., TAPIAS, V. M., NA, H. M., HONICK, A. S., DROLET, R. E. & GREENAMYRE, J. T. 2009. A highly reproducible rotenone model of Parkinson's disease. *Neurobiology of disease,* 34**,** 279-290.

CASSIDY-STONE, A., CHIPUK, J. E., INGERMAN, E., SONG, C., YOO, C., KUWANA, T., KURTH, M. J., SHAW, J. T., HINSHAW, J. E., GREEN, D. R. & NUNNARI, J. 2008. Chemical inhibition of the mitochondrial division dynamin reveals its role in Bax/Bak-dependent mitochondrial outer membrane permeabilization. *Dev Cell,* 14**,** 193-204.

CEREGHETTI, G. M., STANGHERLIN, A., MARTINS DE BRITO, O., CHANG, C. R., BLACKSTONE, C., BERNARDI, P. & SCORRANO, L. 2008. Dephosphorylation by calcineurin regulates translocation of Drp1 to mitochondria. *Proc Natl Acad Sci U S A,* 105**,** 15803-8.

CHANG, C. R. & BLACKSTONE, C. 2007. Cyclic AMP-dependent protein kinase phosphorylation of Drp1 regulates its GTPase activity and mitochondrial morphology. *J Biol Chem,* 282**,** 21583-7.

CHARTIER-HARLIN, M. C., KACHERGUS, J., ROUMIER, C., MOUROUX, V., DOUAY, X., LINCOLN, S., LEVECQUE, C., LARVOR, L., ANDRIEUX, J. & HULIHAN, M. 2004. Alpha-synuclein locus duplication as a cause of familial Parkinson's disease. *Lancet,* 364.

CHEN, H. & CHAN, D. C. 2009. Mitochondrial dynamics–fusion, fission, movement, and mitophagy–in neurodegenerative diseases. *Human Molecular Genetics,* 18**,** R169-R176.

CHEN, L., XIE, Z., TURKSON, S. & ZHUANG, X. 2015. A53T human alpha-synuclein overexpression in transgenic mice induces pervasive mitochondria macroautophagy defects preceding dopamine neuron degeneration. *J Neurosci,* 35**,** 890-905.

CHINOPOULOS, C. & ADAM-VIZI, V. 2001. Mitochondria deficient in complex I activity are depolarized by hydrogen peroxide in nerve terminals: relevance to Parkinson's disease. *Journal of Neurochemistry,* 76**,** 302-306.

CHISTIAKOV, D. A. & CHISTIAKOV, A. A. 2017. alpha-Synuclein-carrying extracellular vesicles in Parkinson's disease: deadly transmitters. *Acta Neurol. Belg,* 117**,** 43-51.

CHO, D.-H., NAKAMURA, T., FANG, J., CIEPLAK, P., GODZIK, A., GU, Z. & LIPTON, S. A. 2009a. S-Nitrosylation of Drp1 Mediates β-Amyloid-Related Mitochondrial Fission and Neuronal Injury. *Science,* 324**,** 102-105.

CHO, D. H., NAKAMURA, T., FANG, J., CIEPLAK, P., GODZIK, A., GU, Z. & LIPTON, S. A. 2009b. S-nitrosylation of Drp1 mediates beta-amyloid-related mitochondrial fission and neuronal injury. *Science,* 324**,** 102-5.

CHOI, S. W., GERENCSER, A. A. & NICHOLLS, D. G. 2009a. Bioenergetic analysis of isolated cerebrocortical nerve terminals on a microgram scale: spare respiratory capacity and stochastic mitochondrial failure. *J Neurochem,* 109**,** 1179-1191.

CHOI, S. W., GERENCSER, A. A. & NICHOLLS, D. G. 2009b. Bioenergetic analysis of isolated cerebrocortical nerve terminals on a microgram scale: spare respiratory capacity and stochastic mitochondrial failure. *J Neurochem,* 109**,** 1179-91.

CHOUBEY, V., SAFIULINA, D., VAARMANN, A., CAGALINEC, M., WARESKI, P., KUUM, M., ZHARKOVSKY, A. & KAASIK, A. 2011. Mutant A53T alpha-synuclein induces neuronal death by increasing mitochondrial autophagy. *J Biol Chem,* 286**,** 10814-24.

CICCHETTI, F., LAPOINTE, N., ROBERGE-TREMBLAY, A., SAINT-PIERRE, M., JIMENEZ, L., FICKE, B. W. & GROSS, R. E. 2005. Systemic exposure to paraquat and maneb models early Parkinson's disease in young adult rats. *Neurobiol Dis,* 20**,** 360-71.

COLE, N. B., DIEULIIS, D., LEO, P., MITCHELL, D. C. & NUSSBAUM, R. L. 2008. Mitochondrial translocation of α-synuclein is promoted by intracellular acidification. *Experimental cell research,* 314**,** 2076-2089.

COSTELLO, S., COCKBURN, M., BRONSTEIN, J., ZHANG, X. & RITZ, B. 2009. Parkinson's disease and residential exposure to maneb and paraquat from agricultural applications in the central valley of California. *Am J Epidemiol,* 169.

COXHEAD, J., KURZAWA-AKANBI, M., HUSSAIN, R., PYLE, A., CHINNERY, P. & HUDSON, G. 2016. Somatic mtDNA variation is an important component of Parkinson's disease. *Neurobiology of Aging,* 38**,** 217.e1-217.e6.

CUERVO, A. M., STEFANIS, L., FREDENBURG, R., LANSBURY, P. T. & SULZER, D. 2004. Impaired degradation of mutant alpha-synuclein by chaperone-mediated autophagy. *Science,* 305**,** 1292-5.

CUI, M., TANG, X., CHRISTIAN, W. V., YOON, Y. & TIEU, K. 2010a. Perturbations in mitochondrial dynamics induced by human mutant PINK1 can be rescued by the mitochondrial division inhibitor mdivi-1. *J Biol Chem,* 285**,** 11740-52.

CUI, M., TANG, X., CHRISTIAN, W. V., YOON, Y. & TIEU, K. 2010b. Perturbations in mitochondrial dynamics induced by human mutant PINK1 can be rescued by the mitochondrial division inhibitor mdivi-1. *J. Biol. Chem,* 285**,** 11740-11752.

DAMIER, P., HIRSCH, E. C., AGID, Y. & GRAYBIEL, A. M. 1999. The substantia nigra of the human brain. II. Patterns of loss of dopamine-containing neurons in Parkinson's disease. *Brain,* 122 (Pt 8)**,** 1437-48.

DANTZIG, P. I. 2006. Parkinson's disease, macular degeneration and cutaneous signs of mercury toxicity. *J Occup Environ Med,* 48**,** 656.

DANZER, K. M., KRANICH, L. R., RUF, W. P., CAGSAL-GETKIN, O., WINSLOW, A. R., ZHU, L., VANDERBURG, C. R. & MCLEAN, P. J. 2012. Exosomal cell-to-cell transmission of alpha synuclein oligomers. *Molecular Neurodegeneration,* 7**,** 42.

DAVIS, G. C., WILLIAMS, A. C., MARKEY, S. P., EBERT, M. H., CAINE, E. D., REICHERT, C. M. & KOPIN, I. J. 1979. Chronic Parkinsonism secondary to intravenous injection of meperidine analogues. *Psychiatry Res,* 1**,** 249-54.

DAWSON, T. M. & DAWSON, V. L. 2010. The Role of Parkin in Familial and Sporadic Parkinson's Disease. *Movement disorders : official journal of the Movement Disorder Society,* 25**,** S32-S39.

DE LAU, L. M. L. & BRETELER, M. M. B. 2006. Epidemiology of Parkinson's disease. *The Lancet Neurology,* 5**,** 525-535.

DECRESSAC, M., MATTSSON, B., LUNDBLAD, M., WEIKOP, P. & BJORKLUND, A. 2012a. Progressive neurodegenerative and behavioural changes induced by AAV-mediated overexpression of alpha-synuclein in midbrain dopamine neurons. *Neurobiol Dis,* 45**,** 939-53.

DECRESSAC, M., MATTSSON, B., LUNDBLAD, M., WEIKOP, P. & BJORKLUND, A. 2012b. Progressive neurodegenerative and behavioural changes induced by AAV-mediated overexpression of alpha-synuclein in midbrain dopamine neurons. *Neurobiol. Dis,* 45**,** 939-953.

DECRESSAC, M., MATTSSON, B., WEIKOP, P., LUNDBLAD, M., JAKOBSSON, J. & BJÖRKLUND, A. 2013. TFEB-mediated autophagy rescues midbrain dopamine neurons from α-synuclein toxicity. *Proceedings of the National Academy of Sciences,* 110**,** E1817-E1826.

DEHAY, B., BOURDENX, M., GORRY, P., PRZEDBORSKI, S., VILA, M., HUNOT, S., SINGLETON, A., OLANOW, C. W., MERCHANT, K. M., BEZARD, E., PETSKO, G. A. & MEISSNER, W. G. 2015a. Targeting alpha-synuclein for treatment of Parkinson's disease: mechanistic and therapeutic considerations. *Lancet Neurol,* 14**,** 855-866.

DEHAY, B., BOURDENX, M., GORRY, P., PRZEDBORSKI, S., VILA, M., HUNOT, S., SINGLETON, A., OLANOW, C. W., MERCHANT, K. M., BEZARD, E., PETSKO, G. A. & MEISSNER, W. G. 2015b. Targeting α-synuclein for treating Parkinson's disease: mechanistic and therapeutic considerations. *The Lancet. Neurology,* 14**,** 855-866.

DESPLATS, P., LEE, H. J., BAE, E. J., PATRICK, C., ROCKENSTEIN, E., CREWS, L., SPENCER, B., MASLIAH, E. & LEE, S. J. 2009a. Inclusion formation and neuronal cell death through neuron-to-neuron transmission of alpha-synuclein. *Proc Natl Acad Sci U S A,* 106.

DESPLATS, P., LEE, H. J., BAE, E. J., PATRICK, C., ROCKENSTEIN, E., CREWS, L., SPENCER, B., MASLIAH, E. & LEE, S. J. 2009b. Inclusion formation and neuronal cell death through neuron-to-neuron transmission of alpha-synuclein. *Proc. Natl. Acad. Sci. U. S. A,* 106**,** 13010-13015.

DESPLATS, P., PATEL, P., KOSBERG, K., MANTE, M., PATRICK, C., ROCKENSTEIN, E., FUJITA, M., HASHIMOTO, M. & MASLIAH, E. 2012. Combined exposure to Maneb and Paraquat alters transcriptional regulation of neurogenesis-related genes in mice models of Parkinson's disease. *Molecular Neurodegeneration,* 7**,** 49.

DEVI, L., RAGHAVENDRAN, V., PRABHU, B. M., AVADHANI, N. G. & ANANDATHEERTHAVARADA, H. K. 2008. Mitochondrial Import and Accumulation of α-Synuclein Impair Complex I in Human Dopaminergic Neuronal Cultures and Parkinson Disease Brain. *The Journal of Biological Chemistry,* 283**,** 9089-9100.

DI MAIO, R., BARRETT, P. J., HOFFMAN, E. K., BARRETT, C. W., ZHARIKOV, A., BORAH, A., HU, X., MCCOY, J., CHU, C. T., BURTON, E. A., HASTINGS, T. G. & GREENAMYRE, J. T. 2016. α-Synuclein binds to TOM20 and inhibits mitochondrial protein import in Parkinson's disease. *Science Translational Medicine,* 8**,** 342ra78-342ra78.

DICKSON, D. W., UCHIKADO, H., FUJISHIRO, H. & TSUBOI, Y. 2010. Evidence in favor of Braak staging of Parkinson's disease. *Mov Disord,* 25 Suppl 1**,** S78-82.

DORSEY, E. R., CONSTANTINESCU, R., THOMPSON, J. P., BIGLAN, K. M., HOLLOWAY, R. G., KIEBURTZ, K., MARSHALL, F. J., RAVINA, B. M., SCHIFITTO, G., SIDEROWF, A. & TANNER, C. M. 2006. Projected number of people with Parkinson disease in the most populous nations, 2005 through 2030. *Neurology*.

DORSEY, E. R., CONSTANTINESCU, R., THOMPSON, J. P., BIGLAN, K. M., HOLLOWAY, R. G., KIEBURTZ, K., MARSHALL, F. J., RAVINA, B. M., SCHIFITTO, G., SIDEROWF, A. & TANNER, C. M. 2007. Projected number of people with Parkinson disease in the most populous nations, 2005 through 2030. *Neurology,* 68**,** 384-6.

EBELING, W., HENNRICH, N., KLOCKOW, M., METZ, H., ORTH, H. D. & LANG, H. 1974. Proteinase K from Tritirachium album Limber. *Eur J Biochem,* 47**,** 91-7.

EBRAHIMI-FAKHARI, D., CANTUTI-CASTELVETRI, I., FAN, Z., ROCKENSTEIN, E., MASLIAH, E., HYMAN, B. T., MCLEAN, P. J. & UNNI, V. K. 2011. Distinct roles in vivo for the ubiquitin-proteasome system and the autophagy-lysosomal pathway in the degradation of α-synuclein. *J Neurosci,* 31**,** 14508-20.

EMMANOUILIDOU, E., MELACHROINOU, K., ROUMELIOTIS, T., GARBIS, S. D., NTZOUNI, M., MARGARITIS, L. H., STEFANIS, L. & VEKRELLIS, K. 2010. Cell-produced alpha-synuclein is secreted in a calcium-dependent manner by exosomes and impacts neuronal survival. *J Neurosci,* 30**,** 6838-51.

EXNER, N., LUTZ, A. K., HAASS, C. & WINKLHOFER, K. F. 2012. Mitochondrial dysfunction in Parkinson's disease: molecular mechanisms and pathophysiological consequences. *EMBO J.* England.

FARES, M. B., AIT-BOUZIAD, N., DIKIY, I., MBEFO, M. K., JOVICIC, A., KIELY, A., HOLTON, J. L., LEE, S. J., GITLER, A. D., ELIEZER, D. & LASHUEL, H. A. 2014. The novel Parkinson's disease linked mutation G51D attenuates in vitro aggregation and membrane binding of alpha-synuclein, and enhances its secretion and nuclear localization in cells. *Hum Mol Genet,* 23**,** 4491-509.

FEARNLEY, J. M. & LEES, A. J. 1991. Ageing and Parkinson's disease: substantia nigra regional selectivity. *Brain,* 114 (Pt 5)**,** 2283-301.

FENG, Y., LIANG, Z. H., WANG, T., QIAO, X., LIU, H. J. & SUN, S. G. 2006. alpha-Synuclein redistributed and aggregated in rotenone-induced Parkinson's disease rats. *Neurosci Bull,* 22**,** 288-93.

FILICHIA, E., HOFFER, B., QI, X. & LUO, Y. 2016a. Inhibition of Drp1 mitochondrial translocation provides neural protection in dopaminergic system in a Parkinson's disease model induced by MPTP. *Sci Rep.*

FILICHIA, E., HOFFER, B., QI, X. & LUO, Y. 2016b. Inhibition of Drp1 mitochondrial translocation provides neural protection in dopaminergic system in a Parkinson's disease model induced by MPTP. 6**,** 32656.

FRANCO-IBORRA, S., VILA, M. & PERIER, C. 2016. The Parkinson Disease Mitochondrial Hypothesis: Where Are We at? *Neuroscientist,* 22**,** 266-277.
FREEMAN, D., CEDILLOS, R., CHOYKE, S., LUKIC, Z., MCGUIRE, K., MARVIN, S., BURRAGE, A. M., SUDHOLT, S., RANA, A., O'CONNOR, C., WIETHOFF, C. M. & CAMPBELL, E. M. 2013. Alpha-synuclein induces lysosomal rupture and cathepsin dependent reactive oxygen species following endocytosis. *PLoS One,* 8**,** e62143.
FREUNDT, E. C., MAYNARD, N., CLANCY, E. K., ROY, S., BOUSSET, L., SOURIGUES, Y., COVERT, M., MELKI, R., KIRKEGAARD, K. & BRAHIC, M. 2012. Neuron-to-neuron transmission of alpha-synuclein fibrils through axonal transport. *Ann. Neurol,* 72**,** 517-524.
FUKUSHIMA, T., TAN, X., LUO, Y. & KANDA, H. 2010. Relationship between blood levels of heavy metals and Parkinson's disease in China. *Neuroepidemiology,* 34**,** 18-24.
GARCIA-REITBOCK, P., ANICHTCHIK, O., BELLUCCI, A., IOVINO, M., BALLINI, C., FINEBERG, E., GHETTI, B., DELLA CORTE, L., SPANO, P., TOFARIS, G. K., GOEDERT, M. & SPILLANTINI, M. G. 2010. SNARE protein redistribution and synaptic failure in a transgenic mouse model of Parkinson's disease. *Brain,* 133**,** 2032-44.
GAUTIER, C. A., KITADA, T. & SHEN, J. 2008. Loss of PINK1 causes mitochondrial functional defects and increased sensitivity to oxidative stress. *Proceedings of the National Academy of Sciences,* 105**,** 11364-11369.
GEY, G. 1952. Tissue culture studies of the proliferative capacity of cervical carcinoma and normal epithelium. *Cancer Res,* 12**,** 264-265.
GIASSON, B. I. & LEE, V. M. Y. 2000. A new link between pesticides and Parkinson's disease. *Nat Neurosci,* 3**,** 1227-1228.
GOEDERT, M., JAKES, R. & SPILLANTINI, M. G. 2017. The Synucleinopathies: Twenty Years On. *J Parkinsons Dis,* 7**,** S53-s71.
GOMES, L. C., DI BENEDETTO, G. & SCORRANO, L. 2011. During autophagy mitochondria elongate, are spared from degradation and sustain cell viability. *Nat Cell Biol,* 13**,** 589-98.
GORELL, J. M., JOHNSON, C. C., RYBICKI, B. A., PETERSON, E. L. & RICHARDSON, R. J. 1998. The risk of Parkinson's disease with exposure to pesticides, farming, well water, and rural living. *Neurology,* 50**,** 1346-50.
GROHM, J., KIM, S. W., MAMRAK, U., TOBABEN, S., CASSIDY-STONE, A., NUNNARI, J., PLESNILA, N. & CULMSEE, C. 2012. Inhibition of Drp1 provides neuroprotection in vitro and in vivo. *Cell Death and Differentiation,* 19**,** 1446-1458.
GUI, Y. X., WANG, X. Y., KANG, W. Y., ZHANG, Y. J., ZHANG, Y., ZHOU, Y., QUINN, T. J., LIU, J. & CHEN, S. D. 2012. Extracellular signal-regulated kinase is involved in alpha-synuclein-induced mitochondrial dynamic disorders by regulating dynamin-like protein 1. *Neurobiol Aging,* 33**,** 2841-54.
GUO, J. L. & LEE, V. M. 2014. Cell-to-cell transmission of pathogenic proteins in neurodegenerative diseases. *Nat Med,* 20**,** 130-8.
HANSEN, C., ANGOT, E., BERGSTROM, A. L., STEINER, J. A., PIERI, L., PAUL, G., OUTEIRO, T. F., MELKI, R., KALLUNKI, P., FOG, K., LI, J. Y. & BRUNDIN, P. 2011. alpha-Synuclein propagates from mouse brain to grafted dopaminergic neurons and seeds aggregation in cultured human cells. *J. Clin. Invest,* 121**,** 715-725.
HEALY, D. G., FALCHI, M., O'SULLIVAN, S. S., BONIFATI, V., DURR, A., BRESSMAN, S., BRICE, A., AASLY, J., ZABETIAN, C. P., GOLDWURM, S., FERREIRA, J. J., TOLOSA, E., KAY, D. M., KLEIN, C., WILLIAMS, D. R., MARRAS, C., LANG, A. E., WSZOLEK, Z. K., BERCIANO, J., SCHAPIRA, A. H., LYNCH, T., BHATIA, K. P., GASSER, T., LEES, A. J. & WOOD, N. W.

2008. Phenotype, genotype, and worldwide genetic penetrance of LRRK2-associated Parkinson's disease: a case–control study. *Lancet Neurol,* 7.

HELLEY, M. P., PINNELL, J., SPORTELLI, C. & TIEU, K. 2017a. Mitochondria: A Common Target for Genetic Mutations and Environmental Toxicants in Parkinson's Disease. *Front Genet,* 8**,** 177.

HELLEY, M. P., PINNELL, J., SPORTELLI, C. & TIEU, K. 2017b. Mitochondria: A Common Target for Genetic Mutations and Environmental Toxicants in Parkinson's Disease. *Frontiers in Genetics,* 8.

HERNANDEZ, D. G., REED, X. & SINGLETON, A. B. 2016. Genetics in Parkinson disease: Mendelian versus non-Mendelian inheritance. *J Neurochem,* 139 Suppl 1**,** 59-74.

HOLLENBECK, P. J. 2005. Mitochondria and neurotransmission: evacuating the synapse. *Neuron,* 47**,** 331-3.

HOSOKAWA, N., HARA, T., KAIZUKA, T., KISHI, C., TAKAMURA, A., MIURA, Y., IEMURA, S., NATSUME, T., TAKEHANA, K., YAMADA, N., GUAN, J. L., OSHIRO, N. & MIZUSHIMA, N. 2009. Nutrient-dependent mTORC1 association with the ULK1-Atg13-FIP200 complex required for autophagy. *Mol Biol Cell,* 20**,** 1981-91.

HUDSON, G., NALLS, M., EVANS, J. R., BREEN, D. P., WINDER-RHODES, S., MORRISON, K. E., MORRIS, H. R., WILLIAMS-GRAY, C. H., BARKER, R. A., SINGLETON, A. B., HARDY, J., WOOD, N. E., BURN, D. J. & CHINNERY, P. F. 2013. Two-stage association study and meta-analysis of mitochondrial DNA variants in Parkinson disease. *Neurology,* 80**,** 2042-8.

INGERMAN, E., PERKINS, E. M., MARINO, M., MEARS, J. A., MCCAFFERY, J. M., HINSHAW, J. E. & NUNNARI, J. 2005. Dnm1 forms spirals that are structurally tailored to fit mitochondria. *The Journal of Cell Biology,* 170**,** 1021-1027.

ISHIHARA, N., NOMURA, M., JOFUKU, A., KATO, H., SUZUKI, S. O., MASUDA, K., OTERA, H., NAKANISHI, Y., NONAKA, I., GOTO, Y.-I., TAGUCHI, N., MORINAGA, H., MAEDA, M., TAKAYANAGI, R., YOKOTA, S. & MIHARA, K. 2009. Mitochondrial fission factor Drp1 is essential for embryonic development and synapse formation in mice. *Nat Cell Biol,* 11**,** 958-966.

ITOH, K., ADACHI, Y., YAMADA, T., SUZUKI, T. L., OTOMO, T., MCBRIDE, H. M., YOSHIMORI, T., IIJIMA, M. & SESAKI, H. 2018. A brain-enriched Drp1 isoform associates with lysosomes, late endosomes, and the plasma membrane. *The Journal of biological chemistry,* 293**,** 11809-11822.

JANETZKY, B., HAUCK, S., YOUDIM, M. B. H., RIEDERER, P., JELLINGER, K., PANTUCEK, F., ZO¨CHLING, R., BOISSL, K. W. & REICHMANN, H. 1994. Unaltered aconitase activity, but decreased complex I activity in substantia nigra pars compacta of patients with Parkinson's disease. *Neuroscience Letters,* 169**,** 126-128.

JI, C. H. & KWON, Y. T. 2017. Crosstalk and Interplay between the Ubiquitin-Proteasome System and Autophagy. *Molecules and cells,* 40**,** 441-449.

KAMEL, F. 2013. Paths from Pesticides to Parkinson's. *Science,* 341**,** 722-723.

KAMP, F., EXNER, N., LUTZ, A. K., WENDER, N., HEGERMANN, J., BRUNNER, B., NUSCHER, B., BARTELS, T., GIESE, A., BEYER, K., EIMER, S., WINKLHOFER, K. F. & HAASS, C. 2010. Inhibition of mitochondrial fusion by alpha-synuclein is rescued by PINK1, Parkin and DJ-1. *Embo j,* 29**,** 3571-89.

KANDIMALLA, R., MANCZAK, M., FRY, D., SUNEETHA, Y., SESAKI, H. & REDDY, P. H. 2016. Reduced Dynamin-related Protein 1 Protects Against Phosphorylated Tau-induced

Mitochondrial Dysfunction and Synaptic Damage in Alzheimer's Disease. *Hum. Mol. Genet*, ddw312.
KANDIMALLA, R. & REDDY, P. H. 2016. Multiple faces of dynamin-related protein 1 and its role in Alzheimer's disease pathogenesis. *Biochim Biophys Acta,* 1862, 814-828.
KASAI, T., TOKUDA, T., YAMAGUCHI, N., WATANABE, Y., KAMETANI, F., NAKAGAWA, M. & MIZUNO, T. 2008. Cleavage of normal and pathological forms of alpha-synuclein by neurosin in vitro. *Neurosci Lett,* 436, 52-6.
KEENEY, P. M., XIE, J., CAPALDI, R. A. & BENNETT, J. P. 2006. Parkinson's Disease Brain Mitochondrial Complex I Has Oxidatively Damaged Subunits and Is Functionally Impaired and Misassembled. *The Journal of Neuroscience,* 26, 5256-5264.
KIM, C., HO, D. H., SUK, J. E., YOU, S., MICHAEL, S., KANG, J., JOONG LEE, S., MASLIAH, E., HWANG, D., LEE, H. J. & LEE, S. J. 2013a. Neuron-released oligomeric alpha-synuclein is an endogenous agonist of TLR2 for paracrine activation of microglia. *Nat Commun,* 4, 1562.
KIM, J., BYUN, J. W., CHOI, I., KIM, B., JEONG, H. K., JOU, I. & JOE, E. 2013b. PINK1 Deficiency Enhances Inflammatory Cytokine Release from Acutely Prepared Brain Slices. *Exp Neurobiol,* 22, 38-44.
KIMURA, S., NODA, T. & YOSHIMORI, T. 2007. Dissection of the autophagosome maturation process by a novel reporter protein, tandem fluorescent-tagged LC3. *Autophagy,* 3, 452-460.
KING, J. S. 2012. Autophagy across the eukaryotes: is S. cerevisiae the odd one out? *Autophagy,* 8, 1159-1162.
KLEIN, C., LOHMANN-HEDRICH, K., ROGAEVA, E., SCHLOSSMACHER, M. G. & LANG, A. E. 2007. Deciphering the role of heterozygous mutations in genes associated with parkinsonism. *Lancet Neurol,* 6, 652-62.
KLEIN, C. & WESTENBERGER, A. 2012. Genetics of Parkinson's Disease. *Cold Spring Harbor Perspectives in Medicine,* 2, a008888.
KLIONSKY, D. J. 2005. The molecular machinery of autophagy: unanswered questions. *J Cell Sci,* 118, 7-18.
KOEHLER, P. J. & KEYSER, A. 1997. Tremor in Latin texts of Dutch physicians: 16th-18th centuries. *Mov Disord,* 12, 798-806.
KORDOWER, J. H., CHU, Y., HAUSER, R. A., FREEMAN, T. B. & OLANOW, C. W. 2008. Lewy body-like pathology in long-term embryonic nigral transplants in Parkinson's disease. *Nat Med,* 14.
KRAYTSBERG, Y., KUDRYAVTSEVA, E., MCKEE, A. C., GEULA, C., KOWALL, N. W. & KHRAPKO, K. 2006. Mitochondrial DNA deletions are abundant and cause functional impairment in aged human substantia nigra neurons. *Nat Genet,* 38, 518-20.
KRUG, A. K., GUTBIER, S., ZHAO, L., POLTL, D., KULLMANN, C., IVANOVA, V., FORSTER, S., JAGTAP, S., MEISER, J., LEPARC, G., SCHILDKNECHT, S., ADAM, M., HILLER, K., FARHAN, H., BRUNNER, T., HARTUNG, T., SACHINIDIS, A. & LEIST, M. 2014. Transcriptional and metabolic adaptation of human neurons to the mitochondrial toxicant MPP(+). *Cell Death Dis,* 5, e1222.
KRUGER, R., KUHN, W., MULLER, T., WOITALLA, D., GRAEBER, M., KOSEL, S., PRZUNTEK, H., EPPLEN, J. T., SCHOLS, L. & RIESS, O. 1998. Ala30Pro mutation in the gene encoding alpha-synuclein in Parkinson's disease. *Nat Genet,* 18, 106-8.

KUMA, A., MIZUSHIMA, N., ISHIHARA, N. & OHSUMI, Y. 2002. Formation of the approximately 350-kDa Apg12-Apg5.Apg16 multimeric complex, mediated by Apg16 oligomerization, is essential for autophagy in yeast. *J Biol Chem,* 277**,** 18619-25.

LANGSTON, J. W., BALLARD, P., TETRUD, J. W. & IRWIN, I. 1983. Chronic Parkinsonism in humans due to a product of meperidine-analog synthesis. *Science,* 219**,** 979-80.

LARSEN, K. E., SCHMITZ, Y., TROYER, M. D., MOSHAROV, E., DIETRICH, P., QUAZI, A. Z., SAVALLE, M., NEMANI, V., CHAUDHRY, F. A., EDWARDS, R. H., STEFANIS, L. & SULZER, D. 2006. Alpha-synuclein overexpression in PC12 and chromaffin cells impairs catecholamine release by interfering with a late step in exocytosis. *J Neurosci,* 26**,** 11915-22.

LASHUEL, H. A., OVERK, C. R., OUESLATI, A. & MASLIAH, E. 2013. The many faces of alpha-synuclein: from structure and toxicity to therapeutic target. *Nat Rev Neurosci,* 14.

LATSOUDIS, H., SPANAKI, C., CHLOUVERAKIS, G. & PLAITAKIS, A. 2008. Mitochondrial DNA polymorphisms and haplogroups in Parkinson's disease and control individuals with a similar genetic background. *J Hum Genet,* 53**,** 349-56.

LAVEDAN, C. 1998. The synuclein family. *Genome Res,* 8**,** 871-80.

LAZAROU, M., SLITER, D. A., KANE, L. A., SARRAF, S. A., WANG, C., BURMAN, J. L., SIDERIS, D. P., FOGEL, A. I. & YOULE, R. J. 2015. The ubiquitin kinase PINK1 recruits autophagy receptors to induce mitophagy. *Nature,* 524**,** 309-314.

LEE, H. J., KHOSHAGHIDEH, F., PATEL, S. & LEE, S. J. 2004. Clearance of alpha-synuclein oligomeric intermediates via the lysosomal degradation pathway. *J Neurosci,* 24**,** 1888-96.

LEE, H. J., SUK, J. E., PATRICK, C., BAE, E. J., CHO, J. H., RHO, S., HWANG, D., MASLIAH, E. & LEE, S. J. 2010. Direct transfer of alpha-synuclein from neuron to astroglia causes inflammatory responses in synucleinopathies. *J Biol Chem,* 285**,** 9262-72.

LEHMAN, J. J., BARGER, P. M., KOVACS, A., SAFFITZ, J. E., MEDEIROS, D. M. & KELLY, D. P. 2000. Peroxisome proliferator–activated receptor γ coactivator-1 promotes cardiac mitochondrial biogenesis. *Journal of Clinical Investigation,* 106**,** 847-856.

LESAGE, S., ANHEIM, M., LETOURNEL, F., BOUSSET, L., HONORE, A., ROZAS, N., PIERI, L., MADIONA, K., DURR, A. & MELKI, R. 2013. G51D alpha-synuclein mutation causes a novel parkinsonian-pyramidal syndrome. *Ann Neurol,* 73.

LI, H., CHEN, Y., JONES, A. F., SANGER, R. H., COLLIS, L. P., FLANNERY, R., MCNAY, E. C., YU, T., SCHWARZENBACHER, R., BOSSY, B., BOSSY-WETZEL, E., BENNETT, M. V. L., PYPAERT, M., HICKMAN, J. A., SMITH, P. J. S., HARDWICK, J. M. & JONAS, E. A. 2008a. Bcl-xL induces Drp1-dependent synapse formation in cultured hippocampal neurons. *Proceedings of the National Academy of Sciences,* 105**,** 2169-2174.

LI, J. Y., ENGLUND, E., HOLTON, J. L., SOULET, D., HAGELL, P., LEES, A. J., LASHLEY, T., QUINN, N. P., REHNCRONA, S. & BJORKLUND, A. 2008b. Lewy bodies in grafted neurons in subjects with Parkinson's disease suggest host-to-graft disease propagation. *Nat Med,* 14.

LILL, C. M., ROEHR, J. T., MCQUEEN, M. B., KAVVOURA, F. K., BAGADE, S., SCHJEIDE, B. M., SCHJEIDE, L. M., MEISSNER, E., ZAUFT, U., ALLEN, N. C., LIU, T., SCHILLING, M., ANDERSON, K. J., BEECHAM, G., BERG, D., BIERNACKA, J. M., BRICE, A., DESTEFANO, A. L., DO, C. B., ERIKSSON, N., FACTOR, S. A., FARRER, M. J., FOROUD, T., GASSER, T., HAMZA, T., HARDY, J. A., HEUTINK, P., HILL-BURNS, E. M., KLEIN, C., LATOURELLE, J. C., MARAGANORE, D. M., MARTIN, E. R., MARTINEZ, M., MYERS, R. H., NALLS, M. A., PANKRATZ, N., PAYAMI, H., SATAKE, W., SCOTT, W. K., SHARMA, M., SINGLETON, A.

B., STEFANSSON, K., TODA, T., TUNG, J. Y., VANCE, J., WOOD, N. W., ZABETIAN, C. P., YOUNG, P., TANZI, R. E., KHOURY, M. J., ZIPP, F., LEHRACH, H., IOANNIDIS, J. P. & BERTRAM, L. 2012. Comprehensive research synopsis and systematic meta-analyses in Parkinson's disease genetics: The PDGene database. *PLoS Genet,* 8**,** e1002548.

LIN, J., WU, H., TARR, P. T., ZHANG, C.-Y., WU, Z., BOSS, O., MICHAEL, L. F., PUIGSERVER, P., ISOTANI, E., OLSON, E. N., LOWELL, B. B., BASSEL-DUBY, R. & SPIEGELMAN, B. M. 2002. Transcriptional co-activator PGC-1α drives the formation of slow-twitch muscle fibres. *Nature,* 418**,** 797.

LIN, M. T., CANTUTI-CASTELVETRI, I., ZHENG, K., JACKSON, K. E., TAN, Y. B., ARZBERGER, T., LEES, A. J., BETENSKY, R. A., BEAL, M. F. & SIMON, D. K. 2012. Somatic mitochondrial DNA mutations in early Parkinson and incidental Lewy body disease. *Ann Neurol,* 71**,** 850-4.

LOTHARIUS, J., BARG, S., WIEKOP, P., LUNDBERG, C., RAYMON, H. K. & BRUNDIN, P. 2002. Effect of Mutant α-Synuclein on Dopamine Homeostasis in a New Human Mesencephalic Cell Line. *Journal of Biological Chemistry,* 277**,** 38884-38894.

LUK, K. C., KEHM, V. M., ZHANG, B., O'BRIEN, P., TROJANOWSKI, J. Q. & LEE, V. M. 2012. Intracerebral inoculation of pathological alpha-synuclein initiates a rapidly progressive neurodegenerative alpha-synucleinopathy in mice. *J. Exp. Med,* 209**,** 975-986.

LUTZ, A. K., EXNER, N., FETT, M. E., SCHLEHE, J. S., KLOOS, K., LÄMMERMANN, K., BRUNNER, B., KURZ-DREXLER, A., VOGEL, F., REICHERT, A. S., BOUMAN, L., VOGT-WEISENHORN, D., WURST, W., TATZELT, J., HAASS, C. & WINKLHOFER, K. F. 2009. Loss of Parkin or PINK1 Function Increases Drp1-dependent Mitochondrial Fragmentation. *The Journal of Biological Chemistry,* 284**,** 22938-22951.

LY, C. V. & VERSTREKEN, P. 2006. Mitochondria at the synapse. *Neuroscientist,* 12**,** 291-9.

LYNCH-DAY, M. A., MAO, K., WANG, K., ZHAO, M. & KLIONSKY, D. J. 2012. The role of autophagy in Parkinson's disease. *Cold Spring Harb Perspect Med,* 2**,** a009357.

MADAY, S., WALLACE, K. E. & HOLZBAUR, E. L. 2012. Autophagosomes initiate distally and mature during transport toward the cell soma in primary neurons. *J Cell Biol,* 196**,** 407-17.

MANCZAK, M., CALKINS, M. J. & REDDY, P. H. 2011. Impaired mitochondrial dynamics and abnormal interaction of amyloid beta with mitochondrial protein Drp1 in neurons from patients with Alzheimer's disease: implications for neuronal damage. *Hum Mol Genet,* 20**,** 2495-509.

MANCZAK, M., KANDIMALLA, R., FRY, D., SESAKI, H. & REDDY, P. H. 2016. Protective effects of reduced dynamin-related protein 1 against amyloid beta-induced mitochondrial dysfunction and synaptic damage in Alzheimer's disease. *Hum. Mol. Genet***,** ddw330.

MANCZAK, M., KANDIMALLA, R., YIN, X. & REDDY, P. H. 2019. Mitochondrial division inhibitor 1 reduces dynamin-related protein 1 and mitochondrial fission activity. *Hum Mol Genet,* 28**,** 177-199.

MANCZAK, M. & REDDY, P. H. 2015. Mitochondrial division inhibitor 1 protects against mutant huntingtin-induced abnormal mitochondrial dynamics and neuronal damage in Huntington's disease. *Hum Mol Genet,* 24**,** 7308-25.

MCCOY, M. K. & COOKSON, M. R. 2011. DJ-1 regulation of mitochondrial function and autophagy through oxidative stress. *Autophagy,* 7**,** 531-532.

MISHIZEN-EBERZ, A. J., GUTTMANN, R. P., GIASSON, B. I., DAY, G. A., 3RD, HODARA, R., ISCHIROPOULOS, H., LEE, V. M., TROJANOWSKI, J. Q. & LYNCH, D. R. 2003. Distinct

cleavage patterns of normal and pathologic forms of alpha-synuclein by calpain I in vitro. *J Neurochem,* 86**,** 836-47.

MISHRA, P. & CHAN, D. C. 2014. Mitochondrial dynamics and inheritance during cell division, development and disease. *Nature Reviews Molecular Cell Biology,* 15**,** 634-646.

MULLIN, S. & SCHAPIRA, A. 2015. The genetics of Parkinson's disease. *British Medical Bulletin,* 114**,** 39-52.

NAIR, S., SOBOTKA, K. S., JOSHI, P., GRESSENS, P., FLEISS, B., THORNTON, C., MALLARD, C. & HAGBERG, H. 2019. Lipopolysaccharide-induced alteration of mitochondrial morphology induces a metabolic shift in microglia modulating the inflammatory response in vitro and in vivo. *Glia,* 67**,** 1047-1061.

NAKAMURA, K., NEMANI, V. M., AZARBAL, F., SKIBINSKI, G., LEVY, J. M., EGAMI, K., MUNISHKINA, L., ZHANG, J., GARDNER, B., WAKABAYASHI, J., SESAKI, H., CHENG, Y., FINKBEINER, S., NUSSBAUM, R. L., MASLIAH, E. & EDWARDS, R. H. 2011. Direct membrane association drives mitochondrial fission by the Parkinson disease-associated protein alpha-synuclein. *J Biol Chem,* 286**,** 20710-26.

NAKAMURA, T., CIEPLAK, P., CHO, D.-H., GODZIK, A. & LIPTON, S. A. 2010. S-Nitrosylation of Drp1 links excessive mitochondrial fission to neuronal injury in neurodegeneration. *Mitochondrion,* 10**,** 573-578.

NARENDRA, D., TANAKA, A., SUEN, D. F. & YOULE, R. J. 2008. Parkin is recruited selectively to impaired mitochondria and promotes their autophagy. *J Cell Biol,* 183**,** 795-803.

NEMANI, V. M., LU, W., BERGE, V., NAKAMURA, K., ONOA, B., LEE, M. K., CHAUDHRY, F. A., NICOLL, R. A. & EDWARDS, R. H. 2010. Increased expression of alpha-synuclein reduces neurotransmitter release by inhibiting synaptic vesicle reclustering after endocytosis. *Neuron,* 65.

NONAKA, T., WATANABE, S. T., IWATSUBO, T. & HASEGAWA, M. 2010. Seeded aggregation and toxicity of {alpha}-synuclein and tau: cellular models of neurodegenerative diseases. *J Biol Chem,* 285**,** 34885-98.

NUMADATE, A., MITA, Y., MATSUMOTO, Y., FUJII, S. & HASHIMOTO, Y. 2014. Development of 2-thioxoquinazoline-4-one derivatives as dual and selective inhibitors of dynamin-related protein 1 (Drp1) and puromycin-sensitive aminopeptidase (PSA). *Chem Pharm Bull (Tokyo),* 62**,** 979-88.

OBESO, J. A., STAMELOU, M., GOETZ, C. G., POEWE, W., LANG, A. E., WEINTRAUB, D., BURN, D., HALLIDAY, G. M., BEZARD, E., PRZEDBORSKI, S., LEHERICY, S., BROOKS, D. J., ROTHWELL, J. C., HALLETT, M., DELONG, M. R., MARRAS, C., TANNER, C. M., ROSS, G. W., LANGSTON, J. W., KLEIN, C., BONIFATI, V., JANKOVIC, J., LOZANO, A. M., DEUSCHL, G., BERGMAN, H., TOLOSA, E., RODRIGUEZ-VIOLANTE, M., FAHN, S., POSTUMA, R. B., BERG, D., MAREK, K., STANDAERT, D. G., SURMEIER, D. J., OLANOW, C. W., KORDOWER, J. H., CALABRESI, P., SCHAPIRA, A. H. V. & STOESSL, A. J. 2017. Past, present, and future of Parkinson's disease: A special essay on the 200th Anniversary of the Shaking Palsy. *Mov Disord,* 32**,** 1264-1310.

OSELLAME, L. D., SINGH, A. P., STROUD, D. A., PALMER, C. S., STOJANOVSKI, D., RAMACHANDRAN, R. & RYAN, M. T. 2016. Cooperative and independent roles of the Drp1 adaptors Mff, MiD49 and MiD51 in mitochondrial fission. *J Cell Sci,* 129**,** 2170-81.

OWUSU-ANSAH, E., YAVARI, A. & BANERJEE, U. 2008. A protocol for in vivo detection of Reactive Oxygen Species. *Protocol Exchange*.

PALACINO, J. J., SAGI, D., GOLDBERG, M. S., KRAUSS, S., MOTZ, C., WACKER, M., KLOSE, J. & SHEN, J. 2004. Mitochondrial dysfunction and oxidative damage in parkin-deficient mice. *J Biol Chem,* 279**,** 18614-22.

PALMER, C. S., ELGASS, K. D., PARTON, R. G., OSELLAME, L. D., STOJANOVSKI, D. & RYAN, M. T. 2013. Adaptor proteins MiD49 and MiD51 can act independently of Mff and Fis1 in Drp1 recruitment and are specific for mitochondrial fission. *J Biol Chem,* 288**,** 27584-93.

PALMER, C. S., OSELLAME, L. D., LAINE, D., KOUTSOPOULOS, O. S., FRAZIER, A. E. & RYAN, M. T. 2011. MiD49 and MiD51, new components of the mitochondrial fission machinery. *EMBO Rep,* 12**,** 565-73.

PALMER, G., HORGAN, D. J., TISDALE, H., SINGER, T. P. & BEINERT, H. 1968. Studies on the respiratory chain-linked reduced nicotinamide adenine dinucleotide dehydrogenase. XIV. Location of the sites of inhibition of rotenone, barbiturates, and piericidin by means of electron paramagnetic resonance spectroscopy. *J Biol Chem,* 243**,** 844-7.

PAN-MONTOJO, F., SCHWARZ, M., WINKLER, C., ARNHOLD, M., O'SULLIVAN, G. A., PAL, A., SAID, J., MARSICO, G., VERBAVATZ, J.-M., RODRIGO-ANGULO, M., GILLE, G., FUNK, R. H. W. & REICHMANN, H. 2012a. Environmental toxins trigger PD-like progression via increased alpha-synuclein release from enteric neurons in mice. 2**,** 898.

PAN-MONTOJO, F., SCHWARZ, M., WINKLER, C., ARNHOLD, M., O'SULLIVAN, G. A., PAL, A., SAID, J., MARSICO, G., VERBAVATZ, J. M., RODRIGO-ANGULO, M., GILLE, G., FUNK, R. H. & REICHMANN, H. 2012b. Environmental toxins trigger PD-like progression via increased alpha-synuclein release from enteric neurons in mice. *Sci Rep,* 2**,** 898.

PARK, J., CHOI, H., MIN, J. S., PARK, S. J., KIM, J. H., PARK, H. J., KIM, B., CHAE, J. I., YIM, M. & LEE, D. S. 2013. Mitochondrial dynamics modulate the expression of pro-inflammatory mediators in microglial cells. *J Neurochem,* 127**,** 221-32.

PARKER, W. D., JR., BOYSON, S. J. & PARKS, J. K. 1989. Abnormalities of the electron transport chain in idiopathic Parkinson's disease. *Ann Neurol,* 26**,** 719-23.

PARKER, W. D., JR. & SWERDLOW, R. H. 1998. Mitochondrial dysfunction in idiopathic Parkinson disease. *Am J Hum Genet,* 62**,** 758-62.

PARKINSON, J. 2002. An essay on the shaking palsy. 1817. *J Neuropsychiatry Clin Neurosci,* 14**,** 223-36; discussion 222.

PARKKINEN, L., PIRTTILA, T. & ALAFUZOFF, I. 2008. Applicability of current staging/categorization of alpha-synuclein pathology and their clinical relevance. *Acta Neuropathol,* 115**,** 399-407.

PASANEN, P., MYLLYKANGAS, L., SIITONEN, M., RAUNIO, A., KAAKKOLA, S., LYYTINEN, J., TIENARI, P. J., POYHONEN, M. & PAETAU, A. 2014. Novel alpha-synuclein mutation A53E associated with atypical multiple system atrophy and Parkinson’s disease-type pathology. *Neurobiol Aging,* 35.

PERA, M., LARREA, D., GUARDIA-LAGUARTA, C., MONTESINOS, J., VELASCO, K. R., AGRAWAL, R. R., XU, Y., CHAN, R. B., DI PAOLO, G., MEHLER, M. F., PERUMAL, G. S., MACALUSO, F. P., FREYBERG, Z. Z., ACIN-PEREZ, R., ENRIQUEZ, J. A., SCHON, E. A. & AREA-GOMEZ, E. 2017. Increased localization of APP-C99 in mitochondria-associated ER membranes causes mitochondrial dysfunction in Alzheimer disease. *Embo j*.

POEHLER, A. M., XIANG, W., SPITZER, P., MAY, V. E., MEIXNER, H., ROCKENSTEIN, E., CHUTNA, O., OUTEIRO, T. F., WINKLER, J., MASLIAH, E. & KLUCKEN, J. 2014. Autophagy modulates SNCA/alpha-synuclein release, thereby generating a hostile microenvironment. *Autophagy,* 10**,** 2171-92.

POLYMEROPOULOS, M. H., LAVEDAN, C., LEROY, E., IDE, S. E., DEHEJIA, A., DUTRA, A., PIKE, B., ROOT, H., RUBENSTEIN, J. & BOYER, R. 1997a. Mutation in the alpha-synuclein gene identified in families with Parkinson's disease. *Science,* 276.

POLYMEROPOULOS, M. H., LAVEDAN, C., LEROY, E., IDE, S. E., DEHEJIA, A., DUTRA, A., PIKE, B., ROOT, H., RUBENSTEIN, J., BOYER, R., STENROOS, E. S., CHANDRASEKHARAPPA, S., ATHANASSIADOU, A., PAPAPETROPOULOS, T., JOHNSON, W. G., LAZZARINI, A. M., DUVOISIN, R. C., DI IORIO, G., GOLBE, L. I. & NUSSBAUM, R. L. 1997b. Mutation in the alpha-synuclein gene identified in families with Parkinson's disease. *Science,* 276**,** 2045-7.

PRASAD, K. N., CARVALHO, E., KENTROTI, S., EDWARDS-PRASAD, J., FREED, C. & VERNADAKIS, A. 1994. Establishment and characterization of immortalized clonal cell lines from fetal rat mesencephalic tissue. *In Vitro Cell Dev Biol Anim,* 30a**,** 596-603.

PRIYADARSHI, A., KHUDER, S. A., SCHAUB, E. A. & PRIYADARSHI, S. S. 2001. Environmental Risk Factors and Parkinson's Disease: A Metaanalysis. *Environmental Research,* 86**,** 122-127.

PRUDENT, J., ZUNINO, R., SUGIURA, A., MATTIE, S., SHORE, GORDON C. & MCBRIDE, HEIDI M. 2015. MAPL SUMOylation of Drp1 Stabilizes an ER/Mitochondrial Platform Required for Cell Death. *Molecular Cell,* 59**,** 941-955.

PRZEDBORSKI, S. 2017. The two-century journey of Parkinson disease research. *Nat Rev Neurosci,* 18**,** 251-259.

PUIGSERVER, P., WU, Z., PARK, C. W., GRAVES, R., WRIGHT, M. & SPIEGELMAN, B. M. 1998. A cold-inducible coactivator of nuclear receptors linked to adaptive thermogenesis. *Cell,* 92**,** 829-39.

PURNELL, P. R. & FOX, H. S. 2013. Autophagy-mediated turnover of dynamin-related protein 1. *BMC Neurosci,* 14**,** 86.

QI, X., QVIT, N., SU, Y. C. & MOCHLY-ROSEN, D. 2013a. A novel Drp1 inhibitor diminishes aberrant mitochondrial fission and neurotoxicity. *J. Cell Sci,* 126**,** 789-802.

QI, X., QVIT, N., SU, Y. C. & MOCHLY-ROSEN, D. 2013b. A novel Drp1 inhibitor diminishes aberrant mitochondrial fission and neurotoxicity. *J Cell Sci,* 126**,** 789-802.

QUADRI, M., FEDERICO, A., ZHAO, T., BREEDVELD, G. J., BATTISTI, C., DELNOOZ, C., SEVERIJNEN, L. A., DI TORO MAMMARELLA, L., MIGNARRI, A., MONTI, L., SANNA, A., LU, P., PUNZO, F., COSSU, G., WILLEMSEN, R., RASI, F., OOSTRA, B. A., VAN DE WARRENBURG, B. P. & BONIFATI, V. 2012. Mutations in SLC30A10 cause parkinsonism and dystonia with hypermanganesemia, polycythemia, and chronic liver disease. *Am J Hum Genet,* 90**,** 467-77.

RAPPOLD, P. M., CUI, M., GRIMA, J. C., FAN, R. Z., DE MESY-BENTLEY, K. L., CHEN, L., ZHUANG, X., BOWERS, W. J. & TIEU, K. 2014. Drp1 inhibition attenuates neurotoxicity and dopamine release deficits in vivo. *Nat Commun,* 5**,** 5244.

REDDY, P. H., MANCZAK, M. & YIN, X. 2017. Mitochondria-Division Inhibitor 1 Protects Against Amyloid-β induced Mitochondrial Fragmentation and Synaptic Damage in Alzheimer's Disease. *Journal of Alzheimer's disease : JAD,* 58**,** 147-162.

REEVE, A. K., LUDTMANN, M. H., ANGELOVA, P. R., SIMCOX, E. M., HORROCKS, M. H., KLENERMAN, D., GANDHI, S., TURNBULL, D. M. & ABRAMOV, A. Y. 2015. Aggregated alpha-synuclein and complex I deficiency: exploration of their relationship in differentiated neurons. *Cell Death Dis,* 6**,** e1820.

RICHARDSON, J. R., QUAN, Y., SHERER, T. B., GREENAMYRE, J. T. & MILLER, G. W. 2005. Paraquat Neurotoxicity is Distinct from that of MPTP and Rotenone. *Toxicological Sciences,* 88**,** 193-201.

ROBOTTA, M., GERDING, H. R., VOGEL, A., HAUSER, K., SCHILDKNECHT, S., KARREMAN, C., LEIST, M., SUBRAMANIAM, V. & DRESCHER, M. 2014. Alpha-Synuclein Binds to the Inner Membrane of Mitochondria in an α-Helical Conformation. *ChemBioChem,* 15**,** 2499-2502.

ROTH, J. A. 2014. Correlation between the biochemical pathways altered by mutated parkinson-related genes and chronic exposure to manganese. *Neurotoxicology,* 44**,** 314-25.

SARKAR, S., MALOVIC, E., HARISCHANDRA, D. S., NGWA, H. A., GHOSH, A., HOGAN, C., ROKAD, D., ZENITSKY, G., JIN, H., ANANTHARAM, V., KANTHASAMY, A. G. & KANTHASAMY, A. 2018. Manganese exposure induces neuroinflammation by impairing mitochondrial dynamics in astrocytes. *Neurotoxicology,* 64**,** 204-218.

SATO, S., UCHIHARA, T., FUKUDA, T., NODA, S., KONDO, H., SAIKI, S., KOMATSU, M., UCHIYAMA, Y., TANAKA, K. & HATTORI, N. 2018. Loss of autophagy in dopaminergic neurons causes Lewy pathology and motor dysfunction in aged mice. *Sci Rep,* 8**,** 2813.

SCHAPIRA, A. H. V., COOPER, J. M., DEXTER, D., CLARK, J. B., JENNER, P. & MARSDEN, C. D. 1990. Mitochondrial Complex I Deficiency in Parkinson's Disease. *Journal of Neurochemistry,* 54**,** 823-827.

SCHILDKNECHT, S., KARREMAN, C., POLTL, D., EFREMOVA, L., KULLMANN, C., GUTBIER, S., KRUG, A., SCHOLZ, D., GERDING, H. R. & LEIST, M. 2013. Generation of genetically-modified human differentiated cells for toxicological tests and the study of neurodegenerative diseases. *Altex,* 30**,** 427-44.

SCHOLZ, D., POLTL, D., GENEWSKY, A., WENG, M., WALDMANN, T., SCHILDKNECHT, S. & LEIST, M. 2011. Rapid, complete and large-scale generation of post-mitotic neurons from the human LUHMES cell line. *J Neurochem,* 119**,** 957-71.

SESAKI, H., ADACHI, Y., KAGEYAMA, Y., ITOH, K. & IIJIMA, M. 2014. In vivo functions of Drp1: Lessons learned from yeast genetics and mouse knockouts. *Biochimica et biophysica acta,* 1842**,** 1179-1185.

SHAVALI, S., BROWN-BORG, H. M., EBADI, M. & PORTER, J. 2008. Mitochondrial localization of alpha-synuclein protein in alpha-synuclein overexpressing cells. *Neuroscience Letters,* 439**,** 125-128.

SHEN, D. N., ZHANG, L. H., WEI, E. Q. & YANG, Y. 2015. Autophagy in synaptic development, function, and pathology. *Neurosci Bull,* 31**,** 416-26.

SHEN, W. & GANETZKY, B. 2009. Autophagy promotes synapse development in Drosophila</em&gt. *The Journal of Cell Biology,* 187**,** 71.

SHERER, T. B., RICHARDSON, J. R., TESTA, C. M., SEO, B. B., PANOV, A. V., YAGI, T., MATSUNO-YAGI, A., MILLER, G. W. & GREENAMYRE, J. T. 2007. Mechanism of toxicity of pesticides acting at complex I: relevance to environmental etiologies of Parkinson's disease. *Journal of Neurochemistry,* 100**,** 1469-1479.

SHIRENDEB, U., REDDY, A. P., MANCZAK, M., CALKINS, M. J., MAO, P., TAGLE, D. A. & REDDY, P. H. 2011. Abnormal mitochondrial dynamics, mitochondrial loss and mutant huntingtin oligomers in Huntington's disease: implications for selective neuronal damage. *Hum Mol Genet,* 20**,** 1438-55.

SINGLETON, A. B., FARRER, M., JOHNSON, J., SINGLETON, A., HAGUE, S., KACHERGUS, J., HULIHAN, M., PEURALINNA, T., DUTRA, A. & NUSSBAUM, R. 2003a. alpha-Synuclein locus triplication causes Parkinson's disease. *Science,* 302.

SINGLETON, A. B., FARRER, M., JOHNSON, J., SINGLETON, A., HAGUE, S., KACHERGUS, J., HULIHAN, M., PEURALINNA, T., DUTRA, A., NUSSBAUM, R., LINCOLN, S., CRAWLEY, A., HANSON, M., MARAGANORE, D., ADLER, C., COOKSON, M. R., MUENTER, M., BAPTISTA, M., MILLER, D., BLANCATO, J., HARDY, J. & GWINN-HARDY, K. 2003b. alpha-Synuclein locus triplication causes Parkinson's disease. *Science,* 302**,** 841.

SMIRNOVA, E., GRIPARIC, L., SHURLAND, D.-L. & VAN DER BLIEK, A. M. 2001a. Dynamin-related Protein Drp1 Is Required for Mitochondrial Division in Mammalian Cells. *Molecular Biology of the Cell,* 12**,** 2245-2256.

SMIRNOVA, E., GRIPARIC, L., SHURLAND, D. L. & VAN DER BLIEK, A. M. 2001b. Dynamin-related protein Drp1 is required for mitochondrial division in mammalian cells. *Mol. Biol. Cell,* 12**,** 2245-2256.

SMITH, G. & GALLO, G. 2017a. To mdivi-1 or not to mdivi-1: Is that the question? *Dev Neurobiol*.

SMITH, G. & GALLO, G. 2017b. To mdivi-1 or not to mdivi-1: Is that the question? *Dev. Neurobiol,* 77**,** 1260-1268.

SOLESIO, M. E., SAEZ-ATIENZAR, S., JORDAN, J. & GALINDO, M. F. 2012. Characterization of mitophagy in the 6-hydoxydopamine Parkinson's disease model. *Toxicol Sci,* 129**,** 411-20.

SONG, W., CHEN, J., PETRILLI, A., LIOT, G., KLINGLMAYR, E., ZHOU, Y., POQUIZ, P., TJONG, J., POULADI, M. A., HAYDEN, M. R., MASLIAH, E., ELLISMAN, M., ROUILLER, I., SCHWARZENBACHER, R., BOSSY, B., PERKINS, G. & BOSSY-WETZEL, E. 2011. Mutant huntingtin binds the mitochondrial fission GTPase dynamin-related protein-1 and increases its enzymatic activity. *Nat Med,* 17**,** 377-82.

SONG, W., SONG, Y., KINCAID, B., BOSSY, B. & BOSSY-WETZEL, E. 2013. Mutant SOD1G93A triggers mitochondrial fragmentation in spinal cord motor neurons: neuroprotection by SIRT3 and PGC-1alpha. *Neurobiol Dis,* 51**,** 72-81.

SPILLANTINI, M. G., CROWTHER, R. A., JAKES, R., HASEGAWA, M. & GOEDERT, M. 1998. alpha-Synuclein in filamentous inclusions of Lewy bodies from Parkinson's disease and dementia with lewy bodies. *Proc Natl Acad Sci U S A,* 95**,** 6469-73.

SPILLANTINI, M. G., SCHMIDT, M. L., LEE, V. M. Y., TROJANOWSKI, J. Q., JAKES, R. & GOEDERT, M. 1997. [alpha]-Synuclein in Lewy bodies. *Nature,* 388**,** 839-840.

STEFANOVIC, A. N., STOCKL, M. T., CLAESSENS, M. M. & SUBRAMANIAM, V. 2014. alpha-Synuclein oligomers distinctively permeabilize complex model membranes. *Febs j,* 281**,** 2838-50.

SU, X., MAGUIRE-ZEISS, K. A., GIULIANO, R., PRIFTI, L., VENKATESH, K. & FEDEROFF, H. J. 2008. Synuclein activates microglia in a model of Parkinson's disease. *Neurobiol Aging,* 29**,** 1690-701.

SUBRAMANIAM, S. R., VERGNES, L., FRANICH, N. R., REUE, K. & CHESSELET, M. F. 2014. Region specific mitochondrial impairment in mice with widespread overexpression of alpha-synuclein. *Neurobiol Dis,* 70**,** 204-13.

SURMEIER, D. J., OBESO, J. A. & HALLIDAY, G. M. 2017. Parkinson's Disease Is Not Simply a Prion Disorder. *The Journal of Neuroscience,* 37**,** 9799-9807.

TAGUCHI, N., ISHIHARA, N., JOFUKU, A., OKA, T. & MIHARA, K. 2007. Mitotic phosphorylation of dynamin-related GTPase Drp1 participates in mitochondrial fission. *J Biol Chem,* 282**,** 11521-9.

TANIK, S. A., SCHULTHEISS, C. E., VOLPICELLI-DALEY, L. A., BRUNDEN, K. R. & LEE, V. M. 2013. Lewy body-like alpha-synuclein aggregates resist degradation and impair macroautophagy. *J Biol Chem,* 288**,** 15194-210.

TANNER, C., KAMEL, F., ROSS, G., HOPPIN, J., GOLDMAN, S., KORELL, M., MARRAS, C., BHUDHIKANOK, G., KASTEN, M., CHADE, A., COMYNS, K., RICHARDS, M., MENG, C., PRIESTLEY, B., FERNANDEZ, H., CAMBI, F., UMBACH, D., BLAIR, A., SANDLER, D. & LANGSTON, J. 2011a. Rotenone, paraquat, and Parkinson's disease. *Environmental Health Perspectives,* 119**,** 866-872.

TANNER, C. M., KAMEL, F., ROSS, G. W., HOPPIN, J. A., GOLDMAN, S. M., KORELL, M., MARRAS, C., BHUDHIKANOK, G. S., KASTEN, M., CHADE, A. R., COMYNS, K., RICHARDS, M. B., MENG, C., PRIESTLEY, B., FERNANDEZ, H. H., CAMBI, F., UMBACH, D. M., BLAIR, A., SANDLER, D. P. & LANGSTON, J. W. 2011b. Rotenone, Paraquat, and Parkinson's Disease. *Environmental Health Perspectives,* 119**,** 866-872.

THIRUCHELVAM, M., RICHFIELD, E. K., BAGGS, R. B., TANK, A. W. & CORY-SLECHTA, D. A. 2000. The nigrostriatal dopaminergic system as a preferential target of repeated exposures to combined paraquat and maneb: implications for Parkinson's disease. *J Neurosci,* 20.

TIEU, K. 2011. A Guide to Neurotoxic Animal Models of Parkinson's Disease. *Cold Spring Harbor Perspectives in Medicine,* 1.

TIEU, K. I. J. 2014. Mitochondrial Dynamics as a Potential Therapeutic Target for Parkinson's Disease? *ADVANCES IN CLINICAL NEUROSCIENCE & REHABILITATION,* 14.

ULUSOY, A., RUSCONI, R., PEREZ-REVUELTA, B. I., MUSGROVE, R. E., HELWIG, M., WINZEN-REICHERT, B. & DI MONTE, D. A. 2013. Caudo-rostral brain spreading of alpha-synuclein through vagal connections. *EMBO Mol Med,* 5**,** 1119-27.

UVERSKY, V. N., LI, J. & FINK, A. L. 2001. Metal-triggered structural transformations, aggregation, and fibrillation of human alpha-synuclein. A possible molecular NK between Parkinson's disease and heavy metal exposure. *J Biol Chem,* 276**,** 44284-96.

VALENTE, E. M., ABOU-SLEIMAN, P. M., CAPUTO, V., MUQIT, M. M., HARVEY, K., GISPERT, S., ALI, Z., DEL TURCO, D., BENTIVOGLIO, A. R., HEALY, D. G., ALBANESE, A., NUSSBAUM, R., GONZALEZ-MALDONADO, R., DELLER, T., SALVI, S., CORTELLI, P., GILKS, W. P., LATCHMAN, D. S., HARVEY, R. J., DALLAPICCOLA, B., AUBURGER, G. & WOOD, N. W. 2004. Hereditary early-onset Parkinson's disease caused by mutations in PINK1. *Science,* 304**,** 1158-60.

VOGIATZI, T., XILOURI, M., VEKRELLIS, K. & STEFANIS, L. 2008. Wild type alpha-synuclein is degraded by chaperone-mediated autophagy and macroautophagy in neuronal cells. *J Biol Chem,* 283.

VOLPICELLI-DALEY, L. A., LUK, K. C. & LEE, V. M. 2014. Addition of exogenous alpha-synuclein preformed fibrils to primary neuronal cultures to seed recruitment of endogenous alpha-synuclein to Lewy body and Lewy neurite-like aggregates. *Nat. Protoc,* 9**,** 2135-2146.

WALCZAK, M. & MARTENS, S. 2013. Dissecting the role of the Atg12-Atg5-Atg16 complex during autophagosome formation. *Autophagy,* 9**,** 424-425.

WANG, H., SONG, P., DU, L., TIAN, W., YUE, W., LIU, M., LI, D., WANG, B., ZHU, Y., CAO, C., ZHOU, J. & CHEN, Q. 2011a. Parkin ubiquitinates Drp1 for proteasome-dependent

degradation: implication of dysregulated mitochondrial dynamics in Parkinson disease. *J Biol Chem,* 286**,** 11649-58.
WANG, W., KARAMANLIDIS, G. & TIAN, R. 2016a. Novel targets for mitochondrial medicine. *Sci Transl Med,* 8**,** 326rv3.
WANG, W., KARAMANLIDIS, G. & TIAN, R. 2016b. Novel targets for mitochondrial medicine. *Sci. Transl. Med,* 8**,** 326rv3.
WANG, W., WANG, X., FUJIOKA, H., HOPPEL, C., WHONE, A. L., CALDWELL, M. A., CULLEN, P. J., LIU, J. & ZHU, X. 2016c. Parkinson's disease-associated mutant VPS35 causes mitochondrial dysfunction by recycling DLP1 complexes. *Nat Med,* 22**,** 54-63.
WANG, X., SU, B., LEE, H.-G., LI, X., PERRY, G., SMITH, M. A. & ZHU, X. 2009. Impaired Balance of Mitochondria Fission and Fusion in Alzheimer Disease. *The Journal of neuroscience : the official journal of the Society for Neuroscience,* 29**,** 9090-9103.
WANG, X., SU, B., LIU, W., HE, X., GAO, Y., CASTELLANI, R. J., PERRY, G., SMITH, M. A. & ZHU, X. 2011b. DLP1-dependent mitochondrial fragmentation mediates 1-methyl-4-phenylpyridinium toxicity in neurons: implications for Parkinson's disease. *Aging Cell,* 10**,** 807-23.
WATERHAM, H. R., KOSTER, J., VAN ROERMUND, C. W., MOOYER, P. A., WANDERS, R. J. & LEONARD, J. V. 2007. A lethal defect of mitochondrial and peroxisomal fission. *New England Journal of Medicine,* 356**,** 1736-1741.
WEBB, J. L., RAVIKUMAR, B., ATKINS, J., SKEPPER, J. N. & RUBINSZTEIN, D. C. 2003a. Alpha-Synuclein is degraded by both autophagy and the proteasome. *J Biol Chem,* 278**,** 25009-13.
WEBB, J. L., RAVIKUMAR, B., ATKINS, J., SKEPPER, J. N. & RUBINSZTEIN, D. C. 2003b. Alpha-Synuclein is degraded by both autophagy and the proteasome. *J Biol Chem,* 278.
WHITE WJ, L. C. 1998. The Development and Maintenance of the Crl:CD(SD) IGS BR Rat Breeding System. *CD (SD) IGS Charles River Laboratories Publications.***,** 8-14.
WINSLOW, A. R., CHEN, C.-W., CORROCHANO, S., ACEVEDO-AROZENA, A., GORDON, D. E., PEDEN, A. A., LICHTENBERG, M., MENZIES, F. M., RAVIKUMAR, B., IMARISIO, S., BROWN, S., O'KANE, C. J. & RUBINSZTEIN, D. C. 2010a. α-Synuclein impairs macroautophagy: implications for Parkinson's disease. *The Journal of Cell Biology,* 190**,** 1023-1037.
WINSLOW, A. R., CHEN, C. W., CORROCHANO, S., ACEVEDO-AROZENA, A., GORDON, D. E., PEDEN, A. A., LICHTENBERG, M., MENZIES, F. M., RAVIKUMAR, B., IMARISIO, S., BROWN, S., O'KANE, C. J. & RUBINSZTEIN, D. C. 2010b. alpha-Synuclein impairs macroautophagy: implications for Parkinson's disease. *J Cell Biol,* 190**,** 1023-37.
WINSLOW, A. R. & RUBINSZTEIN, D. C. 2011. The Parkinson disease protein α-synuclein inhibits autophagy. *Autophagy,* 7**,** 429-431.
WOOTEN, G. F., CURRIE, L. J., BENNETT, J. P., HARRISON, M. B., TRUGMAN, J. M. & PARKER, W. D., JR. 1997. Maternal inheritance in Parkinson's disease. *Ann Neurol,* 41**,** 265-8.
WU, Z., PUIGSERVER, P., ANDERSSON, U., ZHANG, C., ADELMANT, G., MOOTHA, V., TROY, A., CINTI, S., LOWELL, B., SCARPULLA, R. C. & SPIEGELMAN, B. M. 1999. Mechanisms controlling mitochondrial biogenesis and respiration through the thermogenic coactivator PGC-1. *Cell,* 98**,** 115-24.
XIE, W. & CHUNG, K. K. K. 2012. Alpha-synuclein impairs normal dynamics of mitochondria in cell and animal models of Parkinson's disease. *Journal of Neurochemistry,* 122**,** 404-414.

XILOURI, M., BREKK, O. R. & STEFANIS, L. 2016. Autophagy and Alpha-Synuclein: Relevance to Parkinson's Disease and Related Synucleopathies. *Mov Disord,* 31**,** 178-92.

XU, Y. F., GENDRON, T. F., ZHANG, Y. J., LIN, W. L., D'ALTON, S., SHENG, H., CASEY, M. C., TONG, J., KNIGHT, J., YU, X., RADEMAKERS, R., BOYLAN, K., HUTTON, M., MCGOWAN, E., DICKSON, D. W., LEWIS, J. & PETRUCELLI, L. 2010. Wild-type human TDP-43 expression causes TDP-43 phosphorylation, mitochondrial aggregation, motor deficits, and early mortality in transgenic mice. *J Neurosci,* 30**,** 10851-9.

YOULE, R. J. & VAN DER BLIEK, A. M. 2012. Mitochondrial fission, fusion, and stress. *Science,* 337**,** 1062-1065.

YU, S., LI, X., LIU, G., HAN, J., ZHANG, C., LI, Y., XU, S., LIU, C., GAO, Y., YANG, H., UEDA, K. & CHAN, P. 2007. Extensive nuclear localization of alpha-synuclein in normal rat brain neurons revealed by a novel monoclonal antibody. *Neuroscience,* 145**,** 539-55.

YU, W. H., DORADO, B., FIGUEROA, H. Y., WANG, L., PLANEL, E., COOKSON, M. R., CLARK, L. N. & DUFF, K. E. 2009. Metabolic activity determines efficacy of macroautophagic clearance of pathological oligomeric alpha-synuclein. *Am J Pathol,* 175**,** 736-47.

ZARRANZ, J. J., ALEGRE, J., GOMEZ-ESTEBAN, J. C., LEZCANO, E., ROS, R., AMPUERO, I., VIDAL, L., HOENICKA, J., RODRIGUEZ, O. & ATARES, B. 2004a. The new mutation, E46K, of alpha-synuclein causes Parkinson and Lewy body dementia. *Ann Neurol,* 55.

ZARRANZ, J. J., ALEGRE, J., GOMEZ-ESTEBAN, J. C., LEZCANO, E., ROS, R., AMPUERO, I., VIDAL, L., HOENICKA, J., RODRIGUEZ, O., ATARES, B., LLORENS, V., GOMEZ TORTOSA, E., DEL SER, T., MUNOZ, D. G. & DE YEBENES, J. G. 2004b. The new mutation, E46K, of alpha-synuclein causes Parkinson and Lewy body dementia. *Ann Neurol,* 55**,** 164-73.

ZHANG, L., SHIMOJI, M., THOMAS, B., MOORE, D. J., YU, S. W., MARUPUDI, N. I., TORP, R., TORGNER, I. A., OTTERSEN, O. P., DAWSON, T. M. & DAWSON, V. L. 2005a. Mitochondrial localization of the Parkinson's disease related protein DJ-1: implications for pathogenesis. *Hum Mol Genet,* 14**,** 2063-73.

ZHANG, W., WANG, T., PEI, Z., MILLER, D. S., WU, X., BLOCK, M. L., WILSON, B., ZHOU, Y., HONG, J. S. & ZHANG, J. 2005b. Aggregated alpha-synuclein activates microglia: a process leading to disease progression in Parkinson's disease. *FASEB J,* 19.

ZHANG, Z., LIU, L., JIANG, X., ZHAI, S. & XING, D. 2016. The Essential Role of Drp1 and Its Regulation by S-Nitrosylation of Parkin in Dopaminergic Neurodegeneration: Implications for Parkinson's Disease. *Antioxid Redox Signal,* 25**,** 609-622.

ZHAO, Y., HO, P., YIH, Y., CHEN, C., LEE, W. L. & TAN, E. K. 2011. LRRK2 variant associated with Alzheimer's disease. *Neurobiol Aging,* 32**,** 1990-3.

ZHENG, B., LIAO, Z., LOCASCIO, J. J., LESNIAK, K. A., RODERICK, S. S., WATT, M. L., EKLUND, A. C., ZHANG-JAMES, Y., KIM, P. D., HAUSER, M. A., GRÜNBLATT, E., MORAN, L. B., MANDEL, S. A., RIEDERER, P., MILLER, R. M., FEDEROFF, H. J., WÜLLNER, U., PAPAPETROPOULOS, S., YOUDIM, M. B., CANTUTI-CASTELVETRI, I., YOUNG, A. B., VANCE, J. M., DAVIS, R. L., HEDREEN, J. C., ADLER, C. H., BEACH, T. G., GRAEBER, M. B., MIDDLETON, F. A., ROCHET, J.-C., SCHERZER, C. R. & CONSORTIUM, T. G. P. G. E. 2010. PGC-1α, A Potential Therapeutic Target for Early Intervention in Parkinson's Disease. *Science Translational Medicine,* 2**,** 52ra73.